REPUBLIC OF TÜRKİYE

ALTINBAŞ UNIVERSITY

Institute of Graduate Studies

Civil Engineering

INVESTIGATION OF DIFFERENT COLUMN SHAPES MODEL UNDER LATERAL FORCES

Hüseyin TLIMAT

Master's Thesis

Supervisor

Prof. Dr. Sepanta NAİMİ

İstanbul, 2025

INVESTIGATION OF DIFFERENT COLUMN SHAPES MODEL UNDER LATERAL FORCES

Hüseyin TLIMAT

Civil Engineering

Master's Thesis

ALTINBAŞ UNIVERSITY

2025

The thesis titled INVESTIGATION OF DIFFERENT COLUMN SHAPES MODEL UNDER LATERAL FORCES prepared by HÜSEYIN TLIMAT and submitted on 15/09/2025 has been **accepted unanimously** for the degree of Master of Science in Civil Engineering

Prof. Dr. Sepanta NAİMİ
Supervisor

Thesis Defense Committee Members:

Prof. Dr. Sepanta NAİMİ	Department of Civil Engineering, Altınbaş University	__________
Asst. Prof. Dr. Sepehr SAEDI	Department of Civil Engineering, Altınbaş University	__________
Asst. Prof. Dr. Kaveh DEHGHANIAN	Department of Civil Engineering, İstanbul Aydın University	__________

I hereby declare that this thesis meets all format and submission requirements of a Master's Thesis.

I hereby declare that all information/data presented in this graduation project has been obtained in full accordance with academic rules and ethical conduct. I also declare all unoriginal materials and conclusions have been cited in the text and all references mentioned in the Reference List have been cited in the text, and vice versa as required by the abovementioned rules and conduct.

Hüseyin TLIMAT

Signature

ABSTRACT

INVESTIGATION OF DIFFERENT COLUMN SHAPES MODEL UNDER LATERAL FORCES

TLIMAT, Hüseyin

M.Sc., Civil Engineering, Altınbaş University,

Supervisor: Prof. Dr. Sepanta NAİMİ

Date: 09 / 2025

Pages: 95

Columns are one of the most critical components in any structural system, as they serve as primary load-bearing elements that support vertical and lateral forces. The performance and reliability of a structure heavily depend on the efficiency of its columns in transferring loads safely to the foundation. Despite their fundamental role, a major challenge in structural engineering lies in identifying and optimizing the most suitable column shapes that can carry the highest loads under relatively simple and practical conditions, while ensuring structural integrity and material efficiency.

This study aims to explore and analyze a variety of column cross-sectional shapes to determine their mechanical behavior and structural performance under different load scenarios. The research focuses on comparing conventional reinforced concrete columns with specially shaped columns such as L-shaped and T-shaped sections that are proposed as viable alternatives for improving performance and material usage. The investigation involves finite element analysis (FEA) using the ANSYS simulation software to assess the structural behavior of different column geometries.

The methodology consists of two main analytical stages. In the first stage, a lateral load analysis is conducted to measure the displacement response of each column shape under horizontal forces, simulating real-world conditions such as wind or seismic activity. The second stage involves modal analysis, which evaluates the dynamic behavior of the columns by examining their vibration characteristics, specifically the natural frequencies and mode shapes.

Results from the simulations indicate that specially designed concrete columns with non-traditional cross-sections exhibit enhanced performance compared to standard rectangular or square columns. These special-shaped columns demonstrate reduced lateral displacements and improved dynamic responses, making them effective alternatives in scenarios requiring higher stability and resilience. Moreover, the modal analysis using the mode-superposition technique reveals that the special-shaped columns possess distinct vibrational properties, which can be strategically used in displacement-based design approaches.

In conclusion, the findings suggest that alternative column shapes, particularly L-shaped and T-shaped sections, can function as effective replacements or *succedanea* for traditional designs, offering superior structural behaviour under both static and dynamic loads. This research provides valuable insights for structural engineers aiming to optimize column design for enhanced safety, efficiency, and performance in modern building construction.

Keywords: Special-Shaped Concrete Column, ANSYS, Displacement, Flexural Test, Modal Analysis.

TABLE OF CONTENTS

Pages

ABSTRACT .... **v**

LIST OF TABLES .... **ix**

LIST OF FIGURES .... **x**

ABBREVIATIONS .... **xiv**

1. INTRODUCTION **1**

1.1 OVERVIEW 1

1.2 LATERAL LOAD RESPONSE ANALYSIS 2

1.3 PROBLEM STATEMENT 3

1.4 OBJECTIVE OF THE PRESENT STUDY 4

1.5 THESIS LAYOUT 4

2. LITERATURE REVIEW **5**

2.1 OVERVIEW 5

2.2 LATERAL LOAD ANALYSIS 6

2.3 EFFECT OF COLUMN LENGTH 6

2.4 EFFECT OF COLUMN SECTION SHAPE 12

3. RESEARCH METHODOLOGY **25**

3.1 INTRODUCTION 25

3.2 MATERIAL PROPERTIES 25

3.2.1 Fine Aggregate 26

3.2.2 Coarse Aggregate 26

3.2.3 The Used Water 26

3.3 PROPERTIES OF CONCRETE MIXTURE 26

3.4 PRODUCTION SAMPLES 28

3.5 TESTS FOR CONCRETE PROPERTIES 30

3.5.1 Compressive Strength Test 30

3.5.2 Splitting Test 31

3.5.3 Flexural Test Machine 32

3.6 BUILDING THE MODES 34

3.7 ANSYS PRE-PROCESS 37

3.8 DEVELOPING GEOMETRY 39

3.9 MESHING PROCESS 42

3.10 PROCESS TO SOLVE THE MODEL 45

3.11 SET THE LOAD 46

3.12 REQUEST RESULTS 48

4. RESULTS AND DISCUSSION 54

4.1 VALIDATION PROCESS 54

4.2 MODELS CONSIDERED FOR VARIATION IN COLUMN SHAPE +CONCRETE COMPRESSIVE STRENGTH WITH WIND 96 60

4.3 MODELS CONSIDERED FOR VARIATION IN COLUMN SHAPE WITH WIND 110 MPH 63

4.4 MODAL ANALYSIS L 67

4.5 MODAL ANALYSIS T 71

5. CONCLUSION AND RECOMMENDATIONS 76

REFERENCES 78

LIST OF TABLES

Pages

Table 3.1: Mixing Design 27

Table 3.2: The Input Representation of ANSYS Data 38

Table 4.1: Column Models Used in The Present Research 55

Table 4.2: Deviation Rate of Rectangular Column Results 57

Table 4.3: Deviation Rate of Special Column Shape Results 58

Table 4.4: Models Considered for Variation in Column Shape 60

LIST OF FIGURES

Pages

Figure 1.1: Specially Shaped (T, +, L) Columns with Longitudinal and Lateral Reinforcement. 1

Figure 2.1: Comparison between a Short Column and A Long Column [6]......................... 7

Figure 2.2: Behaviour of Short and Regular Columns [7] 8

Figure 2.3. Short Column Damages: (a)-24 January 2020 Elazı˘g Earthquake, (b)-25 January 1999 Armenia Colombia Earthquake, (c)-26 January 2001 (Bhuj) India Earthquake[7] 9

Figure 2.4: Hanging or Floating Columns[8] 10

Figure 2.5: Tree-Like Column Specimen Parameters[9].. 11

Figure 2.6: Tree-Like Column Specimen Parameters[9].. 12

Figure 2.7: On of Column with Lateral and Longitudinal Reinforcement[10] 13

Figure 2.8: Cross sections of Different Shapes of Column[11] 14

Figure 2.9: The Model Shapes [12] 15

Figure 2.10: Cross-Sectional and Longitudinal BRC Column Specimen Detailin[13]....... 17

Figure 2.11: Comparison of Damage Modes at Failure[13]... 18

Figure 2.12: Cross-Section of The Retrofitted Column (unit: mm)[14] 19

Figure 2.13: Dimensions and Reinforcement Details of Specimens (unit: mm)[15] 20

Figure 3.1: Project Samples... 28

Figure 3.2: Oiling The Molds 29

Figure 3.3: Casting Process 30

Figure 3.4: Compressive Test Machine 31

Figure 3.5: Splitting Test Machine 32

Figure 3.6: Flexural Test Machine 33

Figure 3.7: Results of Flexural Samples Test.. 33

Figure 3.8: The Dimensions of The Validation Case Using SolidWork 35

Figure 3.9: The Dimensions of The First Case Using SolidWork..................................... 35

Figure 3.10: THE Dimensions of The Second Case Using SolidWork.............................. 36

Figure 3.11:The Dimensions of The Third Case Using SolidWork 36

Figure 3.12: ANSYS Data Specification 40

Figure 3.13: ANSYS Input Validation Case 40

Figure 3.14: The First Case 41

Figure 3.15: The Second Case 41

Figure 3.16: The Third Case 42

Figure 3.17: Mesh Process for The Validation Case 43

Figure 3.18: Mesh Process for The First Case 44

Figure 3.19: MESH process for The Second Case 44

Figure 3.20: Mesh Process for The Third Case 45

Figure 3.21: Fixing The Base of Column 46

Figure 3.22: Selection Lateral Force Process 47

Figure 3.23: Applying Forces 47

Figure 3.24: Getting Modal Deformation 48

Figure 3.25: Developing Modal Process 49

Figure 3.26: Getting Stresses Results 49

Figure 3.27: Getting Deformation results 50

Figure 3.28: Applying Boundary Conditions 50

Figure 3.29: Checking Mesh Results 51

Figure 3.30: Sample of Modal Results 52

Figure 3.31: Sample of Stress Results 52

Figure 3.32: Sample of Deformation Results 53

Figure 4.1: Comparison of Rectangular Column Results 56

Figure 4.2: Comparison of Special Column Shape Results 57

Figure 4.3: Model 1 ANSYS Results 58

Figure 4.4: Model 2 ANSYS Results 59

Figure 4.5: Model 3 ANSYS Results 59

Figure 4.6: Rectangular Column Results C40 and Wind Velocity 96 mph 60

Figure 4.7: Special Column Shape Results C40 and Wind Velocity 96 mph 61

Figure 4.8: Rectangular Column Results C50 and Wind Velocity 96 mph 61

Figure 4.9: Special Column Shape C50 and Wind Velocity 96 mph 62

Figure 4.10: Rectangular Column Results and Wind Velocity 110 mph 63

Figure 4.11: Rectangular Column Results and Wind Velocity 110 mph 64

Figure 4.12: Rectangular Column Results and Wind Velocity 110 mph 64

Figure 4.13: Special Column Shape and Wind Velocity 110 mph.................................... 65

Figure 4.14: Special Column Shape and Wind Velocity 110 mph.................................... 66

Figure 4.15: Special Column Shape and Wind Velocity 110 mph.................................... 66

Figure 4.16: Modal Analysis L Shape Mode 1 68

Figure 4.17: Modal Analysis L Shape Mode 2 68

Figure 4.18: Modal Analysis L Shape Mode 3 69

Figure 4.19: Modal Analysis L Shape Mode 4 69

Figure 4.20: Modal Analysis L Shape Mode 5 70

Figure 4.21: Modal Analysis L Shape Mode 6 70

Figure 4.22: Modal Analysis T Shape Mode 1 72

Figure 4.23: Modal Analysis T Shape Mode 2 72

Figure 4.24: Modal Analysis T Shape Mode 3 73

Figure 4.25: Modal Analysis T Shape Mode 4 73

Figure 4.26: Modal Analysis T Shape Mode 5 74

Figure 4.27: Modal Analysis T Shape Mode 6 74

ABBREVIATIONS

Arca	:	Average Rate Of Change In Air Age
Cfd	:	Computational Fluid Dynamics
Csv	:	Cross-Side Ventilation
Hvac	:	Heating, Ventilating And Air Conditioning
Nv	:	Natural Ventilation
Ssv	:	Single-Side Ventilation

1. INTRODUCTION

1.1 OVERVIEW

The shape of a column can indeed affect its efficiency. Different shapes can impact the column's load-bearing capacity, stability, and resistance to buckling. For example, a slender column with a larger cross-sectional area may be more efficient in carrying a load compared to a shorter, thicker column. The nature of capacity curve also indicates that the structure almost remains in the elastic range up to the performance point[1]. Within reinforced concrete buildings (RCCs), the columns serve as the primary load-bearing components responsible for withstanding axial compressive stresses, moments, and the transmission of the entire load from the upper structure to the lower structure. Columns can assume various shapes and structures. Less popular but more spacious column designs, such as T-, L-, and plus (+)-shaped columns, provide greater interior space compared to commonly utilized varieties as in figure 1.1. Common shapes for columns include round, rectangular, and square. Columns with unconventional shapes can optimize the utilization of a room's square area by eliminating uncomfortable corners [1].

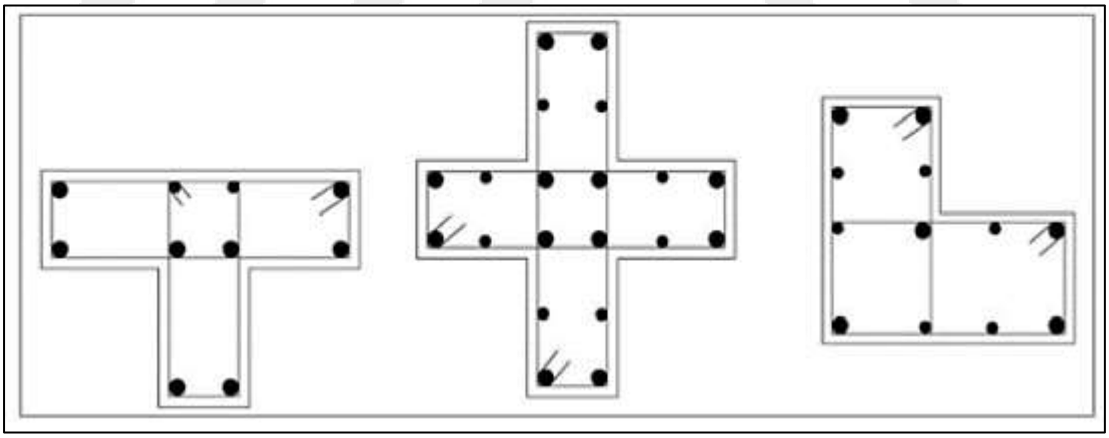

Figure 1.1: Specially Shaped (T, +, L) Columns with Longitudinal and Lateral Reinforcement.

Some researchers developed empirical equations for design parameters using test data, and others have developed behavioral models that use basic principles of mechanics in order to estimate their lateral load capacity[2]. The three variables that remain constant in column chromatography are the solvent type, column temperature, and pressure. Several variables must be taken into account, such as the dimensions of the absorbent particles and the column.

The latest performance assessment recommendations and column codes contain crucial information regarding the nonlinear response properties of structural members, including their ductility, stiffness, and lateral strength, as well as the appropriate modeling parameters for nonlinear analysis [3]. There have been just a few attempts to analytically simulate the nonlinear behavior of shear-controlled columns in research, with most studies employing one of three methodologies. The stress strength of a column can be determined through the application of the strut-and-tie model [4]. To incorporate the interaction between shear and flexure in simulating the column reaction, one can utilize fiber-based or multiple-spring models [5]. One approach is to employ the finite element modeling method [6]. Each of these modeling approaches possesses its own set of benefits and drawbacks, yet none of them are included into commonly utilized commercial software for nonlinear analysis. In addition, the design and testing of the structure do not incorporate squat columns or shear-controlled column segments. Extensive research has been conducted on the behavior and design of slender columns, however, there is limited knowledge on the functioning of squat columns with shear-controlled reactions. Moreover, accurate predictions of the column's reaction to shear may not always be derived from the strength calculations employed in design codes or the backbone curves cited in assessment and rehabilitation standards.

1.2 LATERAL LOAD RESPONSE ANALYSIS

During an earthquake, the Earth's surface undergoes multidirectional displacement. Buildings are most commonly damaged by motions perpendicular to the ground, as columns are primarily built to bear vertical gravity loads [7]. Several buildings possess inherent vertical strength, and the standard safety factor for vertical loading usually considers the vertical impact of an earthquake [8]. Furthermore, the vertical vibrations that occur at all sites will be quite similar as most of their horizontal dimensions are significantly smaller than the wavelength of ground motion during an earthquake. Consequently, there will be minimal or no accumulation of stress as the structures will experience negligible or no movement. Consequently, there is a scarcity of specific standards about the vertical force accompanying the horizontal force of an earthquake. During specific instances, numbers serve as a representation of ground acceleration. In order to faithfully represent the highly disparate fluctuations in acceleration throughout time, it is necessary for these temporal points to be in close proximity to each other [9].

The strong-motion accelerograph [10] is an essential device for recording three distinct types of ground shaking that occur during earthquakes. It is activated by the initial seismic waves, therefore it does not record continuously. This is due to the absence of any notable seismic ground motion that would require documentation, which may extend for several months or even years. Consequently, there would be no justification to persist in documenting numerous instances of these tools. Once the trigger is activated, the recording will persist until the cessation of seismic activity, which may endure for many minutes. Ensuring the proper maintenance of instruments is essential for recording during seismic vibrations [11]. The inaugural strong-motion accelerogram was documented during the seismic event known as the Long Beach earthquake in 1933 [10]. The initial substantial damage to several modern petrochemicals took place during the 1964 Alaskan earthquake [12]. The El Centro earthquake accelerograms, which are aligned in a north-south direction and have been adjusted to isolate ground acceleration peaks, have previously been utilized to analyze the seismic response in the s-direction [13]. The earthquake took place on May 18, 1940, measuring 6.5 on the Richter scale, which ranges from 0 to 8.9. The epicenter was predicted to be around fifteen kilometers northwest of California City. The amount of ground acceleration lasts for 31.18 seconds and peaks at 0.318g [14].

1.3 PROBLEM STATEMENT

The presence of a certain lateral load can cause a column's design to be impacted, leading to failure, displacements, and internal forces. Various types of pressures, such as axial load, can cause columns of different geometries or, more precisely, different types of column materials to exhibit distinct vibrations when exposed to the force of gravity. An essential research field within the study of deformable solids focuses on investigating nonlinear internal stresses in structural columns. The column may experience vibrations and ultimately collapse due to this. The study found two main concerns: the concrete material and the relationship between the column's geometry and its modal qualities. The effectiveness of concrete can be determined by considering its cross-sectional thickness, density, Young's moduli, and form types. The challenge at hand pertains to the efficacy of current methodologies in generating viable solutions for constructing concrete columns, while considering their behavior under lateral forces.

1.4 OBJECTIVE OF THE PRESENT STUDY

The main objective of this research can be summarized as follows:

a. Investigate the modal modes of different structural forms using traditional, readily available column structural concrete.

b. To analyze the reaction of the current column structure to an increase in column height and compare it with an elevated column.

1.5 THESIS LAYOUT

The thesis is divided into five distinct sections. Chapter 1 explores the structural response of a column to lateral loads.

Chapter 2 is a compilation of the properties, shapes, and attributes of columns, which have been derived from multiple investigations conducted by different scholars.

Chapter 3 provides comprehensive coverage of the experimental program, solution methods, examined parameters, applied methodology, and software.

In Chapter 4, we will present and discuss the outcomes of the simulation technique. Chapter Five will present the later part of the work.

2. LITERATURE REVIEW

2.1 OVERVIEW

In the fields of architecture and structural engineering, a column or pillar is a structural component that bears weight and transfers it to lower elements of a building or structure through compression. Thus, a column is a structural element that undergoes compressive forces. A column is a substantial, spherical structure that is elevated by a capital and supplementary supporting elements. The term "columns" is an alternative designation for compression elements that share similarities. Typically, columns provide support for beams or arches, which in turn bear the weight of the top sections of walls or ceilings.

For a structure to be stable and safe, the construction and installation of its columns must adhere to building requirements and standards. The subsequent are few crucial objectives that columns should strive to achieve. Engineers consider lateral resistance while building columns for wind or seismic engineering. The primary goal of structural stabilization is to offer horizontal reinforcement against wind and seismic forces, so guaranteeing the safety and integrity of the building[1]. This chapter investigates the characteristics of columns cross section, lateral buckling that may occur before or simultaneously with torsional buckling, commonly referred to as sudden twisting. The presence of twisting deformations greatly amplifies the intricacy of both theoretical analysis and actual design. The strength of the column is diminished when it is affected by imperfections such initial misalignment or uneven weight distribution. Elastically loaded columns experience non-concentric axial loads, where the axes of these loads do not align exactly with the centroid axis of the column. The column undergoes immediate bending due to the eccentricity or initial curvature of the load[2]. Additionally, they must possess the capacity to withstand natural disasters such as floods, earthquakes, strong winds, and fire. Columns in architecture have both utilitarian and ornamental functions. They may provide the illusion of a building seeming larger and more balanced. Columns are an optimal position for the placement of pipes, wires, and ducts. Typically, this phenomenon is observed in expansive structures such as stadiums, theaters, and museums. In order to guarantee the safety and longevity of a structure, it is imperative that it is meticulously built and constructed, taking into consideration all relevant environmental factors, loads, and pressures. In this chapter, the column shape, design, features and parameters will be presented, and the state of art research will be summarized.

2.2 LATERAL LOAD ANALYSIS

Within the construction sector, buildings have the potential to endure significant harm. The structure must possess the capacity to endure both horizontal forces and the downward pull of gravity, as the latter could lead to significant strain. As the compressive stress in a column's concrete nears its uniaxial compressive strength, there is a notable rise in lateral stresses caused by gradual internal cracking. As a result, the transverse plates (battens) of the steel cage experience significant tensile stresses, which necessitates their reinforcement. The primary objective of the design was to establish connections capable of withstanding high moments with a significant level of rigidity, achieved through the utilization of a robust column weak beam approach. Box-shaped columns are a practical design solution for moment-resisting connections in three-dimensional frameworks [4]. There is a wide range of choices for building analysis, which include both inelastic (nonlinear) and elastic (linear) approaches. The primary approach for inelastic analysis is comprehensive nonlinear history analysis; however, it remains excessively challenging and impractical for widespread application. The determination of capabilities that surpass elastic restrictions can only be achieved by the utilization of nonlinear analysis methods, such as the pushover approach. The pushover analysis is a static analytical technique that involves applying a lateral load profile to the structure and incrementally increasing it by a scaling factor until the displacement at a specific location on the structure reaches a limit state. Nevertheless, there are certain disadvantages associated with this method. Prioritize the meticulous evaluation of the lateral force distribution in the analysis. In order to conduct these inquiries, it is important to have computer software equipped with nonlinear analytical capabilities. In conclusion, the process of creating a nonlinear analysis model is considerably more intricate compared to linear analysis. The models must consider the inelastic load-deformation properties of important components [5].

2.3 EFFECT OF COLUMN LENGTH

Columns in reinforced concrete buildings (RCCs) primarily bear axially compressive stresses, moments, and the transfer of total load from the superstructure to the foundation. The columns have the ability to assume a multitude of shapes. Typical column shapes encompass squares, rectangles, circles, and a limited number of additional options. The floor area of a room can be enhanced by using specifically designed columns to eliminate visually obtrusive corners. The capacity of the column under primary loads is directly proportional to the sectional capacity, regardless of its length. The major function of this column is to transfer the inertia force to other columns. Due to the variation in column stiffness, the majority of these forces are exerted on the shorter column. Hence, the compact column has significant potential for causing structural damage in the case of an inadequately built edifice. The column's stiffness grows inversely with the cube of its height. Consequently, with each halving in length, the column's rigidity and ability to absorb energy multiply by a factor of eight. Figure 2.1 displays both the abbreviated and extended columns[6].

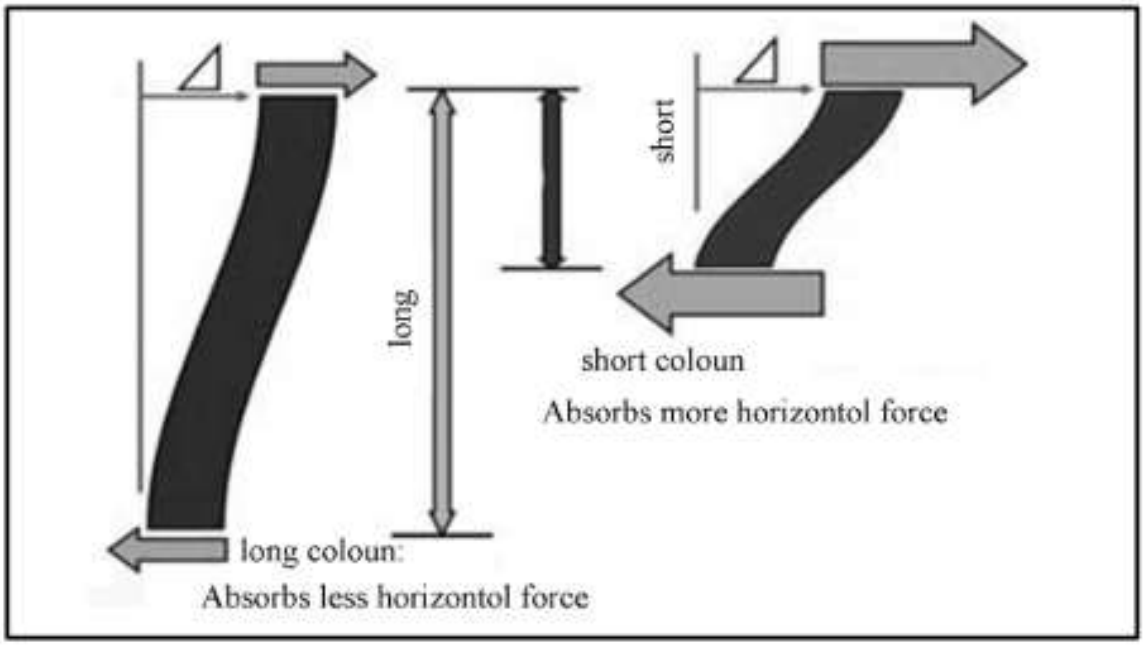

Figure 2.1: Comparison between a Short Column and A Long Column [6].

Ercan Isık et al, in 2023 examine the potential harm that can occur to the column in reinforced concrete structures due to brittle fractures in the structural elements when the shear resistances are exceeded by the intense shear stress exerted on short columns that are formed due to architectural and topographical factors. This study structurally examined three scenarios that could result in the construction of short columns: the hill slope effect, band-type windows, and mezzanine floors. Due to the disparity in height, columns of varying lengths on the same floor encounter distinct shear loads during seismic activity. When earthquake stresses initially strike long and flexible columns, energy is concentrated in shorter columns. X-shaped shear cracks manifest at both the base and top of the column due to the accumulation of forces. Under the influence of seismic forces, both long and short columns of equal cross-sectional area undergo identical displacement (Δ). However, shorter columns endure a higher magnitude of earthquake force as a result of their increased stiffness in comparison to longer columns. Considering the short-column impact is crucial at the first stages of the architectural design process [41]. Figure 2.2 displays the compact column shapes of the buildings.

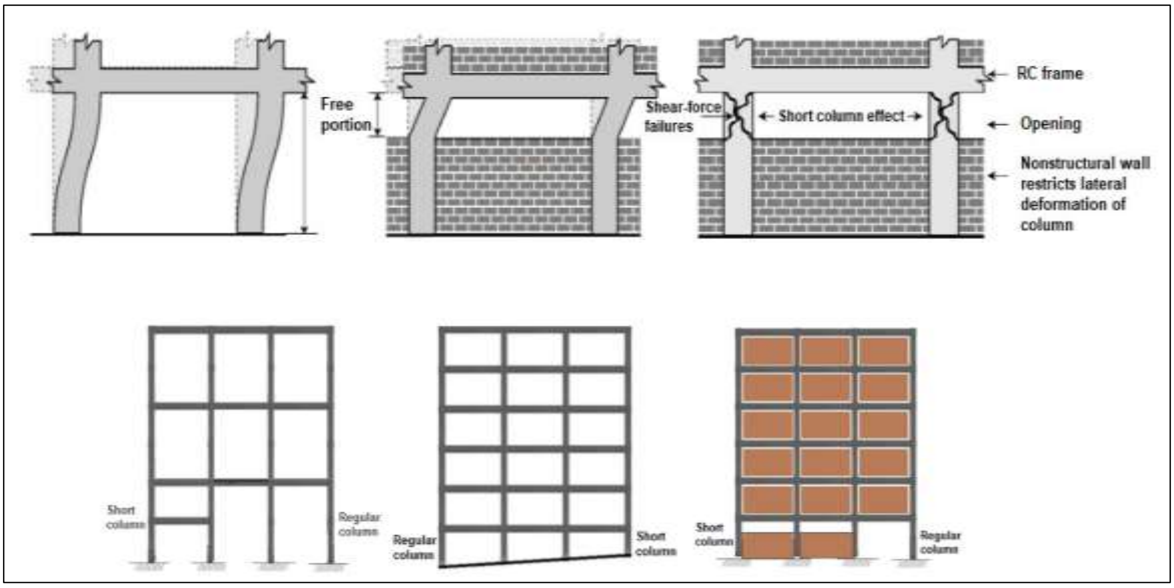

Figure 2.2: Behaviour of Short and Regular Columns [7].

The formation of stubby pillars is a primary factor contributing to the extensive destruction caused by earthquakes. Short columns experience significant shear stress, resulting in brittle collapses when the shear resistance is surpassed. The early loss of strength in these components further diminishes the building's displacement capacity. Hence, structures including columns of limited height will inevitably collapse as a result of their inherent fragility, as they are unable to endure the displacements induced by seismic activity. Additionally, the lateral load capacities of these elements are limited by their shear capacity, which in turn results in underutilization of their bending capacities [43,44]. Earthquakes in different regions of the world result in varying levels of devastation due to their truncated columns. Figure 2.3 displays the observed damage to short columns caused by the earthquake.

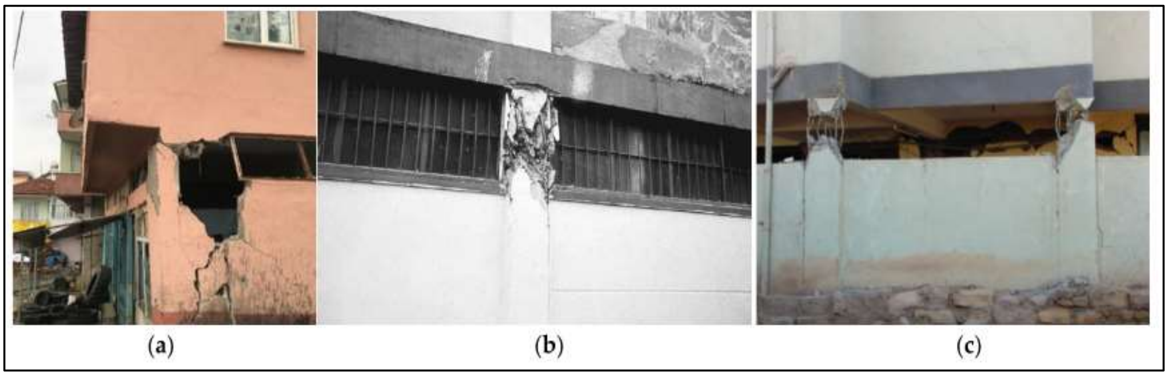

Figure 2.3. Short Column Damages: (a)-24 January 2020 Elazı˘g Earthquake, (b)-25 January 1999 Armenia Colombia Earthquake, (c)-26 January 2001 (Bhuj) India Earthquake[7].

The amended Türkiye Building Earthquake Code (TBEC-2018) mandated separate structural assessments for designs that rely on strength and those that rely on deformation. This study examined the effects of creating short columns on soft-story irregularity, relative story drifts, column shear force, plastic rotation in columns, roof displacement, base shear force, and column damage levels. The analysis determined that the second story was classified as a soft- story due to a significant decrease in relative drifts from the first floor, which was caused by the presence of band-type windows and slope impact. The introduction of shorter columns resulted in a significant increase in the requirement for plastic rotation and shear force within these columns.

The 2023 study conducted by Anil Thote et al. investigates the behaviors exhibited by columns that are capable of floating and those that are not. Disregarding seismic impacts, the comparative study investigates the behavior of floating and non-floating columns under static loading conditions. Floating columns are structural elements that can bear vertical loads and allow for lateral displacements without being attached to the base. On the other hand, non-floating columns are usually secured to the base using bolts and designed to endure horizontal and vertical pressures with minimal displacement. This research aims to investigate the structural behavior of both floating and non-floating columns, specifically focusing on load-carrying capacity, deflection characteristics, and failure modes. The analysis considers several elements, including as the column's dimensions, material properties, and loading conditions. Figure 2.4 displays the outcomes of experimental testing and numerical simulations conducted to analyze the behavior of the two categories of columns.

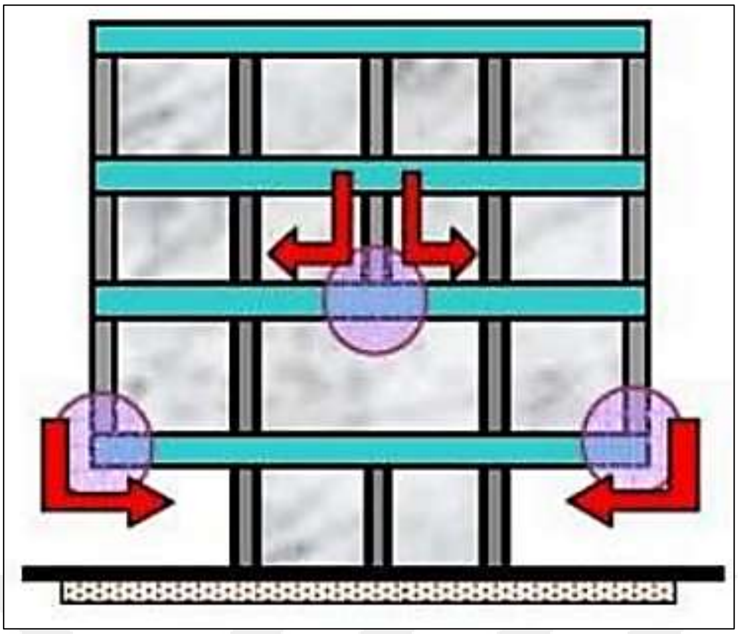

Figure 2.4: Hanging or Floating Columns[8].

The experimental program involves constructing smaller column models and gradually applying loads until they reach their breaking point. Numerical simulations utilize advanced structural analysis tools to predict and analyze the behavior of columns under different loading scenarios. The study's findings elucidate the disparities in load-carrying capacity and general structural behavior between columns that float and those that do not. This comparative analysis aims to assist structural engineers and designers in selecting the most suitable column system for certain applications by outlining the advantages and disadvantages of each column type. Note that this research does not consider the effects of seismic forces. Instead, it focuses solely on the static loading behavior of columns, whether they are floating or non-floating. It is necessary to conduct a separate study on the seismic performance and behavior of columns, considering their dynamic response to earthquake forces [8].

In 2022, Rabab et al. published a study on the structural characteristics of tree-like columns, which are steel columns that have branches. These columns have been incorporated into numerous buildings worldwide. The objective of this study is to analyze the structural behavior of tree-like columns subjected to combined axial and lateral loading conditions. The study intends to identify the ultimate load capacity, as well as the vertical and lateral displacements, and the specific failure mode of the columns. The selected design variable is the ratio of lateral load to axial load. This analysis primarily focuses on the axial and lateral loads applied to branching steel columns. Firstly, a finite element model was generated utilizing the ABAQUS/CAE 2017 software. This model consisted of a single level of branching, with two branches contained within that level. The first phase involved validating the model using experimental data.

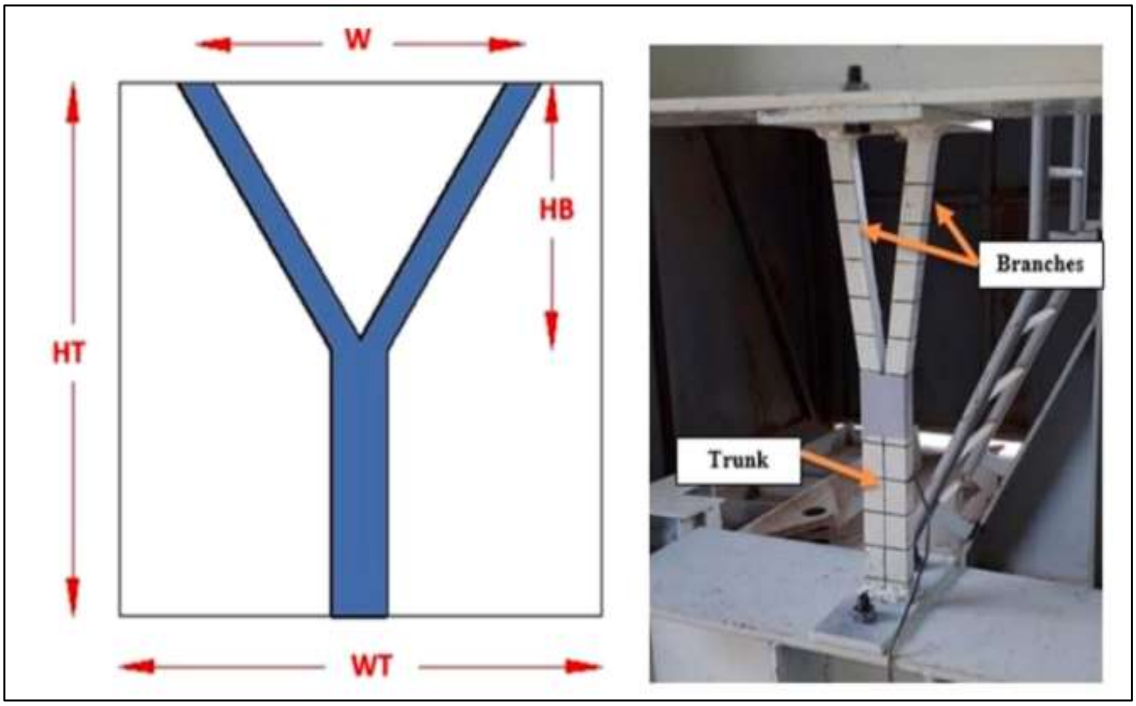

Figure 2.5: Tree-Like Column Specimen Parameters[9].

Figure 2.5 illustrates the outcomes of using the ABAQUS/CAE 2017 software to create the tree-column model. The model's boundary conditions were determined based on the following scenarios: Example 1: Models can only move from the bottom to the top until they experience axial tension, which enables them to move vertically at the top. In the second situation, the model experiences axial and lateral forces that limit its mobility at the bottom end but allow unrestricted movement at the top end.

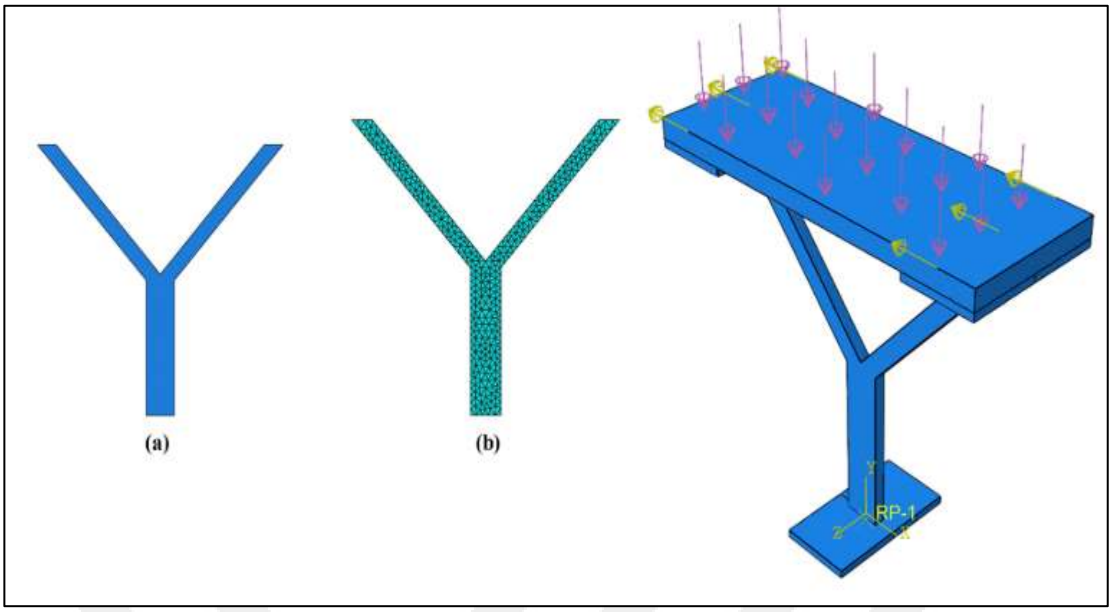

Figure 2.6: Tree-Like Column Specimen Parameters[9].

The three column models were tested using different ratios of lateral to axial stress, and the corresponding findings. Upon implementing a 60% lateral to axial load ratio, the curves exhibited a high degree of proximity, suggesting that the failure loads are almost indistinguishable [9].

2.4 EFFECT OF COLUMN SECTION SHAPE

Civil engineers have the main responsibility of safeguarding the safety of people in buildings by implementing innovative strategies that replace conventional building methods. These approaches enable the construction of expansive commercial areas in limited places, thereby enhancing the living conditions for a significant number of people. Hence, it is imperative to replace conventional construction techniques with modernized ones. One of the significant spatial concepts in the architectural history of urbanization in the twentieth century is buildings, which are primarily designed for office, institutional, or commercial purposes. Their main driving force is the growing necessity for enterprises to be in close proximity to each other, resulting from the rapid urban population growth. Extensive research and studies have been carried out to enhance the structural resilience of buildings against lateral forces and minimize vibrations. Columns are of structural importance as they hold the primary load of a building.

According to the research conducted by Md. Rashidun Rahman et al. in 2020, The columns have the ability to assume many shapes. The most common varieties of columns are square, rectangular, and round. However, there are also less common designs such as L-shaped and T-shaped columns, as well as plus (+) shaped columns that offer greater inside space compared to the more conventional types. Usable floor space in a room can be expanded by employing specifically designed columns to circumvent impediments. The objective of this study is to assess and contrast the ability of multi-story buildings with rectangular columns and those with distinctively curved columns to withstand seismic and wind forces. The intended structure is analyzed using Dhaka city's comparable static analysis for zone II. In construction, columns of various forms are commonly utilized, such as square, rectangular, circular, T-shaped, L-shaped, and cross (+) formed columns. The first three are categorized as "Regular columns," while the latter three are referred to as "Specially shaped columns."

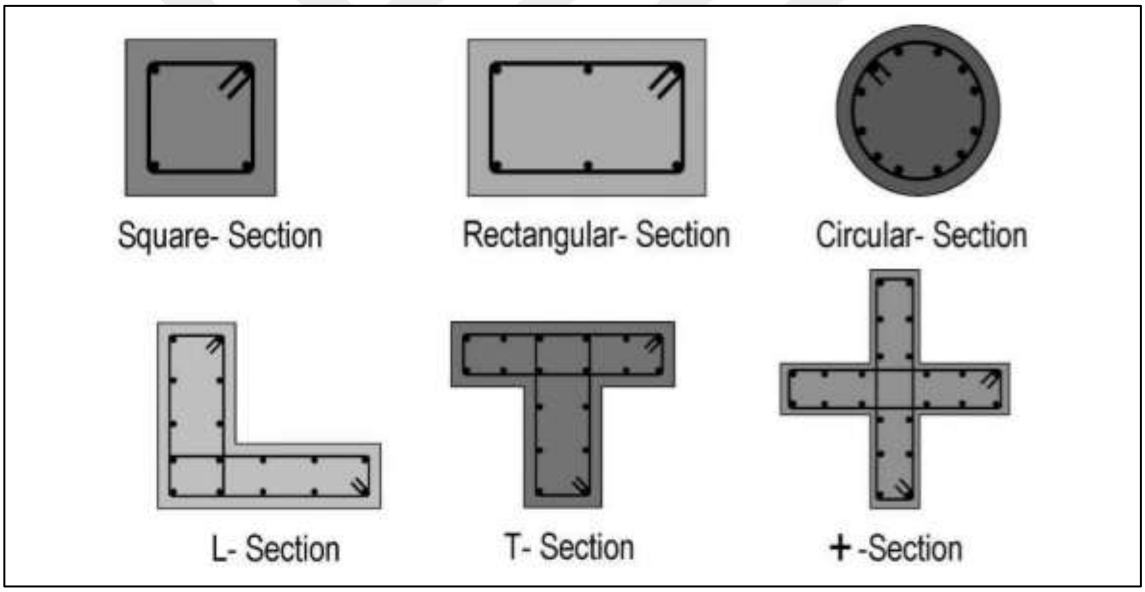

Figure 2.7: On of Column with Lateral and Longitudinal Reinforcement[10].

Based on the results, calculations are drawn showing the effectiveness of different shapes of the column under the effect of seismic loads[10].

Shruti R. Sarage et al, in 2021 also study the square columns, circular columns and combination of column cross sections such as L, T and plus (+) shaped.

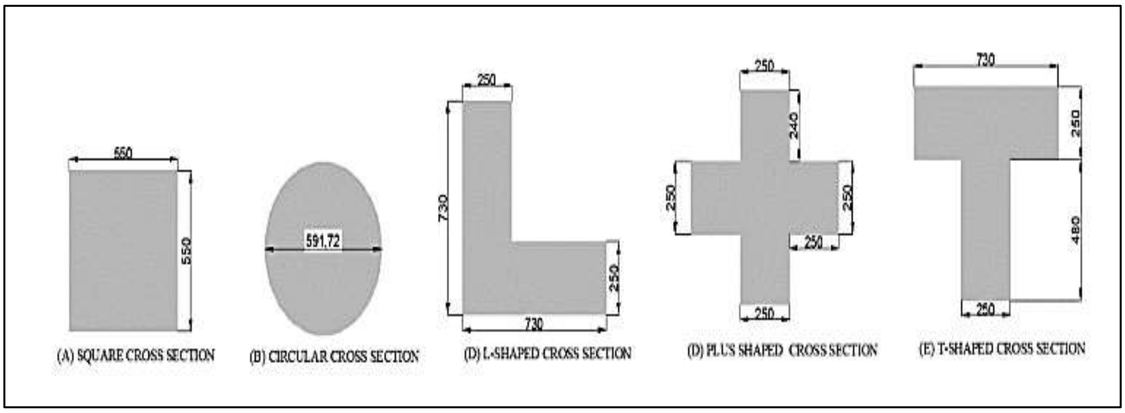

Figure 2.8: Cross Sections of Different Shapes of Column[11].

They measured the present factors:

a. Ductility Factor (Rμ)

b. Overstrength Factor (Rs)

c. Redundancy Factor (Rr)

d. Damping factor (Rξ)

The results indicate that the response modification factor values are greater for structures constructed according to the IS 1893: 2016 standards compared to structures constructed according to the IS 1893: 2002 standards. Structures designed according to ASCE 7-10 have larger response modification factor values compared to those designed according to IS 1893: 2002 and IS 1893:2016. Pushover analysis results indicate that structures constructed according to Indian requirements have lower dissipation capacity and reserved strength. American standards are more elevated. The response modification factor for structures designed according to Indian standards (IS 1893:2002 and IS 1893:2016) grows proportionally with the height of the building. This also applies to constructions that are examined and constructed in accordance with American code requirements [11].

A study conducted in 2018 by Rebecca Aswathy Joseph et al. examined the correlation between punching shear stress in flat plate systems and the compressive strength of concrete as well as the geometry of the columns. The loads on the slab are directly transferred to the columns. Flat plate constructions are widely utilized due to their numerous practical and budgetary advantages. The slab-column connections in such buildings are highly susceptible to experiencing substantial stress, which can result in punching shear failure and final structural collapse.

Sl No.	Model	Column dimensions (mm)
1.	B1	
2.	B2	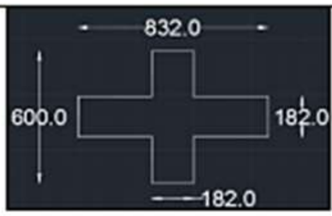
3.	B3	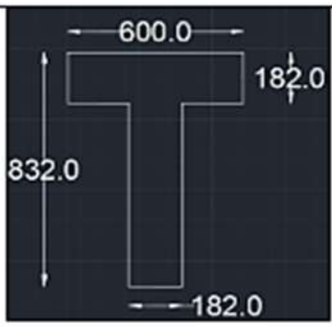
4.	B4	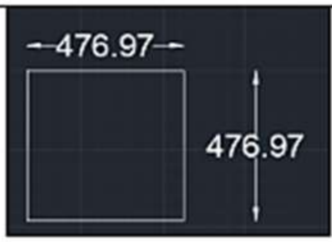

Figure 2.9: The Model Shapes [12].

When flat plate structures experience punching shear failure, a concrete truncated pyramid will be forcefully ejected from the slab. The analysis focuses on the shear stress in flat plate buildings by considering a six-story structure made of reinforced concrete. Various elements are examined to determine their impact. There are three bays aligned with the X and Y axes. the individuals who made the discovery The shear stress at the slab-column connections in flat plate systems varies in direct correlation with the changes in compressive strengths of the concrete. Research has demonstrated that the shear stress experienced at the connections between flat plate systems and columns of different shapes is not consistent. An augmentation in the compressive strength of concrete correlates with a rise in shear stress. M50 concrete exhibits a shear stress that is approximately 40% greater than that of M20 concrete. The shear stress for square columns is calculated to be 3.93 N/mm2. Upon comparing square and rectangular columns, it is shown that the shear stress is decreased by around 15% for the square columns. Connections located in the periphery and corners of an object undergo a higher magnitude of shear stress compared to connections situated in the central region [12].

In 2021, Abreha Abay et al. proposed that bundle reinforced concrete (BRC) columns are affected by lateral impact loads. This study employed explicit finite element (FE) analysis to numerically simulate the behavior of one reinforced concrete (RC) column. The column had a normal reinforcement distribution and was subjected to impact loads. Additionally, three separate bundles of reinforced concrete column specimens were investigated to see their response to these stresses. By examining the impact force-lateral deflection curves, we can determine how different impact velocities affect the horizontal displacement of BRC columns. At the failure point, Figure 2.9 shows the experimental test results that match to the failure modes seen during the Finite Element (FE) analysis. Both the experimental findings of the reinforced concrete (RC) column and the failure modes predicted by the nonlinear finite element (FE) analysis demonstrate a high degree of concordance. All things considered, the results show that the Abaqus/Explicit nonlinear finite element simulation is a good method for predicting how reinforced concrete columns would react to dynamic impact loads.

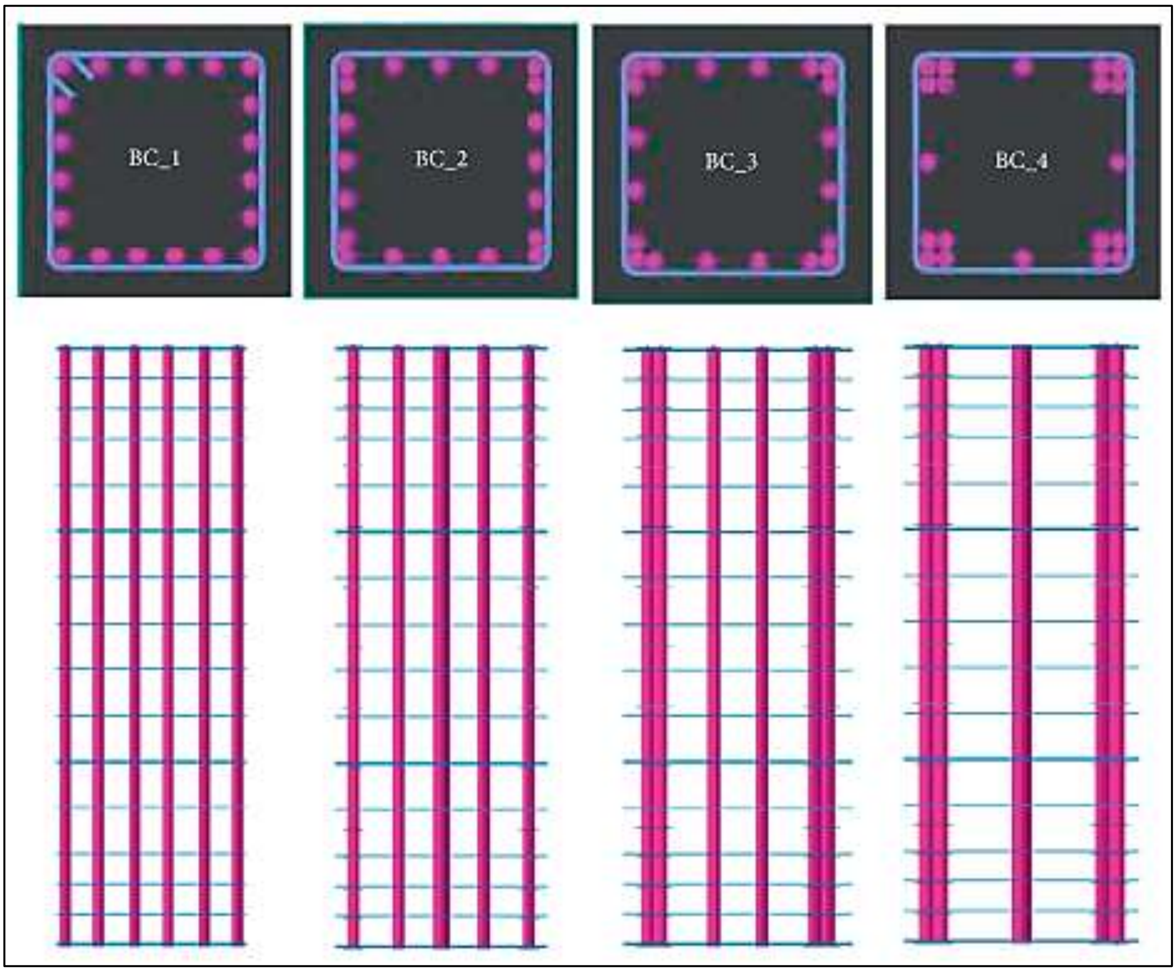

Figure 2.10: Cross-Sectional and Longitudinal BRC Column Specimen Detailin[13].

The findings of the previous experimental test on the same member align well with the lateral impact load response of the RC pier generated by the nonlinear FE analysis, indicating a significant agreement between the two. In general, it is appropriate for forecasting the impact response of the RC column, however there are some inconsistencies in the impact force-time history after reaching the highest value [13].

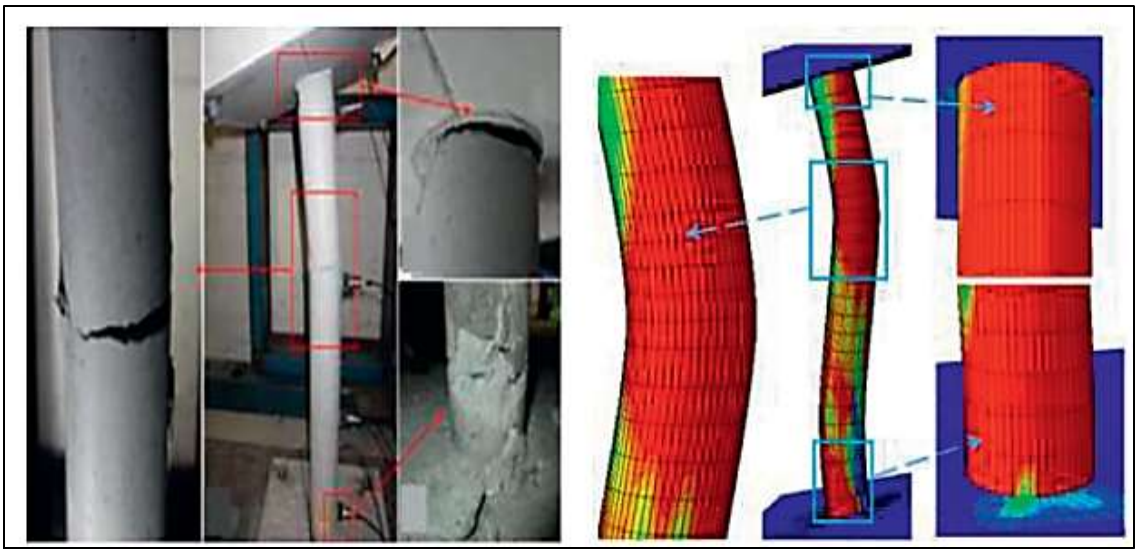

Figure 2.11: Comparison of Damage Modes at Failure[13].

In 2022, Tarikul Islam and his colleagues proposed the utilization of reinforced concrete (RC) jacketing as a method for strengthening columns. This method enhances the RC column's resistance to axial load, while simultaneously enhancing its ductility, stiffness, flexural capacity, and shear capacity. Prior research has demonstrated that RC jacketing is the predominant technique employed to enhance the lateral capacity of a column through composite action. This paper provides a quantitative examination of the sideways resistance of a one-story reinforced concrete frame with a single span, which has been enhanced by the addition of concrete jacketing. The study also includes an analysis of a single reinforced concrete column. Despite the column in the frame being represented by a single column, an examination of the reinforced concrete (RC) frame is still conducted to achieve a thorough comprehension. The shear capacity and ductility of reinforced concrete (RC) columns are significantly enhanced by utilizing fiber reinforced polymer (FRP) and steel jacketing. This also effectively eliminates bond failure. These benefits have been documented in several studies [1,6-8]. However, RC columns that have been reinforced with concrete jacketing demonstrate enhanced ductility, bending, and shear capabilities.

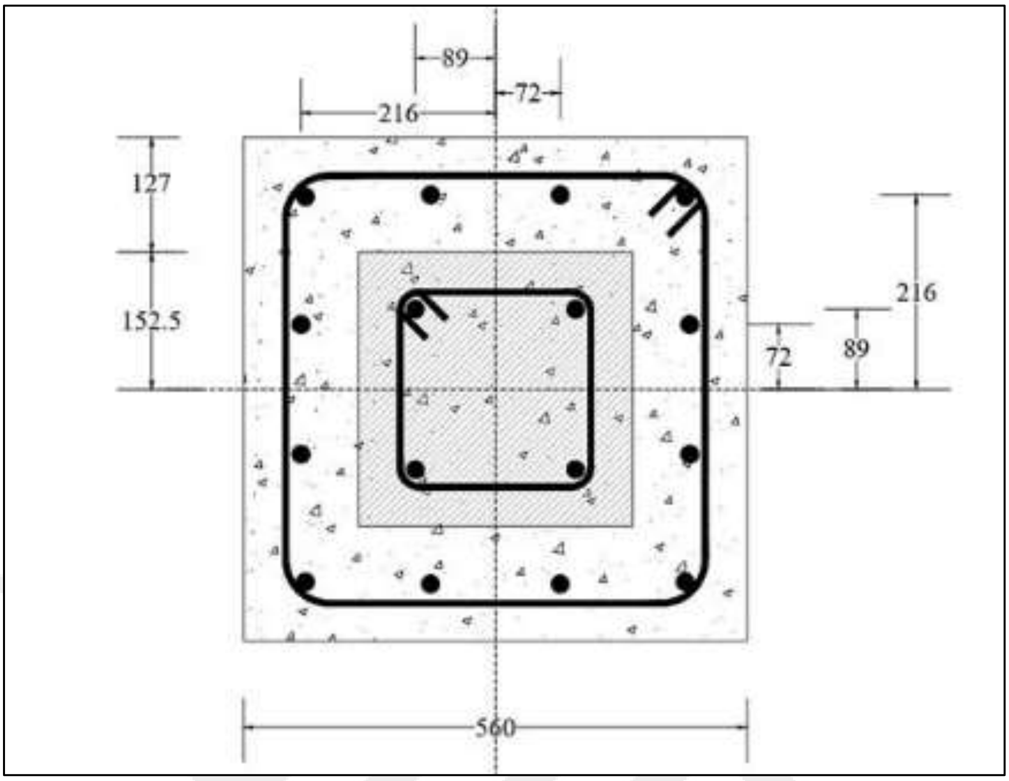

Figure 2.12: Cross-Section of The Retrofitted Column (unit: mm)[14].

The outcomes of the numerical analysis are as follows: The axial load carrying ability and flexural capacity of retrofitted columns are improved by increasing the compressive strength of the RC jacket and the yield strength of the longitudinal reinforcement. The axial compression and flexural capabilities of a jacketed column experience significant improvement as the percentage of reinforcement increases. The compressive strength of the jacket concrete does not impact the initial stiffness of the column when assessing the lateral capacity of retrofitted columns. However, when the ratio of reinforcing material increases, the initial stiffness likewise increases. Compared to the previous column, the average lateral capacity improves tenfold when utilizing a 1.6% reinforcement ratio and allowing for a maximum lateral drift of 2%. The average lateral capacity increases by a factor of thirteen in comparison to the original column when the reinforcement ratio is 2.6%. The study indicated that for lateral drifts ranging from 3 to 4%, there is an additional improvement in the normalized lateral capacity of the retrofitted column [14].

In 2022, Shengshan Pan et al. cast five reinforced concrete columns, specifically labeled as BP-01 through BP-05. All five columns were of the same dimensions and had the same level of reinforcing. This paper's research focuses on the cyclic behavior of bridge columns, using large-strain pre-stressed shape memory alloy (SMA) spirals as the active limiting element. These spirals may be conveniently stretched at room temperature and are stimulated by current. Five specimens underwent quasi-static experimental tests, which were designed and conducted with different improved parameters. The efficacy of utilizing high-strain pre-stressed SMA spirals to strengthen piers has been demonstrated. The hoop effect, facilitated by SMA spirals, effectively mitigated concrete crushing and delayed the progressive deterioration of the reinforcing bars resulting from repetitive cycle shocks. Considering the present exorbitant expense of SMA, a pragmatic approach could involve fortifying the column with FRP. This would additionally reduce the harm to the concrete at the plastic hinge of the column. A column that is reinforced with Shape Memory Alloy (SMA) spirals has significantly improved deformability and the ability to accumulate and dissipate energy. Figure 2.10 illustrates a column with a height of 1050 mm, a diameter of 300 mm, and a concrete cap of 18 mm. The dimensions of the base were 1400 × 600 x 500 mm. Based on the average shear span ratio obtained from the pseudo-static test, the effective shear span ratio was determined to be 3. Additionally, the lateral loading point was located at a distance of 900 mm from the bottom of the column, which corresponds to the effective shear span.

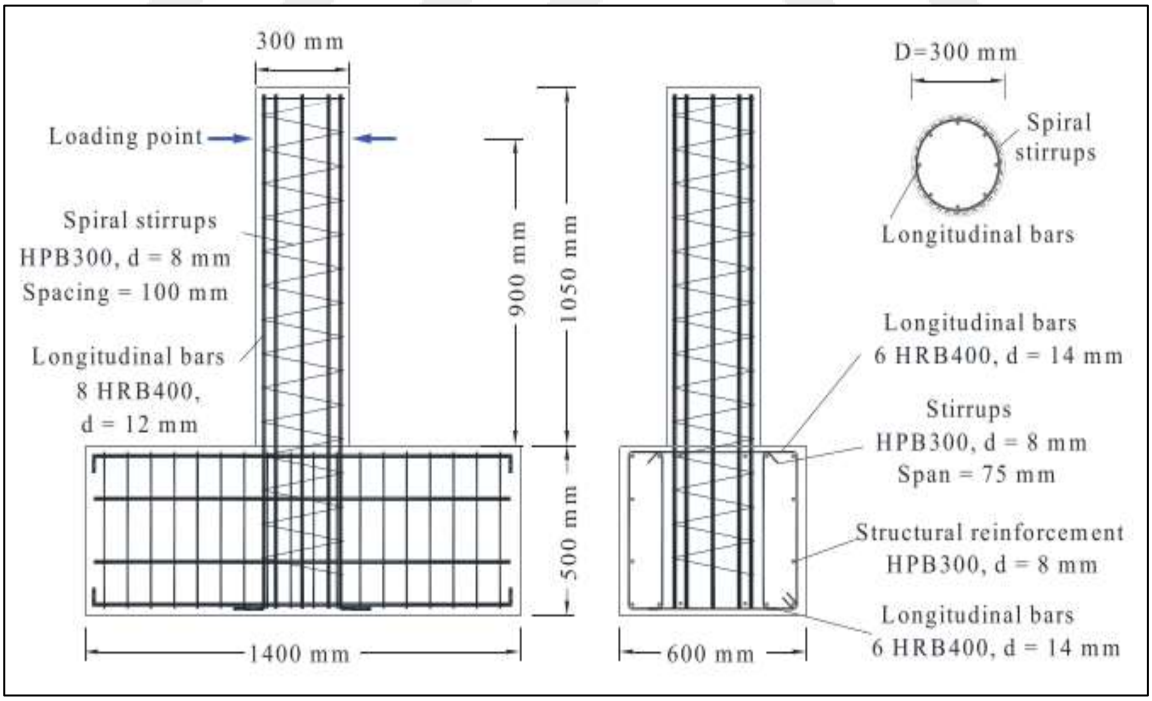

Figure 2.13: Dimensions and Reinforcement Details of Specimens (unit: mm)[15].

Specimens with a smaller wrapping space (SMA volumetric ratio) yield superior results as compared to specimens with wider spacing. The reinforced specimens exhibit superior performance in terms of strength deterioration and residual displacement compared to the as-built column. However, there is minimal disparity observed in the pitch spacing and wrapping height among the specimens. In addition, SMA spirals have minimal impact in reducing the lateral stiffness of columns. The potential result could be favorable. The structural stress remained rather stable due to the limited effect on the stiffness of the column, indicating a positive outlook for the preservation of other structural elements. The seismic behavior of columns with variable wrap heights remains mostly unchanged, provided that the range of SMA spirals includes the plastic hinge region of the column. In light of the failure mechanism, this research proposes a wrap height that exceeds the height of the plastic hinge zone. To achieve the best possible enhancement of the flexibility and ability to absorb energy in bridge columns, it is necessary to conduct additional research using numerical methods or experimental testing. However, it seems that there is an appropriate spacing for wrapping shape memory alloy (SMA) based on the observed patterns of deformability and cumulative energy dissipation. In addition, to accurately assess the seismic behavior of bridge piers reinforced with Shape Memory Alloy (SMA) jackets, it is imperative to carry out shaking table tests, nonlinear dynamic analysis, and quasi-static testing. These approaches are insufficient in capturing the dynamic characteristics of the restricted columns and ground movements [15].

This study compares the structural analysis results of seven steel building models symmetric, L-shaped asymmetric (3-, 10-, and 15-story), and a single-story industrial structure using StaSTEEL and SAP2000 software. At the time of the study, no literature using StaSTEEL was found. Results such as story weights, natural periods, and internal forces (axial, shear, moment) were compared. Both programs use the 2019 Turkish Seismic Code, and the differences in N, V, and M values were within 3.0%, 3.5%, and 2.7%, respectively. StaSTEEL was found more user-friendly and offered more detailed and visually rich reports [51].

Time is a crucial resource in construction project management, with delays significantly impacting project success. Human error is a leading cause of such delays, which occur when actual work exceeds planned schedules. Delays can lead to increased costs, lost productivity, and even contract termination, making them an inevitable challenge in construction. This study aims to identify and analyze the main causes of project delays through a literature review and consultation with key stakeholders contractors, developers, designers, and clients. The Relative Importance Index (RII), considering both severity and frequency, is used to determine the primary delay factors [52].

This study aims to examine the yearly developments in transportation from economic, technical, social, and political perspectives, highlighting its interdisciplinary nature. With advancements in information and technology, current transportation trends are analyzed in light of modern needs. The mutual relationship between transportation and urbanization is emphasized, recognizing transportation as a driver of societal progress. In this context, the development and ongoing investments in high-speed railways are also evaluated as part of future-oriented transportation strategies [53].

This study investigates the role of project management in achieving project success, focusing on three key objectives: (1) assessing the impact of feasibility studies, (2) examining managerial activities, and (3) evaluating the project manager's role. Using 100 surveys collected through practical sampling across various regions, the study analyzed managerial processes such as planning, staffing, collaboration, and control, alongside human resource management. Results indicate positive correlations between these factors and project success, supported by multiple regression and correlation analyses [54].

This study addresses challenges in adaptive façade construction in Iraq by identifying key economic, social, and technological factors using expert surveys and the Weighted Decision Matrix. Results show that factors like urbanization, facility usage, and equipment demand improve the Cost Performance Index (CPI). SPC charts help detect deviations, enabling timely corrective actions. The proposed model supports dynamic project monitoring and success prediction [55].

This study investigates the influence of soil properties on liquefaction during earthquakes, focusing on the Karakaya Dam area. Two approaches Excel extrapolation and linear regression optimization were applied. Findings predict a moderate temperature increase of 3–6°C over the next decade and a significant rise in Euphrates River discharge from 100–350 m^3 to 2,590–2,640 m^3 by 2029, both potentially affecting liquefaction risk. Soil temperature and chemical composition are expected to remain stable, except for a notable pH shift from 4.14 to 9.74. The dominant chemical species identified is the phosphite anion, with concentrations ranging between 1 and 2 μg/m² [56].

This study presents a case analysis comparing manual quantity surveying with BIM-based digital take-off using Revit for a selected construction project. Key elements such as steel, concrete, and architectural components were evaluated. Results show strong agreement between traditional estimation and BIM-based calculations, demonstrating that BIM offers a reliable and efficient solution for accurate cost estimation, especially in complex projects [57].

This study explores the use of Statistical Process Control (SPC) charts for monitoring water resource projects, focusing on dam construction. Traditional SPC methods often fall short in real-time applications due to the complexity of water systems. To address this, an AI-based SPC framework is proposed, integrating machine learning for anomaly detection and performance prediction. Applied to a dam project case study, the framework outperforms traditional SPC in accuracy, efficiency, and responsiveness. The results highlight its potential to enhance project management and support the sustainable operation of water infrastructure [58].

This study explores the use of Building Information Modeling (BIM) for clash detection in the design phase of a 24-classroom school building. In Iraq, most government projects still rely on 2D CAD, leading to coordination issues among disciplines. By integrating architectural and structural BIM models using Autodesk Revit and Navisworks Manage, hard clashes (element overlaps) were identified and resolved, demonstrating BIM's effectiveness in improving design coordination before construction begins [59].

This study investigates the thermal performance of composite walls with added insulation layers across four climatic regions in Iraq. U-value calculations, based on material properties and indoor/outdoor temperatures, assess heat transfer through wall elements. While composite walls offer advantages in durability, efficiency, and worker safety, thermal bridging remains a challenge. Statistical analysis highlights the impact of regional climate on heat load and the varying effectiveness of insulation materials in enhancing energy performance toward nZEB standards [60].

This study evaluates two five-story residential buildings using experimental material data and soil parameters. Nonlinear analyses (AEDY and AMBY) based on DBYBHY2007 were performed in Sta4CAD. Each building was retrofitted with jacketing and shear walls, improving performance to life safety levels. Retrofitting methods were compared [61].

This paper investigates soil improvement techniques for soft clay using geogrids and stone columns through numerical analysis with PLAXIS 3D. Due to low shear strength and instability, reinforcement was applied to enhance soil behavior. Results show geogrids have limited effect on horizontal and vertical displacements but significantly improve the safety factor. Stone columns, especially when combined with geogrid reinforcement and subjected to a 50 kPa traffic load, effectively reduce settlement, increase bearing capacity, and shorten consolidation time. The finite element model indicates up to a 50% improvement in soil performance during construction [62].

3. RESEARCH METHODOLOGY

3.1 INTRODUCTION

Columns are the primary means of support for reinforced concrete structures, as they hold the full weight of the building. The integration of rectangular columns into a structure may have possible aesthetic drawbacks due to the columns' protrusion from the walls and angles. One potential resolution to this matter has been identified, namely the implementation of columns specifically tailored for concrete constructions. Columns with unique configurations are effective for both structural and aesthetic objectives. To address the impact of wind, adjustments were made to the scale geometry of the columns by incorporating setbacks and tapering. Additionally, architectural remedies were taken into account in some cases. Most of the lateral loads are categorized as live loads, with the main force acting on the structure being horizontal. Frequent occurrences of lateral loads include seismic activity, wind, ground pressure exerted on retaining walls along the beach, and the weight of the earth acting on foundation walls. Lateral forces are defined as the force that is applied to a structure parallel to its horizontal axis. The above listed phenomena may encompass wind, seismic activity, and soil pressure. Inadequate resistance in the structural design can lead to substantial harm or total collapse. Moment resistant frames are composed of columns and pillars that endure lateral stresses as a result of the inflexible connections between the columns and pillars and the bending of their components. The given result is determined by dividing the effective length by the marginal lateral dimension of the column, namely the dimension that is perpendicular to the bending axis. When designing a column capable of withstanding lateral forces, it is imperative to consider two essential factors: the geometry of the column and the specifications of the materials used. The technique of the research given in this chapter will incorporate the integration of these two parts.

3.2 MATERIAL PROPERTIES

The physical, molecular, and mechanical qualities of a product are considered material attributes, which determine its value and suitability for large-scale manufacture. The subsequent determination of function is contingent upon the qualities of the materials employed in its construction. In the creation of concrete and bituminous materials, sand and gravel are commonly employed as coarse and fine aggregates, respectively. Additionally, they find application in the construction of roadways, serving as fill, base, and top layers. In addition to mill refuse and cement, they are employed as backfill in the mining industry. Many vocations associated to concrete necessitate the use of river sediment. Furthermore, they have the ability to execute a wide range of block configurations. The sand exhibits a higher degree of uniformity in terms of particle texture and granule size distribution. Only a small amount of water is enough to support the river and dunes.

3.2.1 Fine Aggregate

Medium size sand from Euphrates river with a modulus of fineness = 2.20 [46]; normal grading with the silt content 0.8%, Specific gravity 2.677 [50].

3.2.2 Coarse Aggregate

Crush gravel with a size of 5-20 mm and normal continuous grading was used. The crushing index d"6% and the specific gravity 2.738 [47].

3.2.3 The Used Water

The quantity of water in concrete determines its workability, compressive strengths, permeability and watertightness, durability and weathering, drying shrinkage and potential cracking.

3.3 PROPERTIES OF CONCRETE MIXTURE

Despite the comparatively high compressive strength of concrete, its tensile strength is significantly reduced. Consequently, concrete has the ability to undergo compression without experiencing breaking. The mixture maintains the physical and chemical qualities of each constituent. Furthermore, the process of isolating specific constituents within a mixture is generally not arduous. Ultimately, the ratios of the constituents differ across the composition. The concrete created by mix design incorporates a range of desirable attributes, such as workability, durability, setting time, strength, and impermeability. The design processing takes into account crucial parameters such as the water-cement ratio and aggregate gradation. Concrete with a C30 designation has an average strength of 30 MPa, equivalent to roughly 4350 psi, after a 28-day curing period. This specific grade of concrete with a moderate strength is commonly utilized in the construction of floors, driveways, and commercial constructions of light to medium strength. In order to conduct this experiment, the column was constructed using C30 concrete. It was meant to incorporate the elements indicated in Table 3.1.

Table 3.1: Mixing Design.

	material	Quantity (kg)
1	Cement (kg)	310
2	River sand (kg)	605
3	Gravel (kg)	1220
4	Water in liters (W/C: 0/55%)	0.55

The water-to-cement ratio in both combinations was calculated to be 0.55% by weight based on the characteristics of the different ingredients. The selection of the most suitable cement type is contingent upon the particular task being undertaken. Before proceeding, it is crucial to evaluate the projected performance of cement in the design blend. Kubaisa cement, sourced from the western part of Iraq, was utilized in the project. This item adheres to the standards set by ASTM C 494 and is made up of a Type A superplasticizer. There is a general consensus that the concentration of cement does not have a major effect on strength until a certain ratio of cement to aggregate is reached. When the concentration of cement drops below the minimum required level to make concrete with adequate strength, it becomes necessary to add more cement (American Society of Concrete Contractors, 2005). These tests demonstrate a link between the concentration of cement and its strength, which is in contradiction to the Abrams principle. The strength of a material at a certain age is determined by the degree of hydration of cementitious components and the cement-to-water ratio (W/C). These variables have an impact on both the porosity of the cement paste and the interfacial transition zone between the coarse aggregate and the cement paste. since the temperature of the moist bulb increases, it is advisable to decrease the water content since it leads to a loss in strength and an increase in capillary porosity. Furthermore, there will be a decrease in the water-to-cement ratio.

3.4 PRODUCTION SAMPLES

The production of a fluid slurry involves the amalgamation of Portland cement, water, and aggregate, resulting in a highly malleable and malleable substance. Concrete hydration is a chemical reaction involving cement that necessitates a protracted duration for the concrete components to harden into a stone-like consistency. During this time frame, a wide range of premade tools and procedures can be produced, in addition to the ability to pour concrete into molds. Before pouring concrete, the mixture is strengthened by adding reinforcing materials, such as steel rebar, to enhance its tensile strength. This technology facilitates the production of reinforced concrete.In order to conduct a comprehensive experiment including a wide range of fracture velocities, it was necessary for the specimen design to effectively support the interaction between reflected stress waves and the crack site during its rapid propagation. The specimens chosen for the model, as seen in Figure 3.2, comprise cubes with dimensions of 15 cm by 15 cm by 15 cm, cylinders with dimensions of 200 cm by 100 cm, and blocks with dimensions of 100 cm by 100 cm by 500 cm.

Figure 3.1: Project Samples.

To initiate the process, the dehydrated constituents, namely sand, gravel, cement, and additives, are subjected to rotation within a mixer until they are fully integrated. The fusion of all the elements resulted in the formation of a solid mass. The casting slurry is prepared by carefully including water into the mixture, which is subsequently followed by the addition of fibers. In order to mitigate the adhesion and separation of the concrete sample, a substantial amount of oil was applied to the mold.

Figure 3.2: Oiling The Molds.

An exact amount of sediment is evenly dispersed. Before being evenly distributed, the sand and cement are mixed together in the appropriate ratios. The sand and cement ought to be amalgamated using a shovel until the resulting mixture exhibits a homogeneous hue and lacks any anomalies.In order to generate newly poured, high-quality concrete, it is imperative to meticulously amalgamate the constituent elements. The blending process results in the coating of aggregate particles due to the presence of the cement component. Accurate mixing is crucial for ensuring the workability and proper functionality of concrete in both its fresh and hardened forms. Inadequately mixed concrete often experiences bleeding and segregation. Prior to commencing the process of amalgamating the constituents to generate a homogeneous aggregate, ascertain the precise quantity of each individual component. The qualities of the substance undergo modifications when it is combined with other compounds, although limited research has been conducted to investigate the impact of varying amounts and components on performance. The panel was produced by compressing the prepared slurry into the mold using a vibrating machine. An accurate rod leveler was used to level the spaces between the three layers of regular concrete that were poured into a steel fiber cylinder mold. Vibrations were used to carefully eliminate the air bubble from the surface of the specimen. It is advisable to produce three samples for each of the three scenarios in order to obtain precise measurements of the modulus of elasticity, tensile strength, and compressive strength of the material. A vibrating device is utilized to externally induce vibrations in the timbers during the process of filling the hole with concrete.

Figure 3.3: Casting Process.

The moisture content of pottery, wood, soil, or rock can be estimated by comparing the weights of two samples that were obtained at different time intervals. The scientific and technological applications of the water content of a substance, defined as the ratio of zero (totally dry) to the porosity of the substance during saturation, are many.

3.5 TESTS FOR CONCRETE PROPERTIES

3.5.1 Compressive Strength Test

One methodology for evaluating the overall quality of concrete entails the analysis of its compressive strength. The strength of concrete is directly influenced by the structure of the hydrated cement mortar. The determination of the compressive strength of concrete specimens can be achieved through the utilization of this test. The compressive strengths of cube specimens were determined at 7 and 28 days, using the guidelines described in BS 1881: Part 103: 1983. These procedures are employed to accurately measure the kjk compressive capabilities of concrete cylinders. Following the preparation and placement of the sample at the central location of the apparatus, it is subsequently exposed to a compressive axial force until it undergoes rupture.

Figure 3.4: Compressive Test Machine.

3.5.2 Splitting Test

The process of determining the tensile strength of concrete through the utilization of the split tensile test is a more intricate procedure. In this experiment, a radial force is exerted on the surface of a cylindrical object as it is overturned onto its side. The objective of this experiment is to induce a vertical fracture that spans the entire diameter of the specimen.The compressive strength of the concrete used in building construction can have a substantial impact on the probability of fracture. Moreover, concrete is extremely susceptible to strain because of its inherent fragility. Consequently, it is quite improbable to resist the stress. Fracture of concrete occurs when the applied tensile stresses surpass the tensile strength of the material. The determination of the strain at which concrete elements may fail can be achieved by utilizing their tensile strength. A different approach to evaluating the tensile strength of concrete entails the fracture of a cylindrical sample of the material being analyzed.This rule conforms to the ASTM C496 (Standard Test Method of Cylindrical Concrete Specimen) standard, which is based on IS 5816 1999. The subsequent sections will provide a comprehensive description of the split cylinder test conducted on a concrete specimen

Figure 3.5: Splitting Test Machine**.**

3.5.3 Flexural Test Machine

The measurement acquired from the flexural test yielded a specific outcome. It is easier to determine the average deformation between two opposing sites when longitudinal tensions are supplied using either a bonded or unbonded sensor. During the failure stage, the compression zone concrete underwent pulverization, resulting in the failure of all tested columns in flexure due to the occurrence of flexural cracks. In the region of maximal bending moment, which is located between the two point loads, the first observable fractures became apparent. It can be shown from the load deflection curve that specimens consisting of copper slag-reinforced concrete demonstrate improved resistance to external forces. The energy absorption of these columns was evaluated by analyzing the area under the load versus deflection curves when assessing flexure failure. The results of the study revealed that columns including copper slag shown enhanced capabilities in absorbing energy. Their ductility may be responsible for the increase in energy absorption by the columns.

Figure 3.6: Flexural Test Machine.

Figure 3.7: Results of Flexural Samples Test.

Additional information regarding fracture patterns and failure modes was gathered once the machine had reached its maximum capacity, prior to the machine being deactivated and the crane being removed. After the radius of failure has been calculated and the sample has been photographed, a fresh sample is introduced into the testing apparatus.

3.6 BUILDING THE MODES

The ANSYS program can be used to construct the model by employing well-defined geometric primitives such as volumes, areas, and lines. Once a primordial is created, the application will automatically generate all connected "lower" entities. Both bottom-up and top-down modeling methodologies can be integrated into a logical model. However, the approach of developing the model "from the top down" involves an initial emphasis on "higher" primitive elements. Differentiating between bottom-up techniques, which are defined based on the current coordinate system, and geometric primitives, which are constructed on the working plane, is of utmost importance. If the organization employs blending techniques, it may contemplate implementing a directive to guarantee that the coordinate system aligns with the operational plane.

Before performing data analysis, the user must furnish the IGS files with the device's dimensions. This methodology allows for the easy generation of complex mathematical entities, such as composite components, volumes, and areas, by assembling a panel consisting of several points and lines. The samples provided above demonstrate a restricted array of possible choices. The occurrence of panel formation necessitates the presence of this particular panel. The process of creating a model in SolidWorks often begins with the creation of a two-dimensional representation. The image's remaining components were constructed with basic geometric shapes, including points, curves, lines, and conics. The process of constructing a SolidWorks model involves the following steps:

Before initiating the panel creation process in SolidWorks, it is necessary for the user to select a (Part Format) that aligns with the intended panel type. The significance of panel form design was emphasized by the researcher through the utilization of many panel forms, each demonstrating a unique level of reduction.

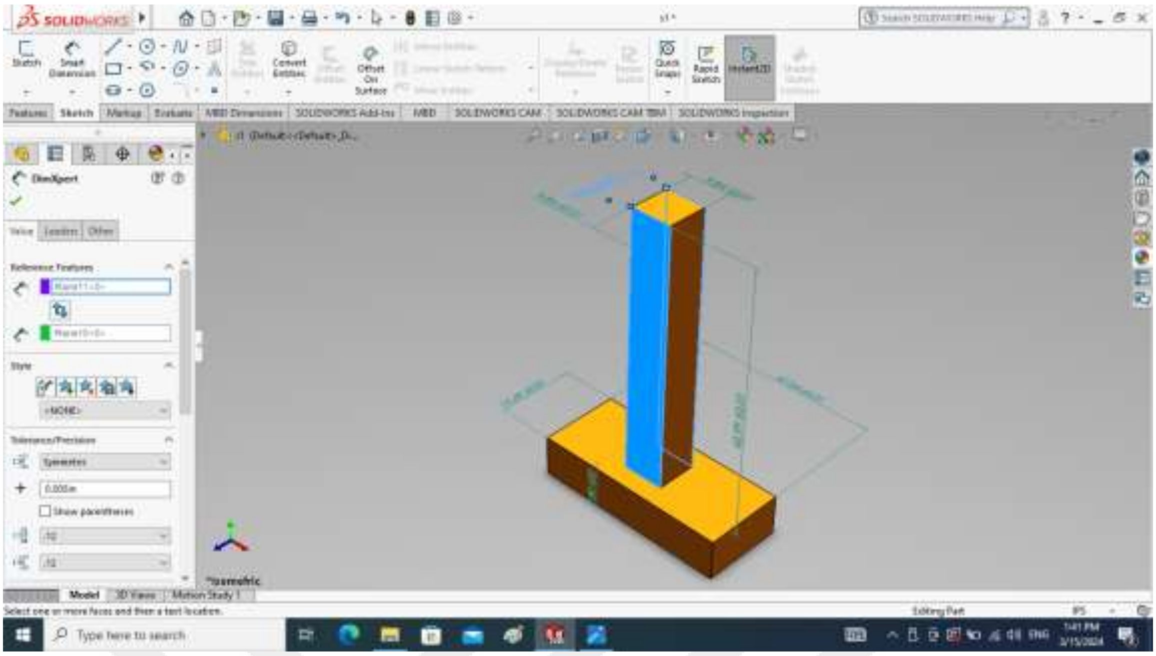

Figure 3.8: The Dimensions of The Validation Case Using SolidWork.

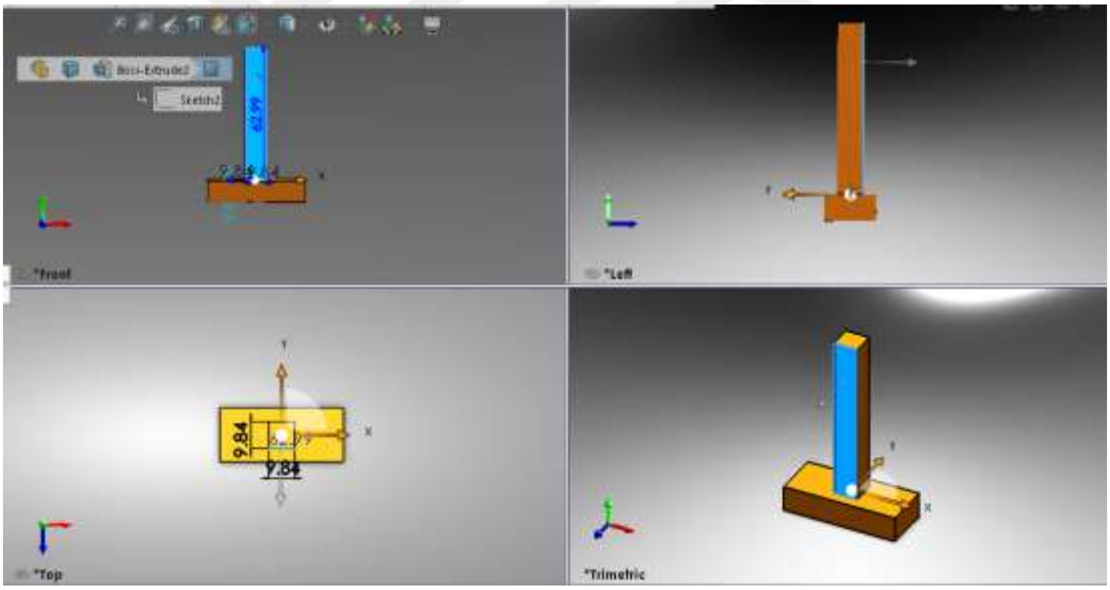

Figure 3.9: The Dimensions of The First Case Using SolidWork.

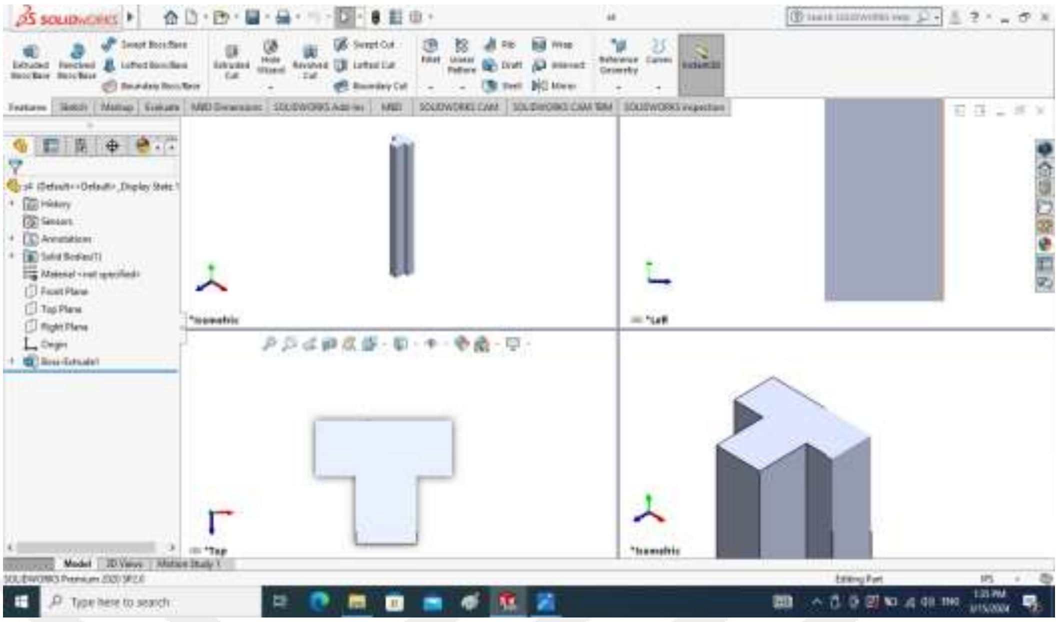

Figure 3.10: THE Dimensions of The Second Case Using SolidWork.

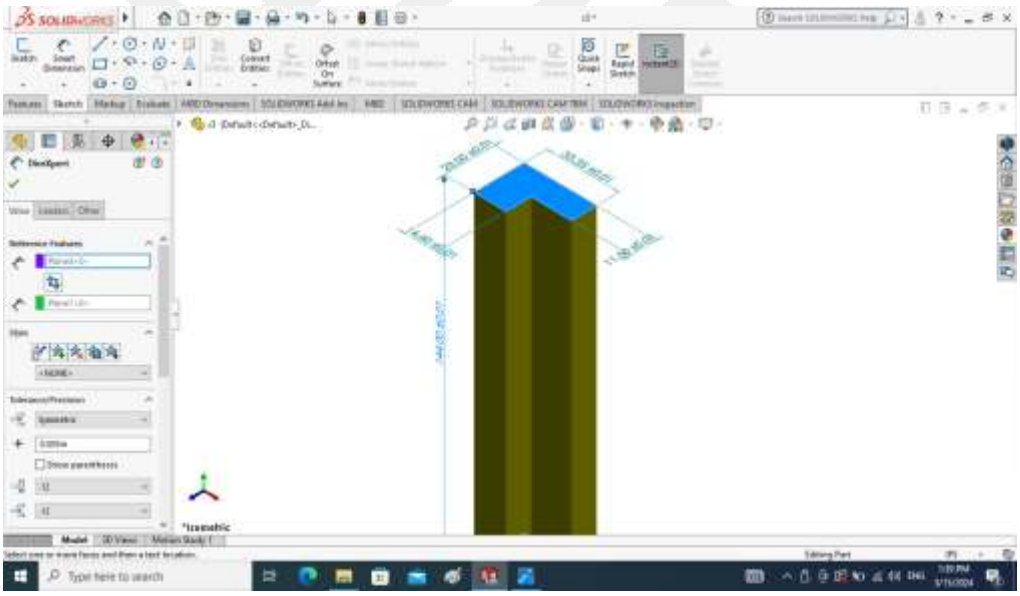

Figure 3.11: The Dimensions of The Third Case Using SolidWork.

In the subsequent step, the data acquired during the initial phase will be imported using one of the various import tools offered by the SolidWorks software. The successful completion of the current project necessitates the execution of two crucial procedures: inputting the precise measurements of the panel component into the SolidWorks program. The correlations among the various components of the section exhibit a proportional relationship with the magnitude of the curve.

The first phase of the modeling process involves examining the panel's reaction to various forces by employing its constituent elements, which are determined from its geometric properties. The responses will be analyzed using modeling software.

After the conclusion of the calculation, it is imperative to save the file with the IGS extension appended.

3.7 ANSYS PRE-PROCESS

In order to get the desired result, the parameters were determined by configuring the model and then performing a numerical calculation on the model database. The purpose was to integrate the material model into the ANSYS file. Any approach used to improve or assess a process must be based on accurate information about the characteristics of the material. The expenses related to exploratory research might be significantly impacted by the characteristics and extent of the inquiry. When performing preliminary research, it is crucial to prioritize the utilization of consistent data sources to create limitations and objectives. Following this, we will now proceed to study the following sector. In order to proceed with further analysis with a panel model, it is imperative to establish the characteristics of the panel and any extra attributes of its constituent elements. Erroneous forecasts produced during the modeling stage would make that stage ineffectual. This document provides a comprehensive description of the procedures involved in the utilization of ANSYS.

Before commencing the task, it is imperative to verify that all items are appropriately positioned. The response of the chosen model to various external stimuli is contingent upon the three vectors that constitute the model. At this stage of the production process, it is postulated that the panel consists of a predetermined amount of steel to preserve its worth. We began our investigation assuming that the material we sampled was steel that was structurally stable.

Table 3.1 presents a comprehensive summary of the transmission coefficients, compressive values, and tensile stresses pertaining to several solid panel materials. Within this particular framework, variables encompass transmission parameters, tension stress, and compressive values, among various other elements.

Table 3.2: The Input Representation of ANSYS Data [48,49].

MECHANICAL PROPERTIES	SYMBOL	STEEL
Young's modulus (GPa)	E	207.0
Shear modulus (GPa)	G	80.0
Poisson's ratio	v	0.3
Density (kg/m^3)	ρ	7600
Yield strength (MPa)	S_y	370
Shear strength (MPa)	S_x	370

The effectiveness of the study relies on the user's capacity to accurately determine the suitable geometry and element type for the model in relation to the "real object," as well as the proper working of the model's simplifications. Furthermore, the outcome of the research is contingent upon the user's level of proficiency. The expected level of output arising from the inquiry will depend on the conclusion of the probe. The process of developing the model involves incorporating it into the broader system, going beyond the initial preprocessing phase. This ensures the comprehensive development of the complete model. Individuals have the capability to create a three-dimensional digital representation of the component being evaluated by employing the graphics application that is embedded within the processor. The aforementioned capacity is facilitated by the inbuilt graphics processing unit (GPU) of the central processor unit (CPU). In the context of data entry, the term "deck" is commonly used to refer to the input file that contains perforated cards. This document incorporates data acquired from diverse sources, including the pre-geometrical processor. The incorporation of limitations inside the model is crucial as they function to limit the movement of particular nodes. Furthermore, it is imperative that the material employed in the building of the model has specific physical or mechanical characteristics. The researcher has the ability to modify the input file in order to include the study methodology and expected outcomes (results). Subsequent to the registration process, the gathered data is transmitted to the designated department tasked with conducting the evaluations. An input file pre-processor is unnecessary when the model itself is sufficiently simple. This phenomenon can be attributed to the potential absence of necessity for such actions. The preprocessor possesses the capacity to extract geometric data from the computer-aided design (CAD) program when needed. This feature is exclusively relevant in particular situations. The following information offers a thorough explanation of the essential activities that must be completed in order to implement the proposed strategy.

3.8 DEVELOPING GEOMETRY

Before evaluating the pavement model, it is imperative to thoroughly characterize the concrete and any other constituent elements. An essential requirement for the process of modeling is the assurance of precise results that correctly depict the intrinsic characteristics of the model. Below are comprehensive instructions on how to effectively utilize ANSYS. Prefabricating structural frameworks is a necessary requirement for the placement of concrete pavements.

The susceptibility of this position to displacement by external forces, commonly referred to as degrees of freedom, is attributed to its limited internal mobility. Furthermore, through the analysis of degrees of freedom, it is possible to determine the transmission of forces and the occurrence of delays among various components. The initial stage of model construction involves the delineation of the constituent elements and their corresponding physical interconnections. The accuracy of the geometries generated by ANSYS is contingent upon the quantity of nodes, which symbolize coordinate points inside a designated area where the degrees of freedom (DOF) are ascertained. Nevertheless, the next part provides a full examination of the fundamental elements of finite element analysis. The term "degree-of-freedom relationship" refers to the mathematical expression that represents the correlation between the degrees of freedom of two separate components. There is a wide variety of component sizes and shapes available. Examples of unique components that constitute the system include annotations such as trusses, plates in two or three dimensions, masonry, or tetrahedral constructions. The proper completion of the ongoing inquiry necessitates the utilization of numerous specialist components. The ANSYS application offers a wide range of options for constructing models.

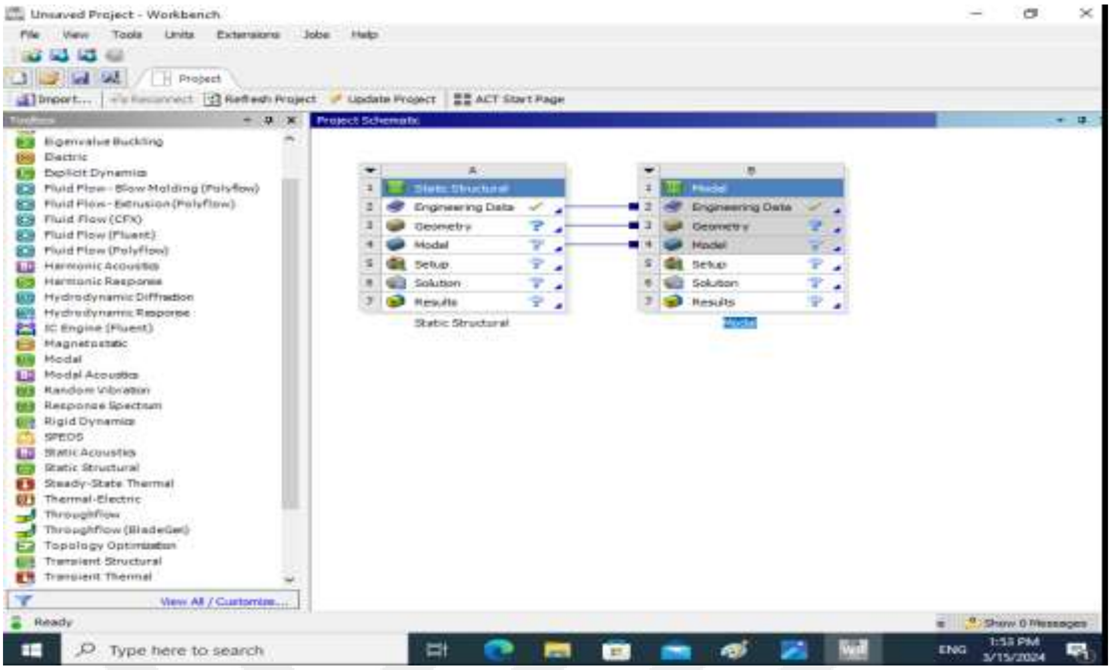

Figure 3.12: ANSYS Data Specification, This figure Illustrates the Project Schematic Window in ANSYS Workbench, Showing how Different Analysis Systems are Organized and Interconnected.

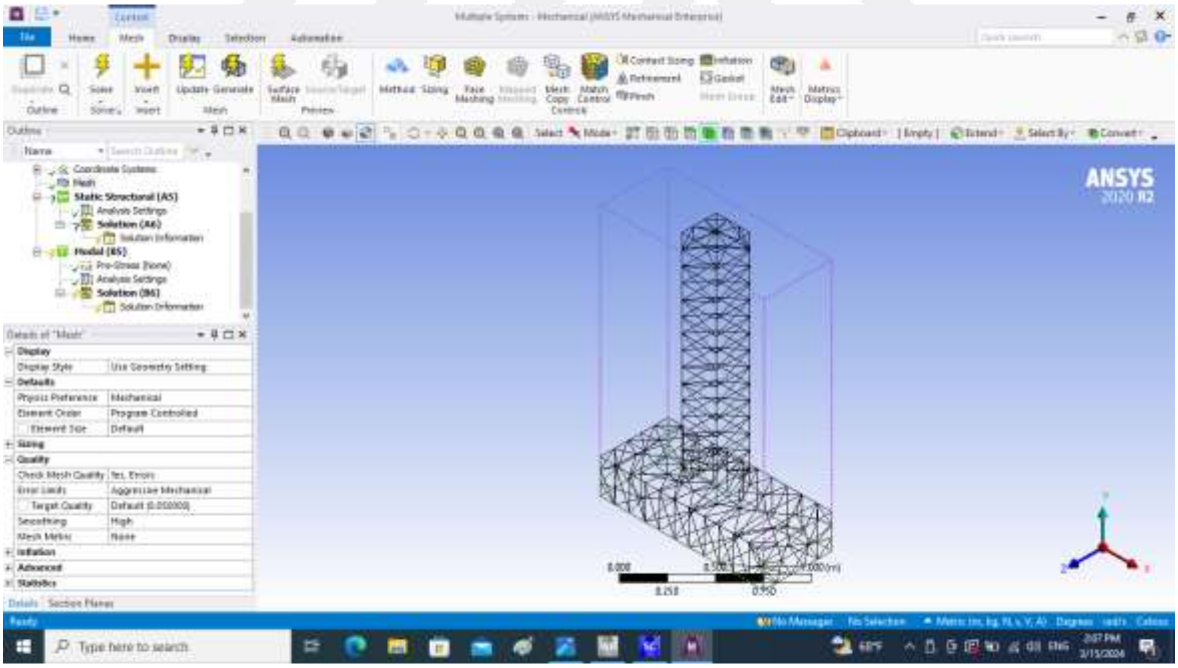

Figure 3.13: ANSYS Input Validation Case.

This Figure Displays the Meshing stage of a Finite Element Model in ANSYS 2020 R2, Specifically for an Input Validation case. The Geometry Appears to be a Vertical Structural Component with a base, Possibly Representing a Simplified Structure Like a Column on a Foundation or Support Block.

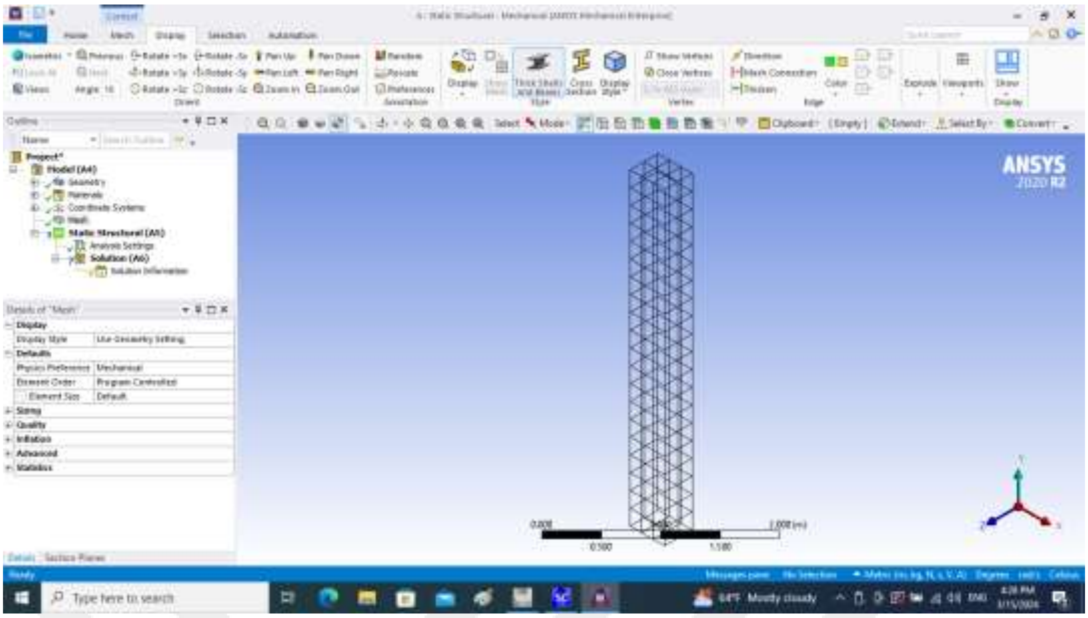

Figure 3.14: The First Case.

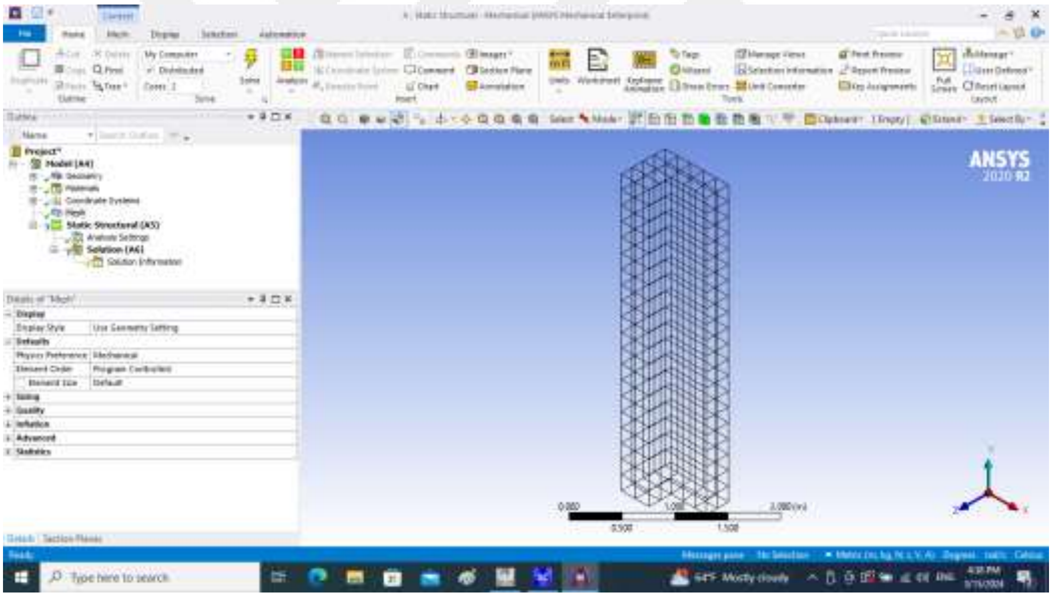

Figure 3.15: The Second Case.

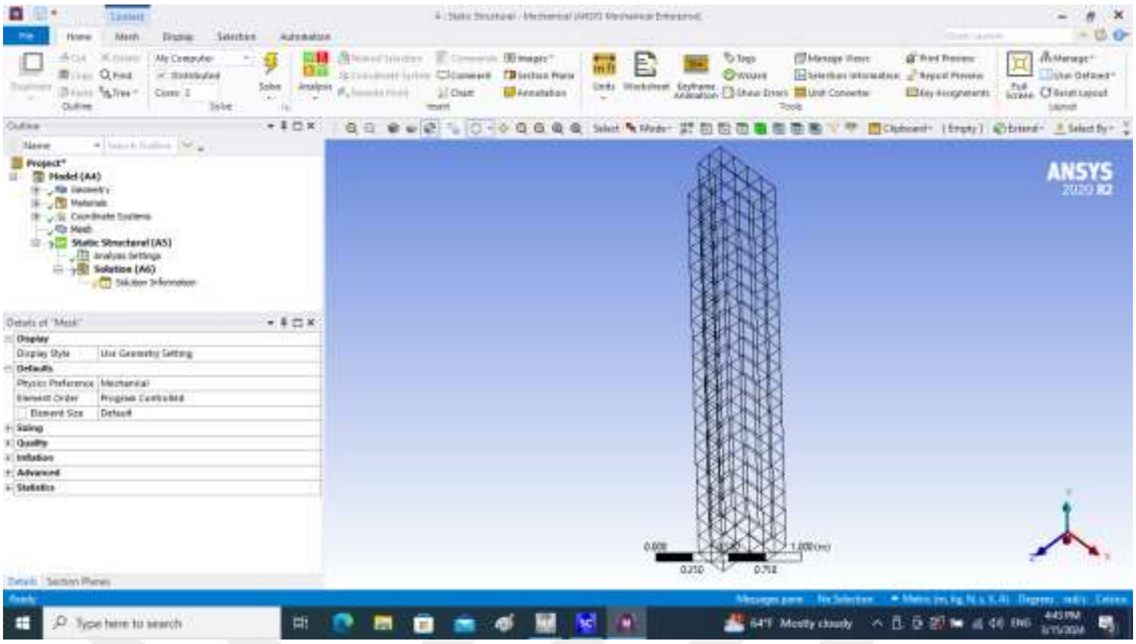

Figure 3.16: The Third Case.

To obtain realistic and precise outcomes from the ANSYS model, it is necessary to incorporate concrete, rebar, and other readily identifiable elements. Consequently, this could prompt further investigation into the framework. The evaluation of concrete behavior under various stress conditions can be achieved by manipulating the quantities of concrete features. The process of importing the functional model into ANSYS is time-consuming.

3.9 MESHING PROCESS

Constructing a theoretical framework of the material and acquiring knowledge about its characteristics constitutes the initial stage in attaining comprehensive comprehension. The essential characteristics of a substance can be deduced from its demonstration of traits that are commonly observed in materials with moderate strength. In order to provide a formal account of the matter: The material under consideration is concrete, which is composed of Portland cement.

The subsequent step in the sequence involves the development of a mesh.

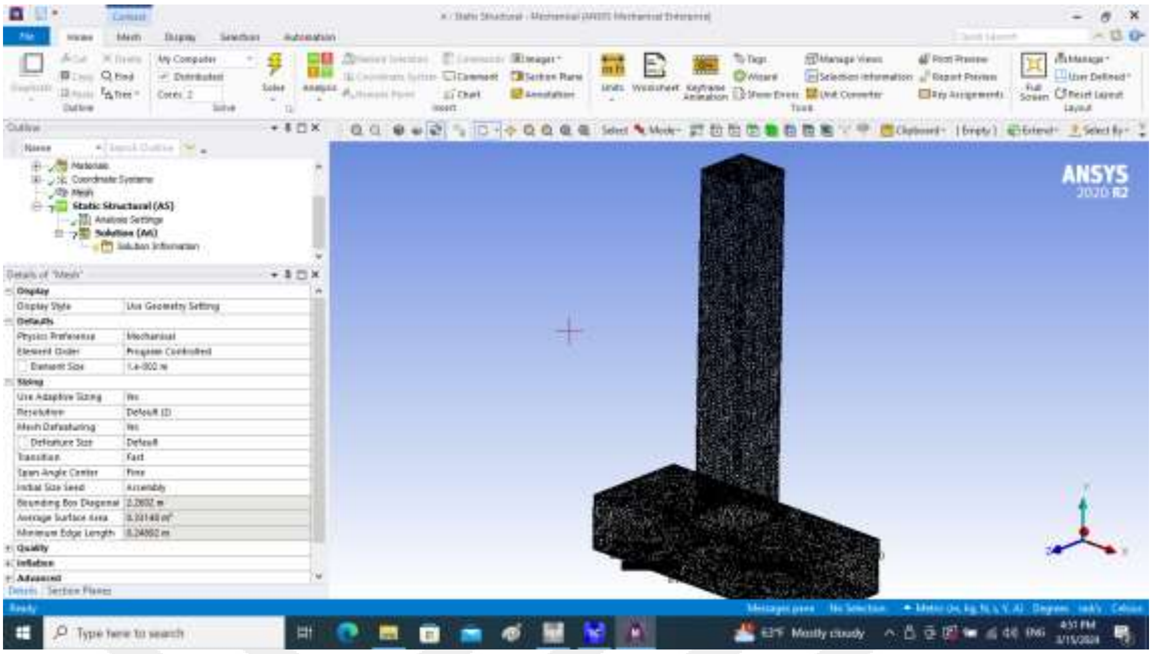

Figure 3.17: Mesh Process for The Validation Case.

Ansys provides users with a wide range of choices to tailor the shape to their own needs. In the Main Menu, the ANSYS Mesh Tool may be found in the Preprocessor area. This tool offers quick accessibility to a variety of commonly utilized mesh settings and workflows. The tool enables users to seamlessly switch between several settings with a single touch. Subsequently, it is important to incorporate the framework. It is crucial to use ANSYS Meshing to create a computational grid in order to do a thorough structural analysis of the complete concrete sidewalk. Optimizing the quality of both individual and collective meshes is crucial when creating a mesh structure from its component pieces. The Mesh Tool is an essential component of a diverse toolbox, used in PREP7 from beginning to end. By following the recommendations offered and adjusting the ANSYS parameters, it is feasible to attain similar results without utilizing the Mesh Tool. Nevertheless, it is evident that use the tool is the most expedient alternative. The capabilities of the Mesh Tool can be increased in two ways by adjusting the parameters of the geometry and examining the subsequent effects.

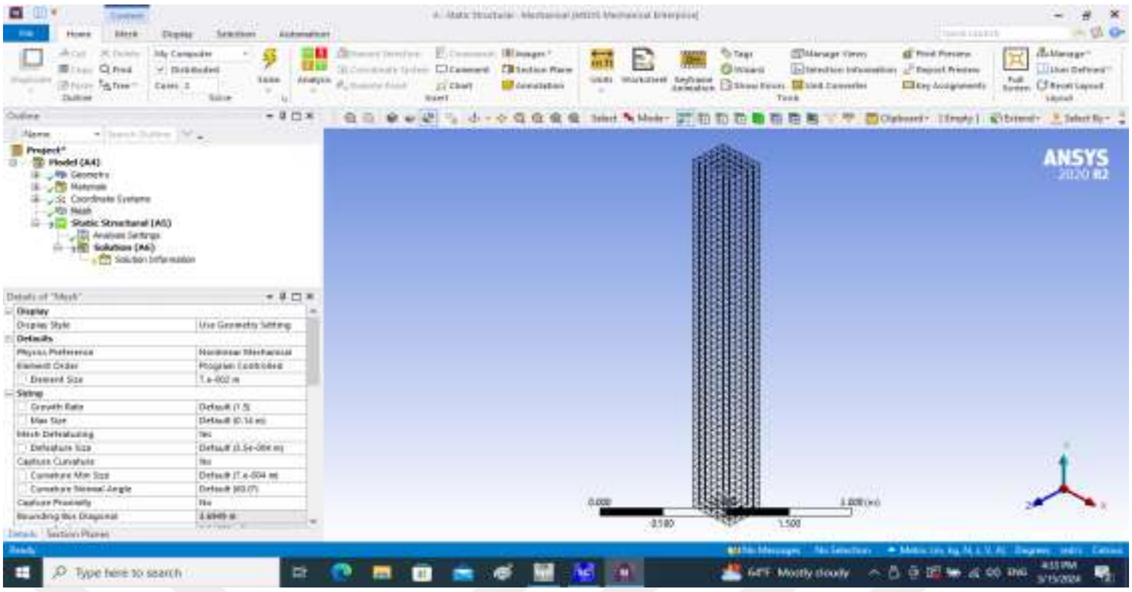

Figure 3.18: Mesh Process for The First Case.

This image shows the meshing stage of a finite element analysis (FEA) process in ANSYS 2020 R2 for a structural model. The structure, likely a column or beam-like component, has been discretized into smaller finite elements, which is a crucial step before performing simulations such as stress, deformation, or thermal analysis.

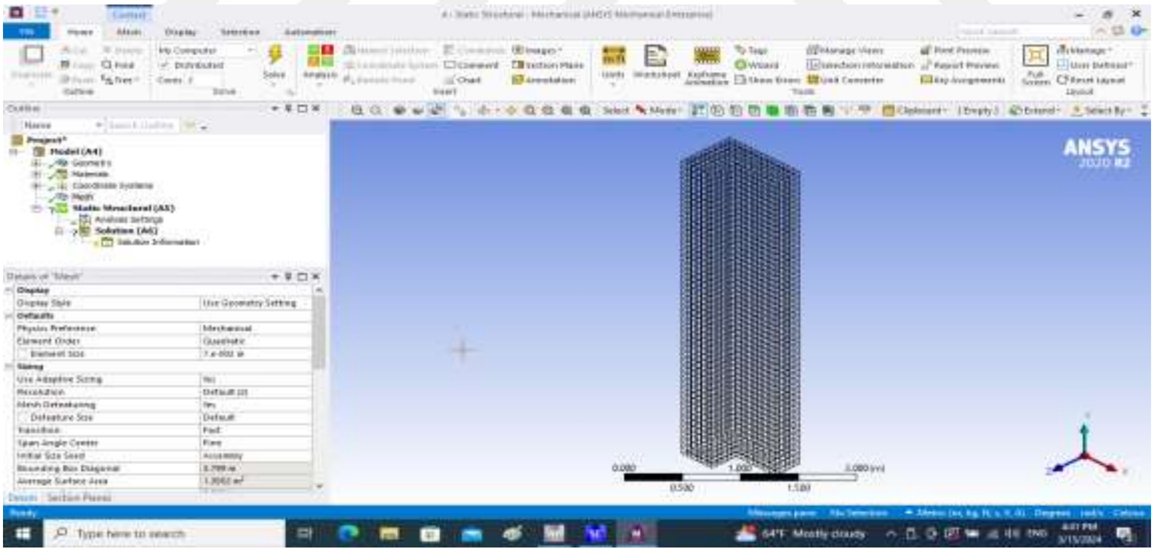

Figure 3.19: MESH process for The Second Case.

This image shows the meshing stage of a finite element analysis (FEA) process in ANSYS 2020 R2 for a structural model. The structure, likely a column or beam-like component, has been discretized into smaller finite elements, which is a crucial step before performing simulations such as stress, deformation, or thermal analysis.

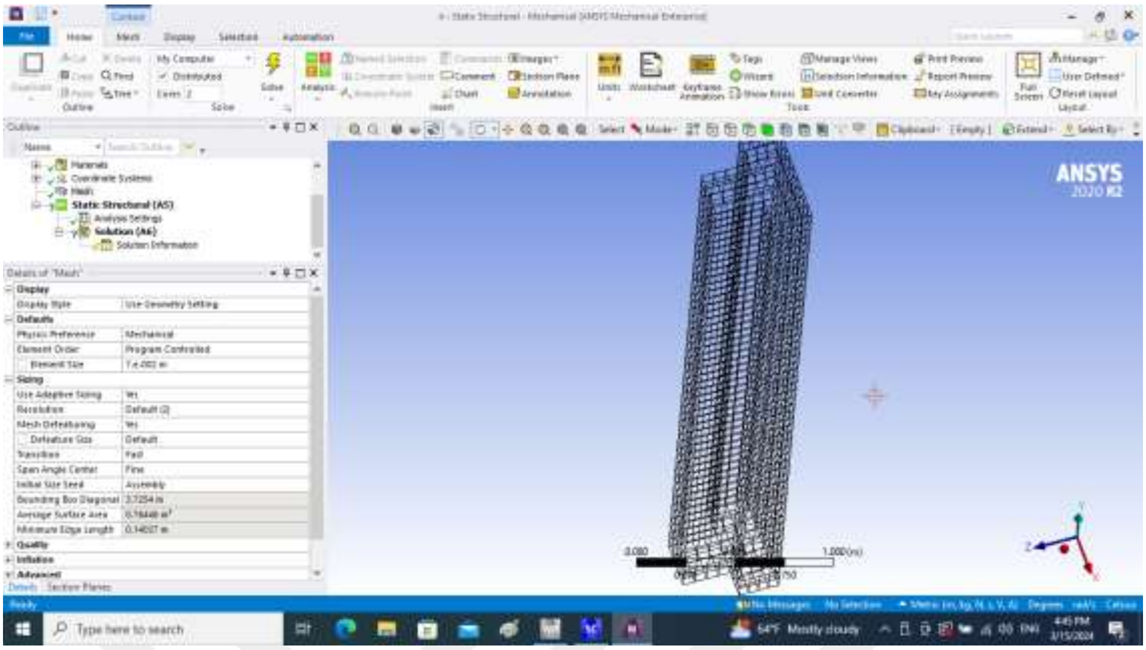

Figure 3.20: Mesh Process for The Third Case.

Unrestricted access to the solid model is facilitated by free meshing processes. The process of mesh generation can be used to models of any shape, regardless of the level of irregularity present. The utilization of element shapes is contingent upon whether regions or volumes are being meshed. For area meshing purposes, free meshes can be composed exclusively of quadrilaterals or a combination of triangles and quadrilaterals. As a usual practice in volume meshing, it is customary to limit the free mesh exclusively to tetrahedral components. To enhance the process of transitions, it is possible to integrate pyramid-shaped elements into the tetrahedral lattice. The aforementioned geometric properties will be employed just during the process of meshing. However, in the event that the designated element type is capable of accommodating various shapes, the subsequent stage entails the identification of relevant information. The construction of a roadway involves the utilization of steel rods as stabilizers, concrete as the foundation, and concrete tension as the concluding stage.

3.10 PROCESS TO SOLVE THE MODEL

The commencement of the analysis phase of the Finite Element (FE) programme is contingent Afterwards, a flawless input file has been confidently checked. After the analysis is conducted, the procedure will be executed, leading to the production of output files. The extent of the inquiry suggests that a substantial amount of data may be required. After the files have been processed and the relevant information has been extracted, it is still required to have a display that is well-organized and easy to explore. The role of the post-processor involves the management of the computer system by executing the necessary procedures. The pretreatment and postprocessing software exhibit a high degree of similarity in terms of their functionality and features. During the post-processing stage, the data obtained from the output files is combined and then displayed to the user in visually appealing formats, such as tables and charts. The term "post-processing" is used to refer to this particular stage. There are two distinct approaches available for the representation of stress components at a particular position on a surface. The initial approach, as demonstrated in the previous example, utilizes color. Moreover, contour lines can be employed to represent indistinguishable degrees of tension. The person is provided with access to both of these methods. Identify the characteristics of the analysis. Commence the process by navigating to the New Analysis menu. Next, choose Static Structural Analysis.

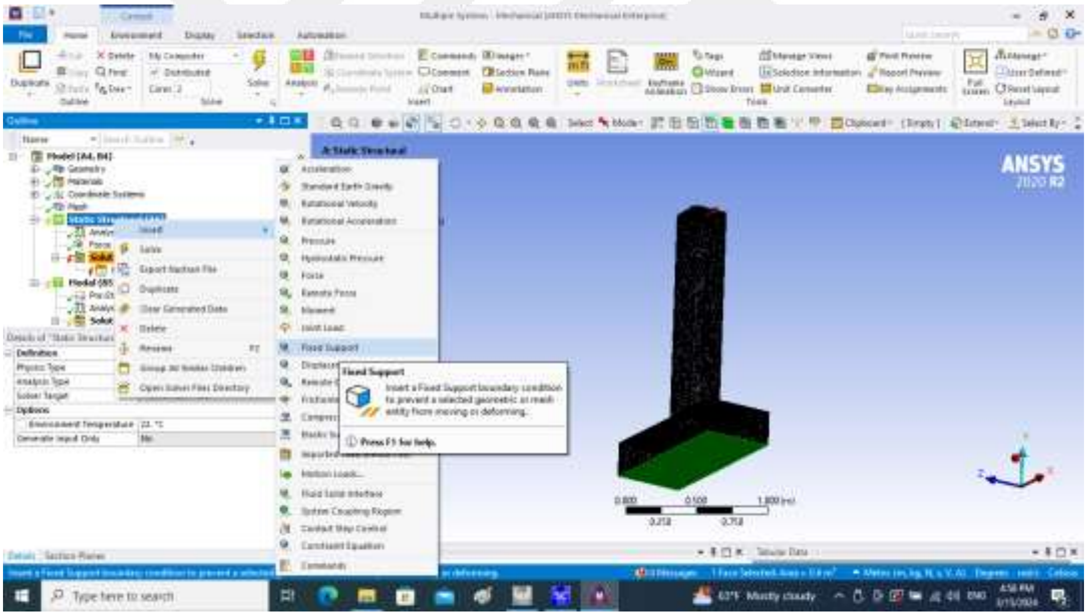

Figure 3.21: Fixing The Base of Column.

3.11 SET THE LOAD

In the context of this analysis, "loading" denotes the fundamental force acting in the desired direction. To initiate the process, navigate to the Static Structural folder within the Outline view. Visible is the Environment toolbar. Following this, rotate the column in a manner that aligns one of its extremities with the horizontal plane at a right angle to the essential axis, as illustrated. It is necessary to utilize the Y-axis to determine your position. Following the identification of the visible end face, activate the Face selection mode in Design Modeler by selecting the face icon from the graphics toolbar, which is referred to as the Selection toolbar. Following that, in order to access The Force menu, one must click the Loads icon that appears on the toolbar. If the Define by option has not yet been selected, proceed to the Details page and modify it to Components.

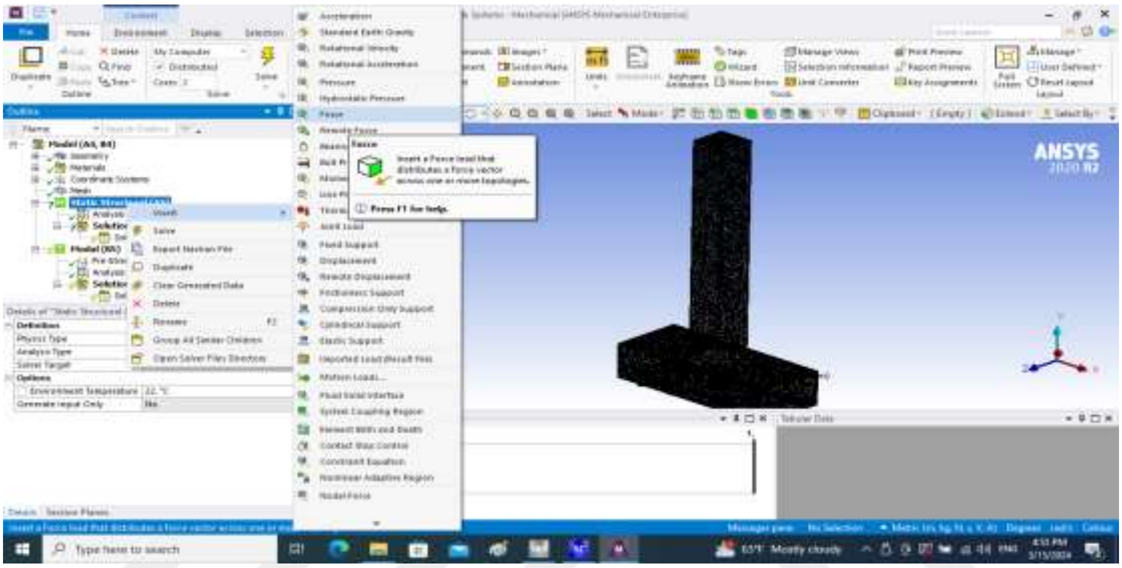

Figure 3.22: Selection Lateral Force Process.

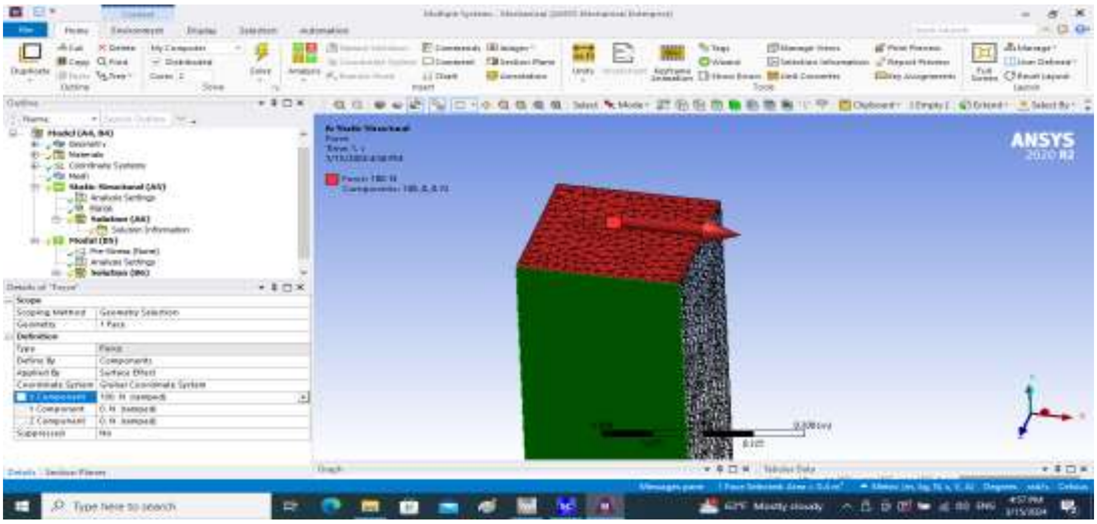

Figure 3.23: Applying Forces.

This figure shows the ANSYS Mechanical interface during a static structural analysis where a force is being applied to a model.

3.12 REQUEST RESULTS

First request deformation, Select the Solution folder. then In the Solution toolbar click on Deformation and select DeformationDirectional. In the Details pane change the Orientation to the required Axis. Click on Stress in the toolbar and select Stress-Normal. In the Details pane change the Orientation to Y-direction

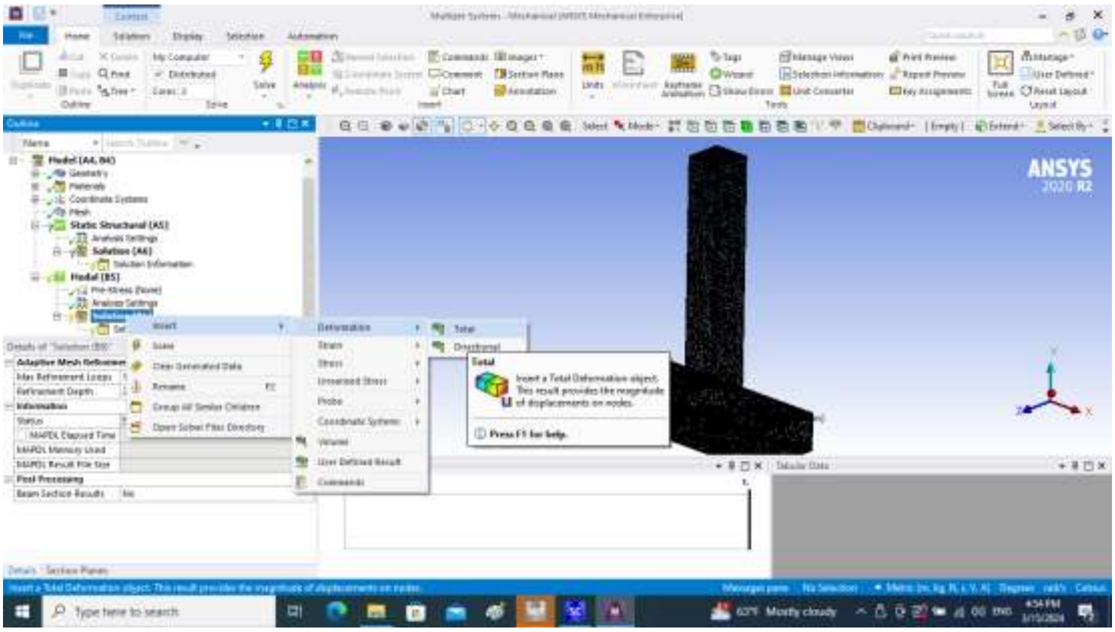

Figure 3.24: Getting Modal Deformation.

This figure displays the ANSYS Mechanical workspace during the process of obtaining modal deformation results.

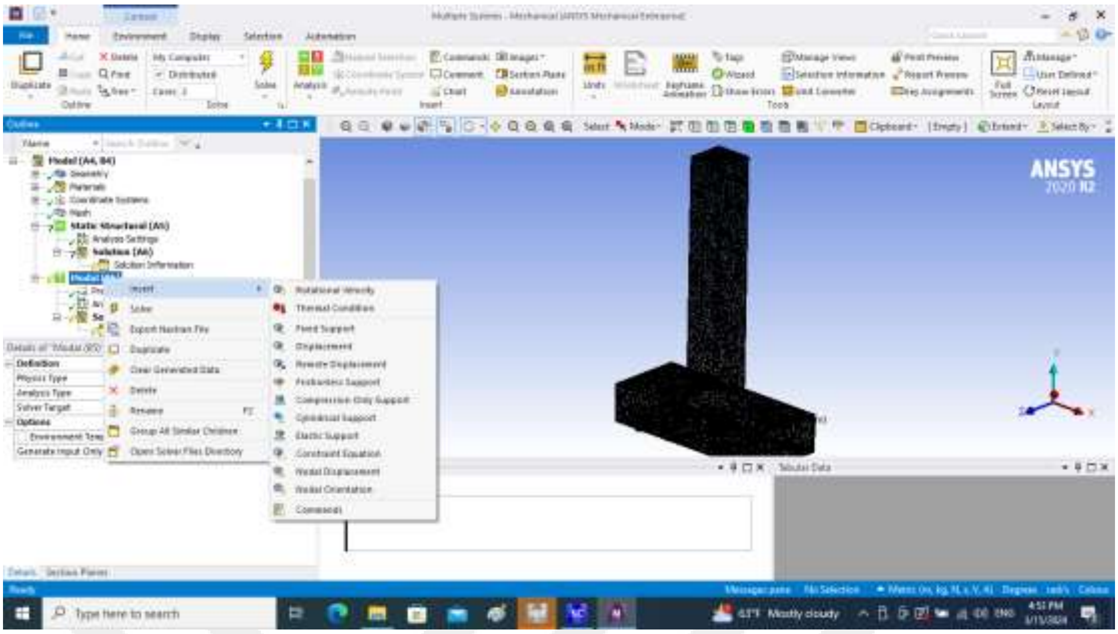

Figure 3.25: Developing Modal Process.

This figure shows the ANSYS Mechanical interface during the setup of a modal analysis.

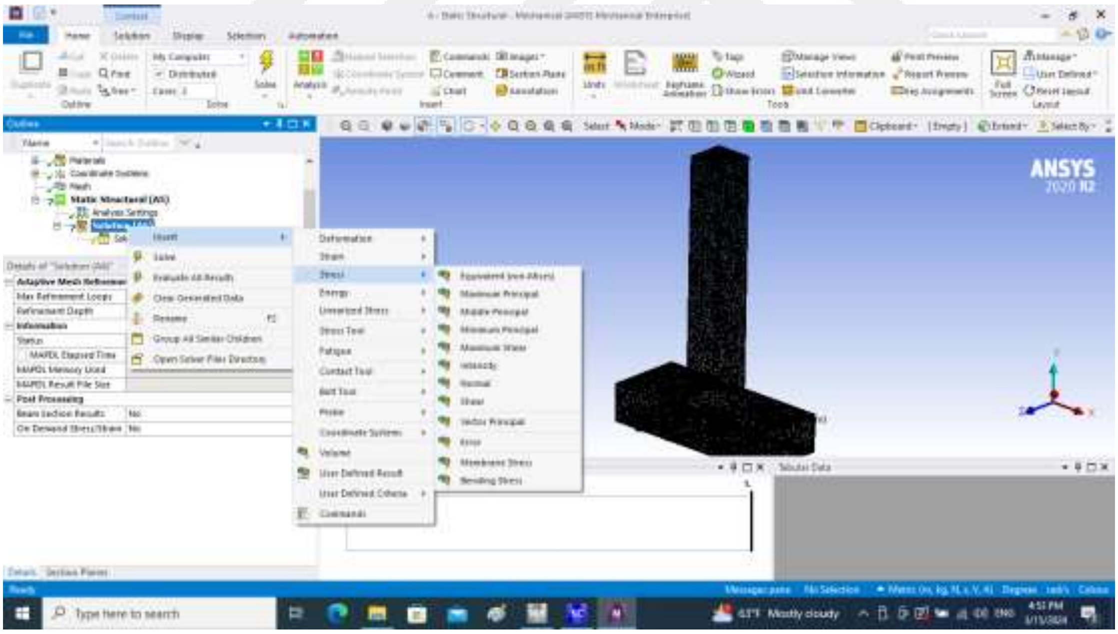

Figure 3.26: Getting Stresses Results.

This figure presents the ANSYS Mechanical environment at the stage of extracting stress results from a static structural analysis.

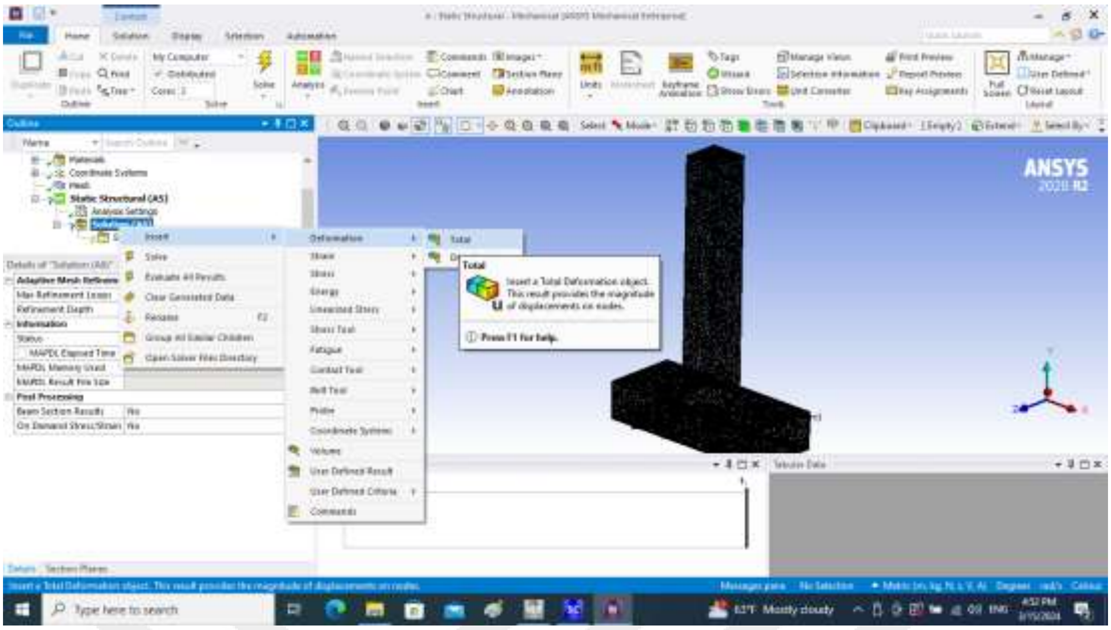

Figure 3.27: Getting Deformation Results.

This figure shows the ANSYS Mechanical interface while setting up deformation results in a static structural analysis.

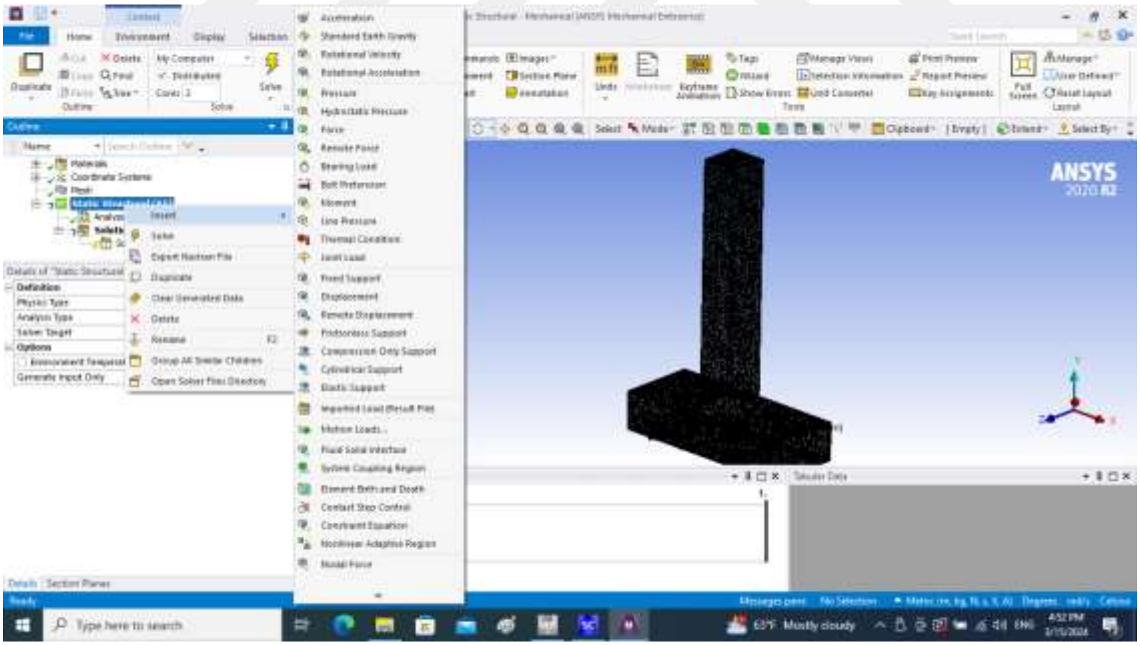

Figure 3.28: Applying Boundary Conditions.

This figure illustrates the ANSYS Mechanical interface during the step of applying boundary conditions in a static structural analysis.

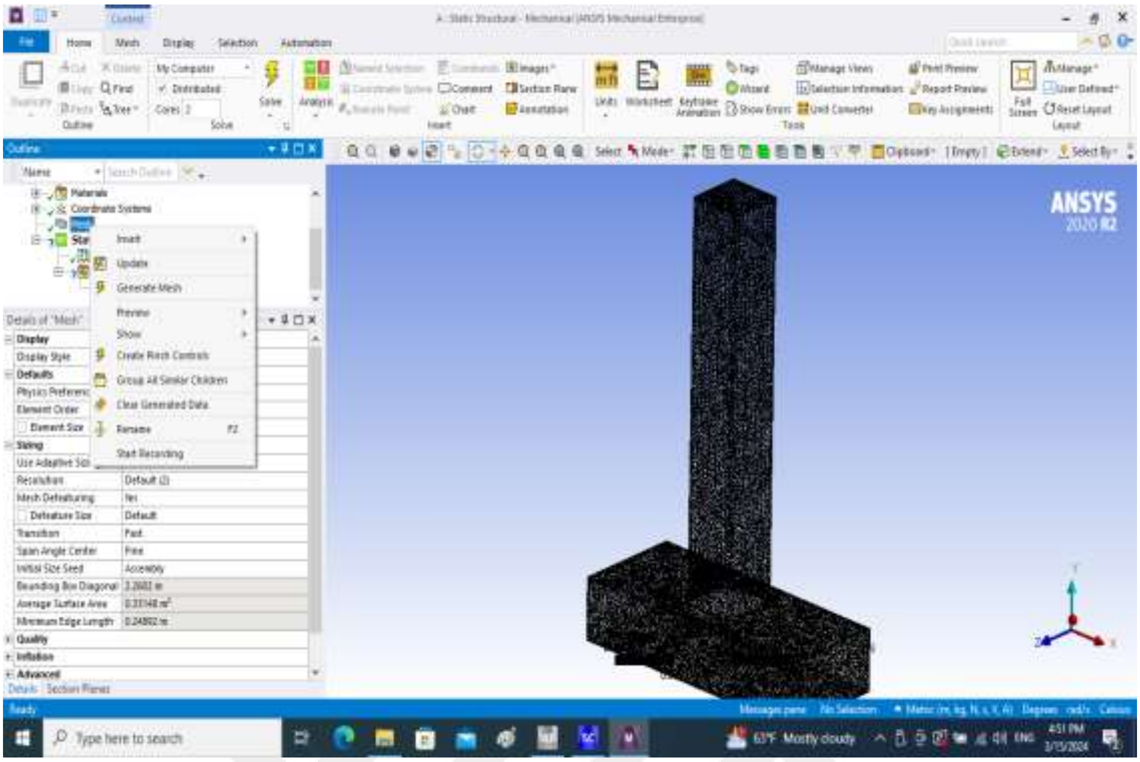

Figure 3.29: Checking Mesh Results.

Enlarge the results area displayed. By default, when displaying graphical results, a considerable portion of the Workbench window is occupied by windowpanes such as the Timeline and Tabular Data windowpanes. These windowpanes can be unpinned (collapsed) in order to enlarge the graphical results, display as described in section 3.4.3, Window Manager Features. To unpin the Timeline and Tabular Data Windowpanes, click on the pushpins located at the top right-hand corner of each plane. The resulting display is shown below.

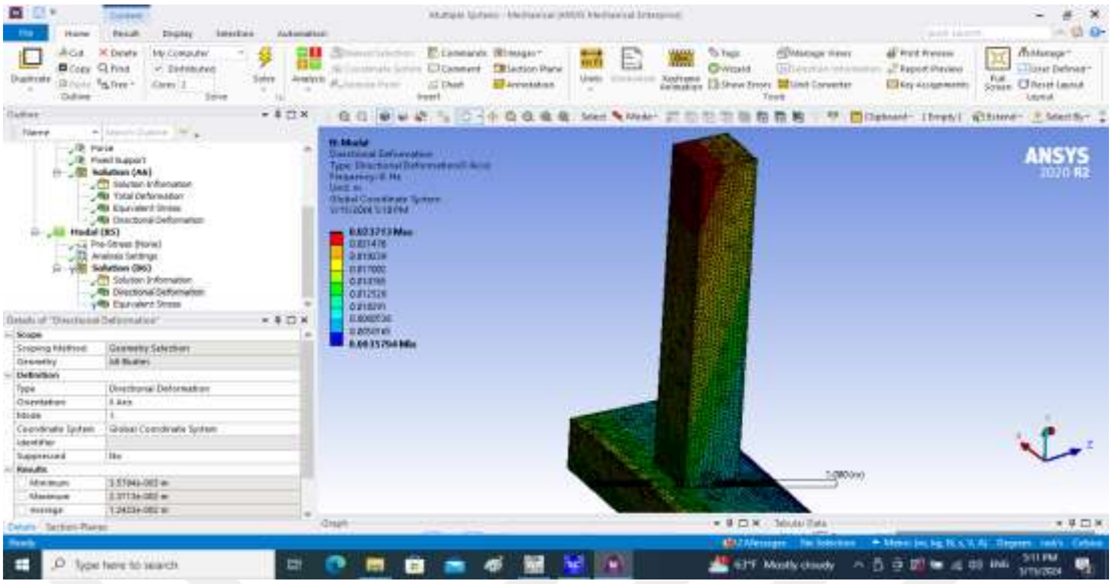

Figure 3.30: Sample of Modal Results.

This figure shows the modal analysis results in ANSYS, where the model is displayed with a colour contour indicating vibration displacements. The legend shows the range from minimum (blue) to maximum (red) deformation, and the details panel provides values like frequency and maximum displacement. It illustrates the structure's natural mode shape and how it deforms at a specific vibration frequency.

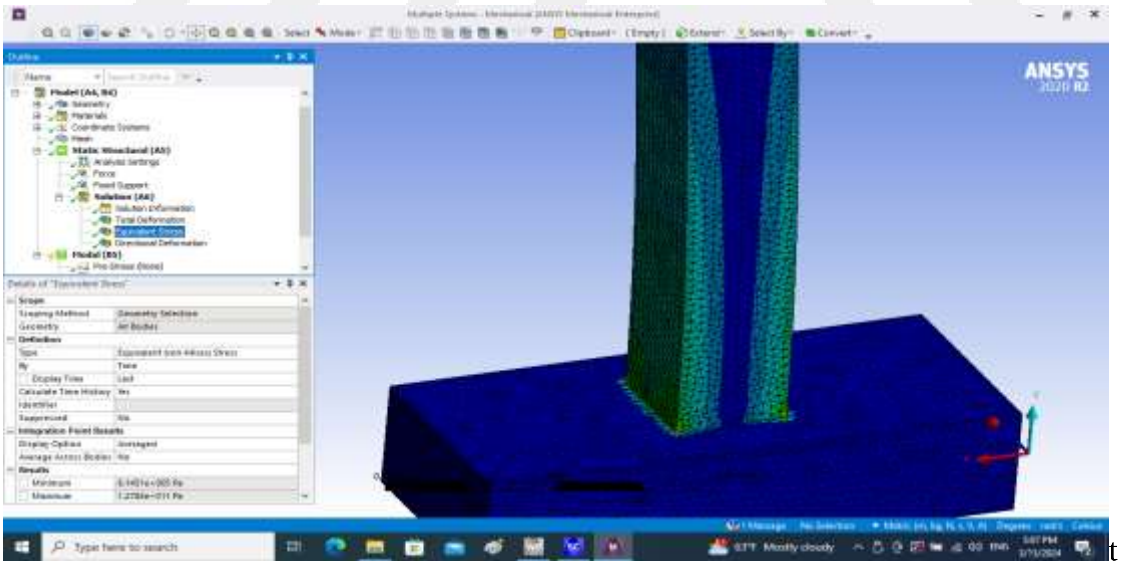

Figure 3.31: Sample of Stress Results.

This figure displays an ANSYS stress analysis result, showing a colour contour of von Mises stress across the model. The legend indicates stress levels from low to high, and the details panel lists the maximum and minimum stress values, highlighting areas of highest structural loading.

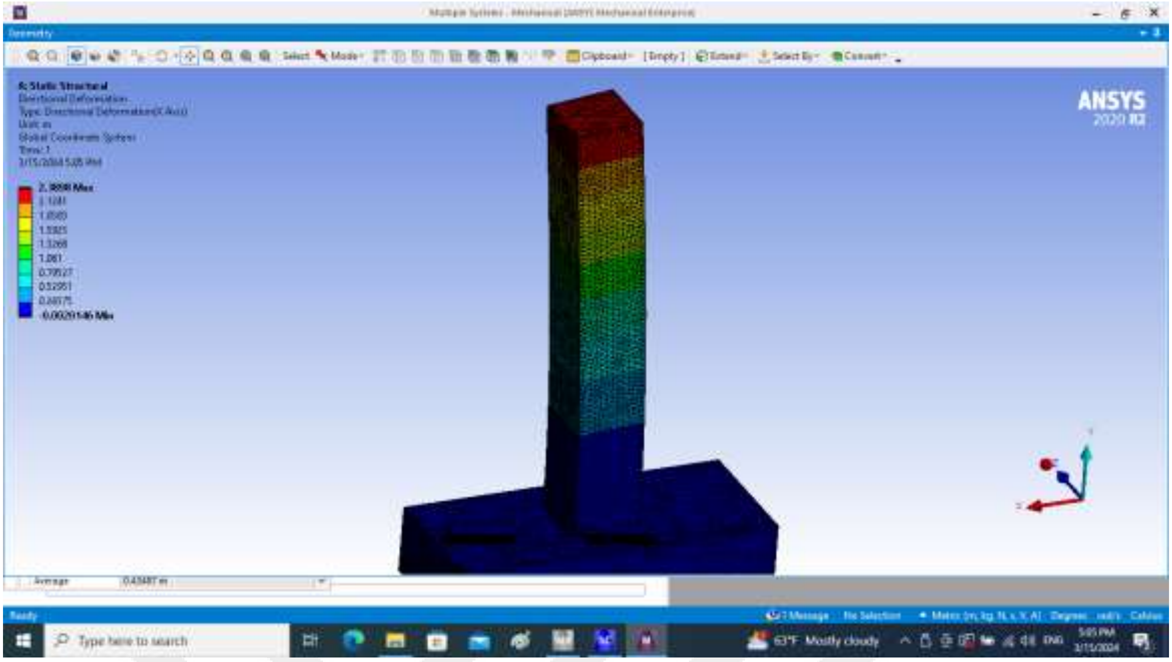

Figure 3.32: Sample of Deformation Results.

This figure shows ANSYS deformation results, using a colour scale from blue (minimum) to red (maximum) to display how much different parts of the structure displace under load.

4. RESULTS AND DISCUSSION

In this chapter, the solution of improving the building structure that is described in the problem statement was found. concrete constructions with slender non-rectangular columns. These structures demonstrated structural integrity, since all analytical results fell within permissible parameters. This building method effectively fulfills the spatial requirements of corners and intersections, ensuring that there are no visible edges or columns in the constructions. The usable floor area is expanded, enabling the inclusion of extra furniture within the buildings. Frame constructions with specially designed columns provide several advantages for various sorts of buildings, such as villas and multi-story complexes.

4.1 VALIDATION PROCESS

Increasingly, individuals are relying on simulation models to aid problem-solving and decision-making. Ensuring the accuracy of the models and their conclusions is crucial for all individuals involved in constructing and employing these models, as well as for those who depend on the data provided by the models' outputs and are impacted by the resulting judgments. In order to alleviate this concern, we utilize model validation methodologies. In order to demonstrate the adequacy of your model for its intended use, validation must be conducted to provide evidence of its accuracy. Regardless of the quality of a simulation model, it will always fall short by accurately predicting the behavior of the actual object or system it represents, as it is only a representation. Consequently, it is necessary to test and validate models just to the extent necessary for their applications. To verify the proper functioning of a model and address the relevant issue, further procedures are required following the training process. To validate a model, it is necessary to initially assess its assumptions, analyze its structure, logic, and causal connections, compare the behavior of the model and the system under various experimental situations, and evaluate the theories that influenced the model's creation. During the process of developing a model, it is customary to create many models in order to choose one that may be considered authentic. This approach can utilize a diverse range of validation tools. Currently, there is no standardized protocol or strategy for selecting among the different validation techniques. Their utilization, whether subjective or objective, depends on the specific model, system, and current circumstances for most of them. The issue statement or the problem description should explicitly indicate that the decision is an integral component of the problem. Based on the model presented in table 4.1,

Table 4.1: Column Models Used in The Present Research.

Column Model		**Dimensions**	
Model 1	**Rectangular column**	**13' 16'**	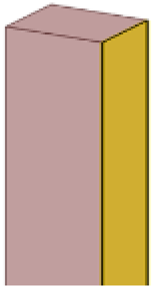
Model 2	**Special column shape type T**	**21'' 26'' 5''**	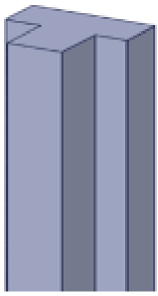
Model 3	**Special column shape type L**	**23'' 24'' 5''**	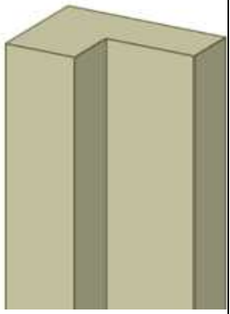

The simulation results present a juxtaposition of autonomous numerical outcomes with outcomes obtained from ANSYS testing conducted under the same settings. Common kinds of deformation include displacement in the center. Due to its curved shape, the column is likely to have the lowest moment of inertia in its core. This research considers a rectangular construction with a Y-dimension of 51 feet and an X-dimension of 50 feet. By utilizing the

ANSYS software, we analyze a single structure using four different models consisting of 6, 10, 15, and 20 stores. Each model incorporates columns with varied shapes, specifically L and T shapes. Next, we compute the economically feasible dimensions of the columns.

The findings indicate that properties related to central stiffness have a considerable influence on load. The mass of a column and the load of a model are influenced by same variables. The model illustrates a second bending mode that may withstand greater stresses while still preserving one or more nodes centered around the item. The alteration was particularly evident when observed from a higher vantage point. Introducing greater rigidity in a certain direction results in the formation of bends in the node-based model. The simulation test results of the current study and the experimental testing results of the previous study are shown in Figures 4.1 and 4.2, respectively.

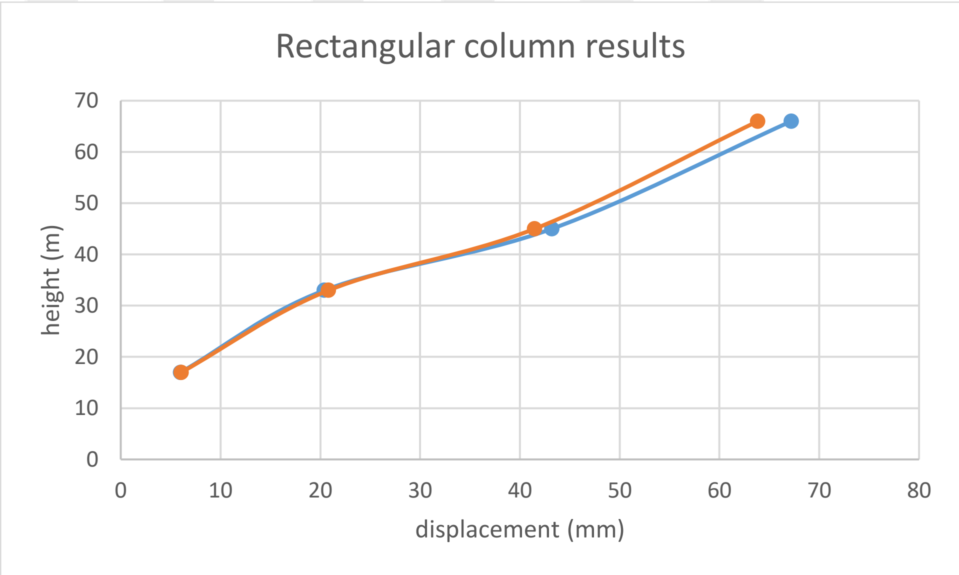

Figure 4.1: Comparison of Rectangular Column Results.

This figure compares rectangular column results, with blue representing my study and orange showing previous studies. It plots displacement (mm) against height (m), revealing closely matching trends with slight differences between your results and earlier findings.

Table 4.2: Deviation Rate of Rectangular Column Results.

Rectangular column results			
recent study	previous study	height	error
displacement (mm)	displacement (mm)	(m)	
6.07	6	17	1%
20.83	20.4	33	2%
41.47	43.2	45	4%
63.84	67.2	66	5%

A common procedure involves comparing the anticipated behavior of the model with the real behavior of the system under various experimental conditions to establish a strong level of confidence in the model. In order to do this, it is necessary to have the ability to get the system's input-output data and the model's input-output data in specific experimental conditions. To assess the accuracy of the model, it is essential to define a suitable range of accuracy for comparing the model's output behaviors with those of the system. The author has not uncovered any scientific approach to get such a high level of precision. The process of model validation typically neglects the establishment of a suitable range of accuracy.

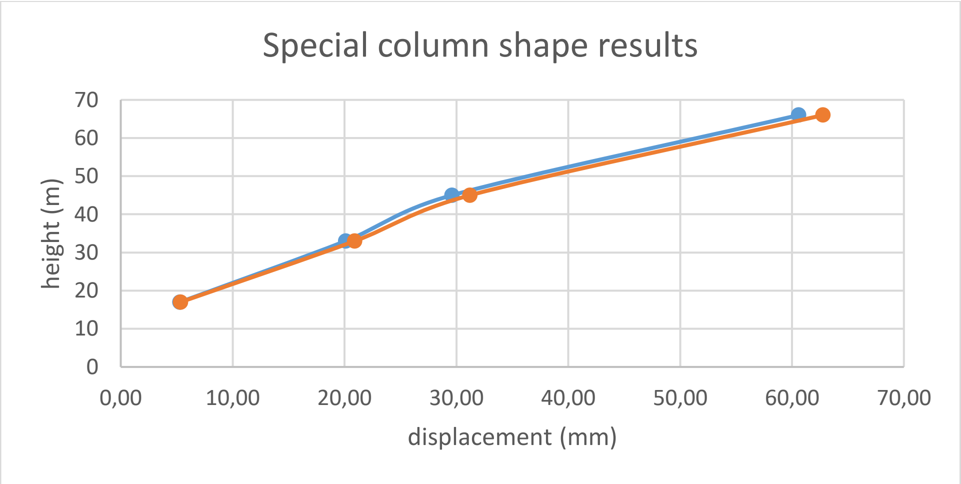

Figure 4.2: Comparison of Special Column Shape Results.

Comparison of Special Column Results, this figure compares rectangular column results, with blue representing my study and orange showing previous studies. It plots displacement (mm) against height (m), revealing closely matching trends with slight differences between your results and earlier findings.

Table 4.3: Deviation Rate of Special Column Shape Results.

Special column shape results			
recent study	previous study	height	error
displacement (mm)	displacement (mm)	(m)	
5.35	5.30	17	1%
20.92	20.10	33	4%
31.22	29.60	45	5%
62.78	60.60	66	4%

Different sets of labels were assigned to the columns next to the loading criterion. The sets and labels were implemented in several stories to derive analytical findings. In addition, the wind load was specified in ANSYS, and the axial forces were obtained from both the center and corner columns. Subsequently, the findings were compared.

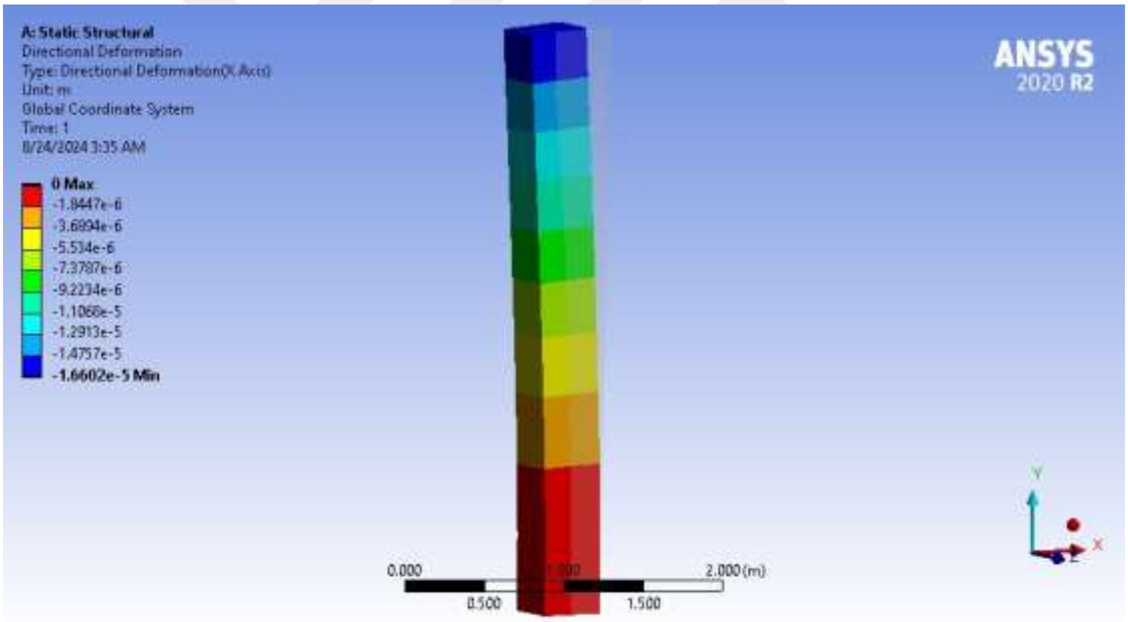

Figure 4.3: Model 1 ANSYS Results.

This figure shows Model 1 ANSYS results with a colour contour of directional deformation along the X-axis. The scale ranges from blue (minimum displacement) to red (maximum displacement), illustrating how the column deforms under applied loads.

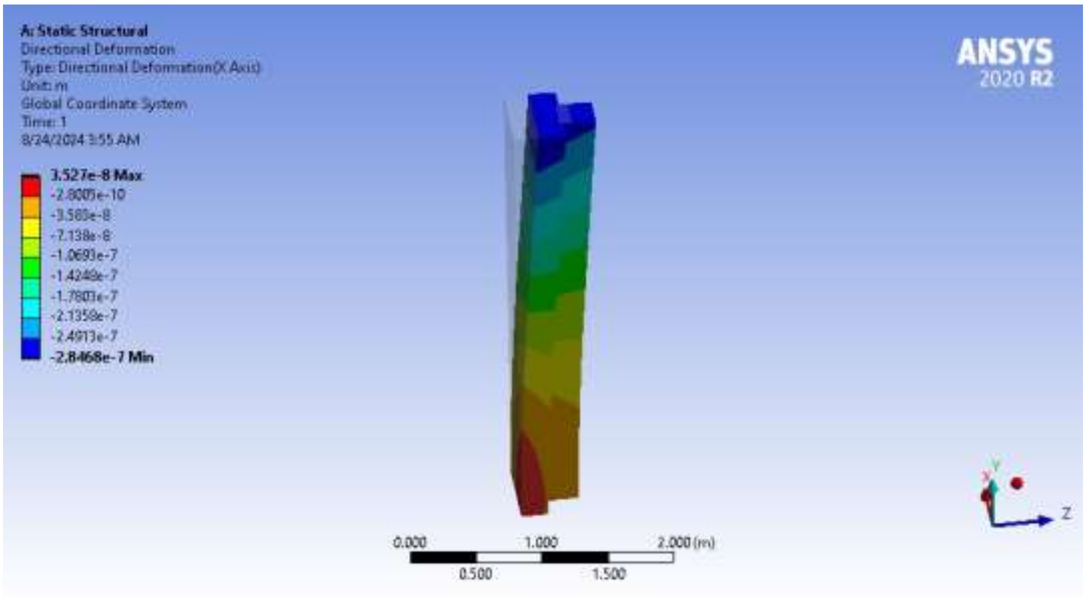

Figure 4.4: Model 2 ANSYS Results.

This figure shows Model 2 ANSYS results with a colour contour of directional deformation along the X-axis. The scale ranges from blue (minimum) to red (maximum), indicating how the column displaces under the applied loading conditions.

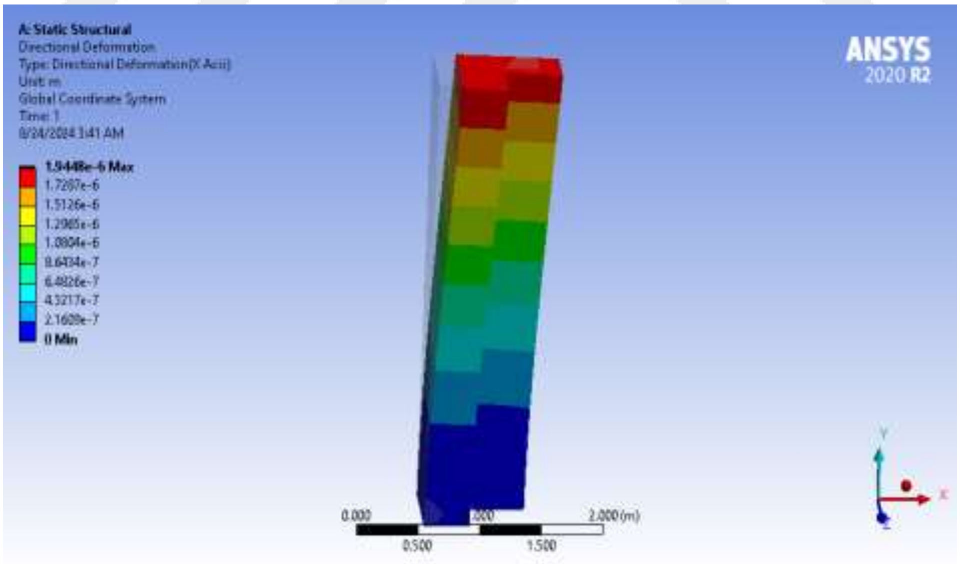

Figure 4.5: Model 3 ANSYS Results.

This figure shows Model 3 ANSYS results with a colour contour of directional deformation along the X-axis. The scale runs from blue (minimum) to red (maximum), highlighting how different regions of the column deform underloading.

Table 4.5: Models Considered for Variation in Column Shape.

Column Model	Dimensions	Wind velocity	Concrete grade
Model 1	13’ 16’	96	C30
Model 2	21’’ 26’’ 5’’	96	C30
Model 3	23’’ 24’’ 5’’	96	C30
Model 1	13’ 16’	96	C40
Model 2	21’’ 26’’ 5’’	96	C40
Model 3	23’’ 24’’ 5’’	96	C40
Model 1	13’ 16’	110	C50
Model 2	21’’ 26’’ 5’’	110	C50
Model 3	23’’ 24’’ 5’’	110	C50

4.2 MODELS CONSIDERED FOR VARIATION IN COLUMN SHAPE +CONCRETE COMPRESSIVE STRENGTH WITH WIND 96

Statistics show a strong relationship between building height and displacement, with wind-load combinations having the largest impact on structural displacement.

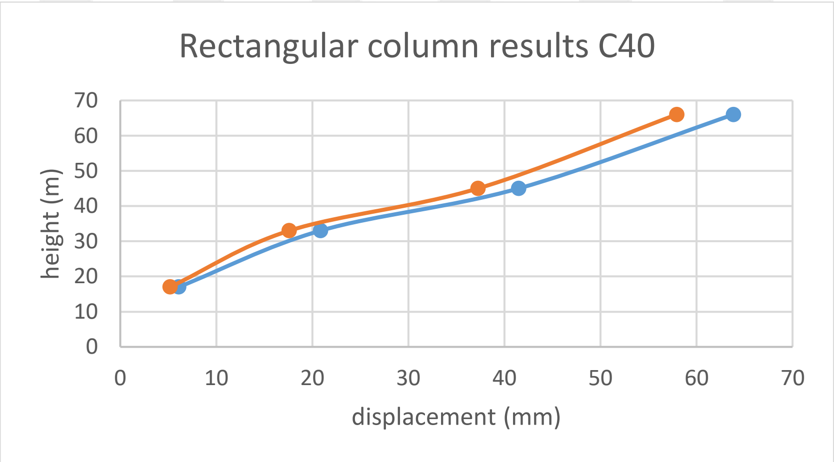

Figure 4.6: Rectangular Column Results C40 and Wind Velocity 96 mph.
This figure compares rectangular column C40 results under a 96-mph wind load, plotting displacement (mm) versus height (m).

The blue curve represents my study, while the orange curve shows previous data, indicating closely matching trends with slight variations in displacement at different heights.
The phrase "special-shaped column structure" is used to describe a construction that includes components with L-shaped or T-shaped columns. The distinctive design of the shaped

column allows it to bear a larger load and exhibit better flexibility in bending compared to L-shaped and T-shaped columns. The performance of standard reinforced concrete columns can be improved by including specially designed substitute columns. Despite its unconventional appearance, the concrete tower exhibits exceptional performance.

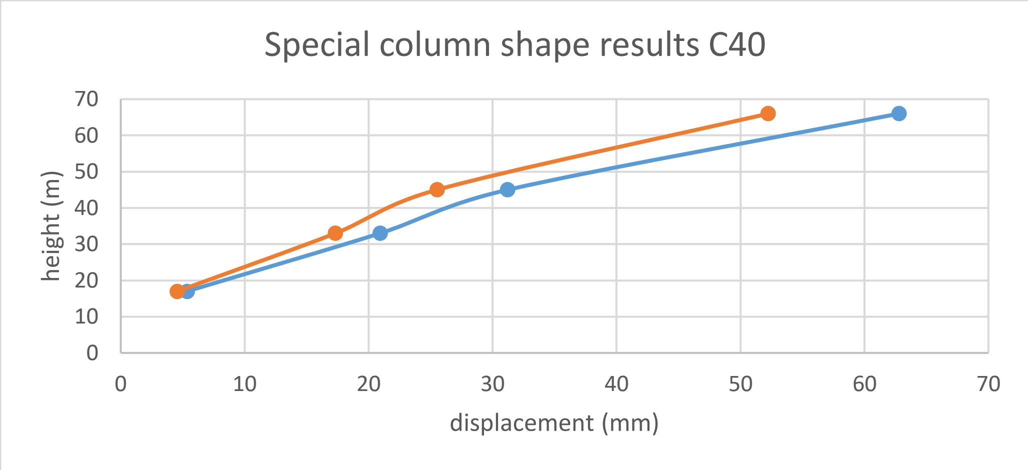

Figure 4.7: Special Column Shape Results C40 and Wind Velocity 96 mph.
This figure compares special column shape C40 results under a 96-mph wind load, plotting displacement (mm) against height (m).

The blue line shows my study, while the orange line represents previous studies, highlighting similar trends with slightly higher displacements in the earlier data.

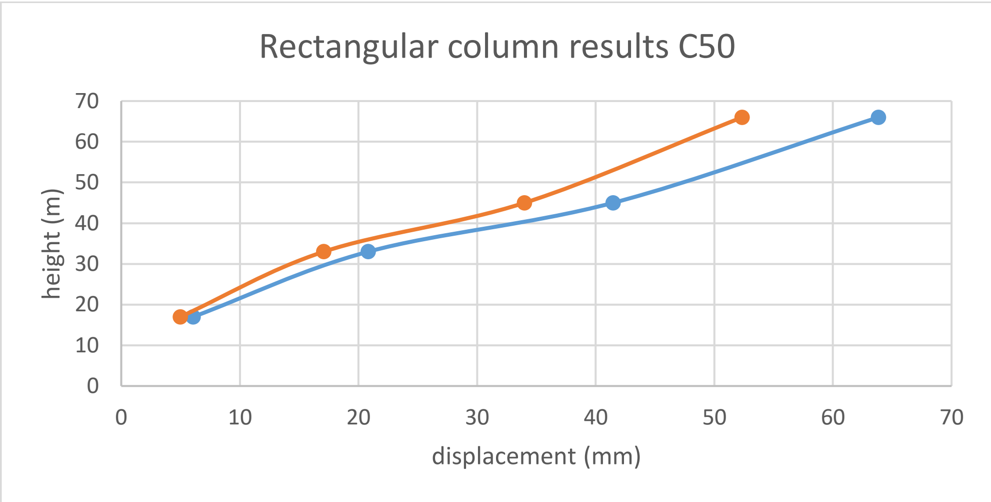

Figure 4.8: Rectangular Column Results C50 and Wind Velocity 96 mph.
This figure compares rectangular column C50 results under a 96-mph wind load, plotting displacement (mm) versus height (m).

The blue curve represents my study, while the orange curve shows previous data, indicating closely matching trends with slight variations in displacement at different heights.

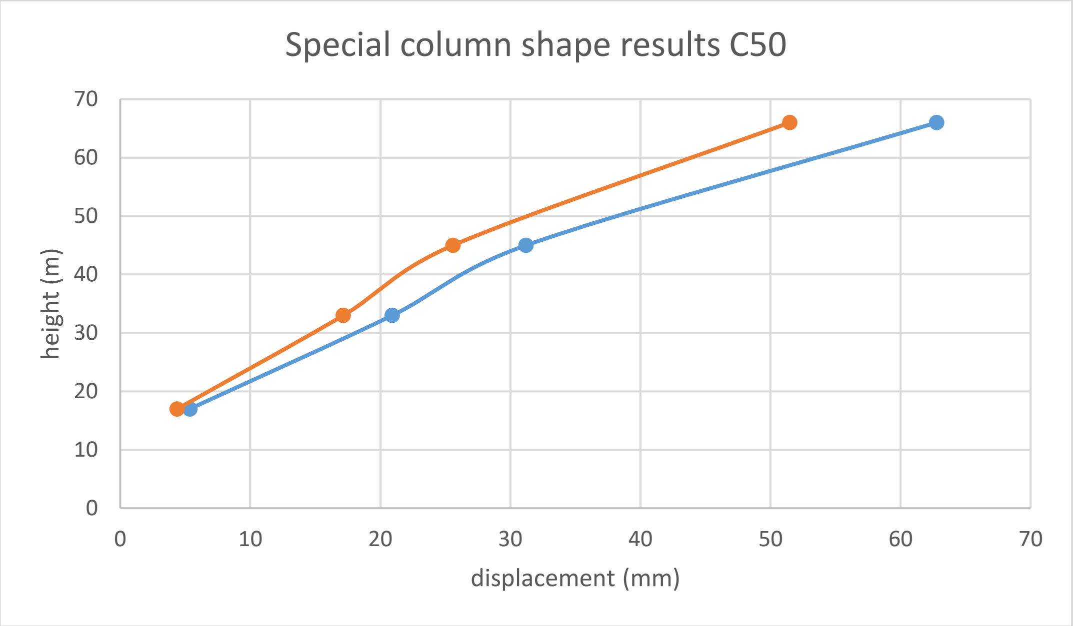

Figure 4.9: Special Column Shape C50 and Wind Velocity 96 mph.
This figure compares special column shape C50 results under a 96-mph wind load, plotting displacement (mm) against height (m).

The blue line shows my study, while the orange line represents previous studies, highlighting similar trends with slightly higher displacements in the earlier data.

When the column components are formed like an L or T, the structure is referred to as a "special-shaped column structure". The shaped column has a lot lower carrying capacity and is much less flexible than the three special-shaped columns we have just discussed because of its drastically different form from the L-shaped and T-shaped columns. Using a succedaneum, a unique kind of column, can improve the performance of normal reinforced concrete columns. The unique concrete tower's efficiency and height are both excellent.

4.3 MODELS CONSIDERED FOR VARIATION IN COLUMN SHAPE WITH WIND 110 MPH

The results indicate that the most significant structural displacement is caused by wind-load combinations, which is a clear indication that displacement is directly correlated with building height.

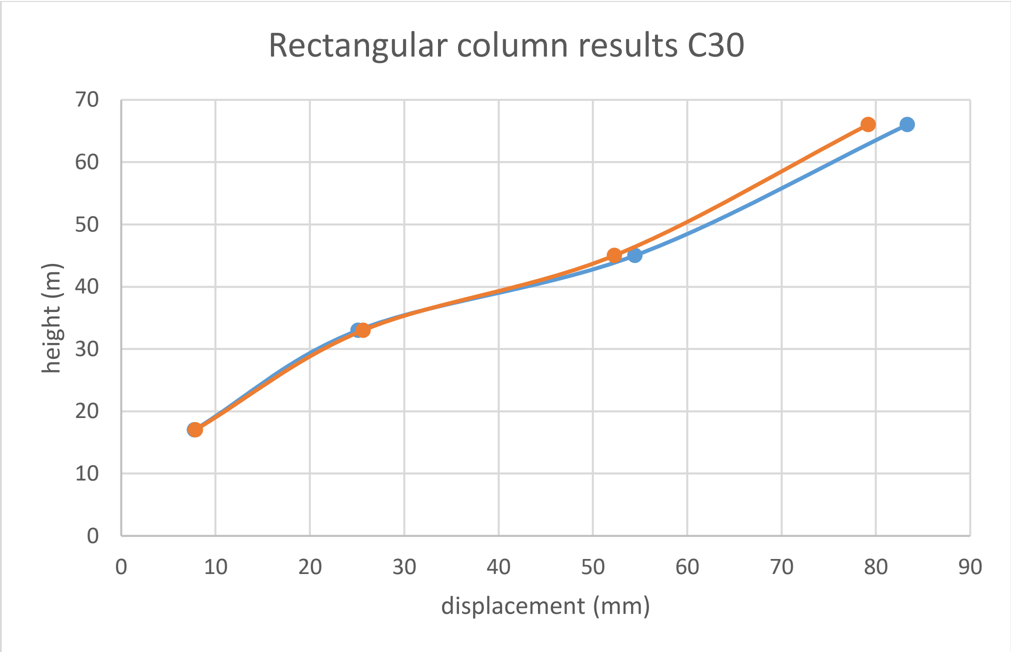

Figure 4.10: Rectangular Column Results and Wind Velocity 110 mph.
This figure compares rectangular column C50 results under a 110-mph wind load, plotting displacement (mm) versus height (m).

The blue curve represents my study, while the orange curve shows previous data, indicating closely matching trends with slight variations in displacement at different heights.

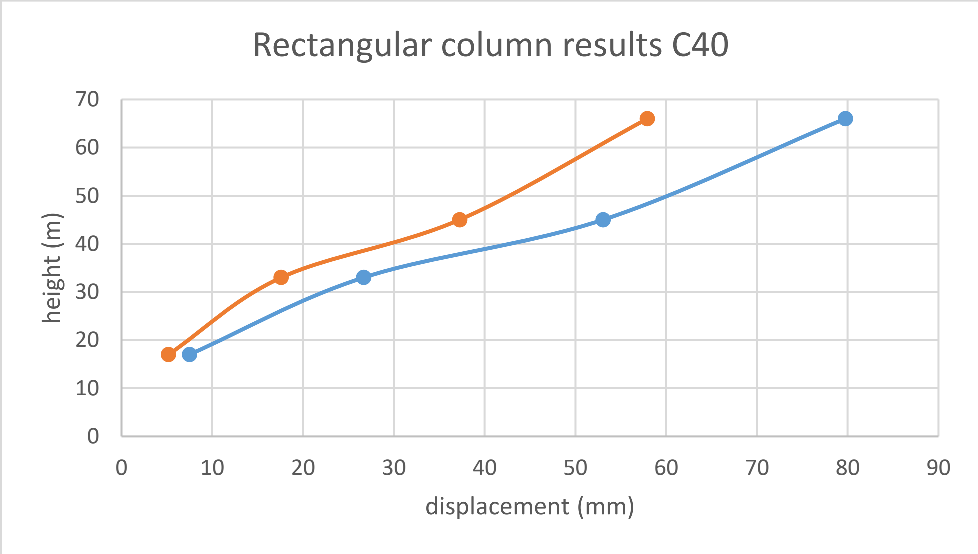

Figure 4.11: Rectangular Column Results and Wind Velocity 110 mph.

This figure compares rectangular column C40 results under a 110-mph wind load, plotting displacement (mm) versus height (m).

The blue curve represents my study, while the orange curve shows previous data, indicating closely matching trends with slight variations in displacement at different heights.

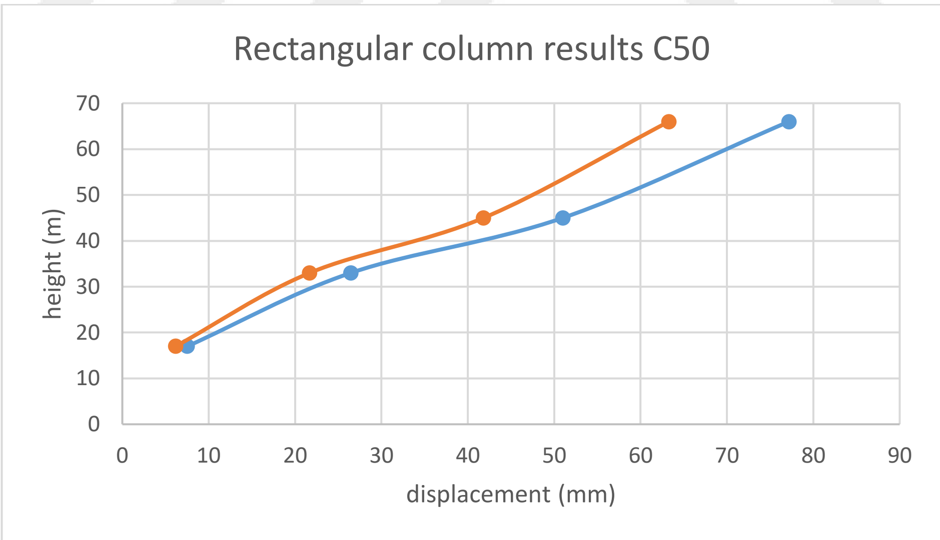

Figure 4.12: Rectangular Column Results and Wind Velocity 110 mph.

This figure compares rectangular column C50 results under a 110-mph wind load, plotting displacement (mm) versus height (m).

The blue curve represents my study, while the orange curve shows previous data, indicating closely matching trends with slight variations in displacement at different heights.

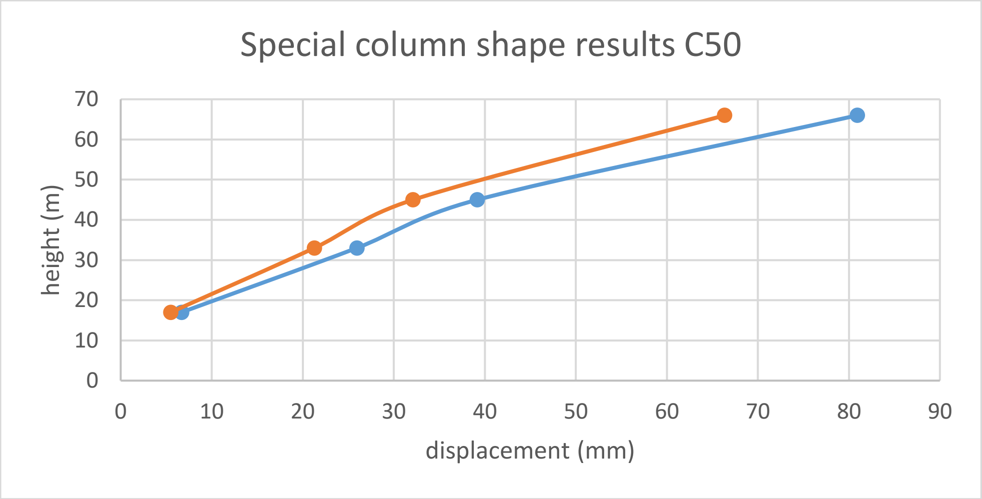

Figure 4.13: Special Column Shape and Wind Velocity 110 mph.

This figure compares special column shape C50 results under a 110-mph wind load, plotting displacement (mm) against height (m).

The blue line shows my study, while the orange line represents previous studies, highlighting similar trends with slightly higher displacements in the earlier data.

An L-shaped or T-shaped column segment makes up a special-shaped column structure. Due to its major form variation from L and T shaped columns, the shaped columns differ greatly in carrying capacity and ductility from the special-shaped columns with the three shapes listed above. As succedaneums, specially shaped columns are used to improve the performance of regular reinforced concrete columns. The concrete column with a unique design exhibits remarkable effectiveness.

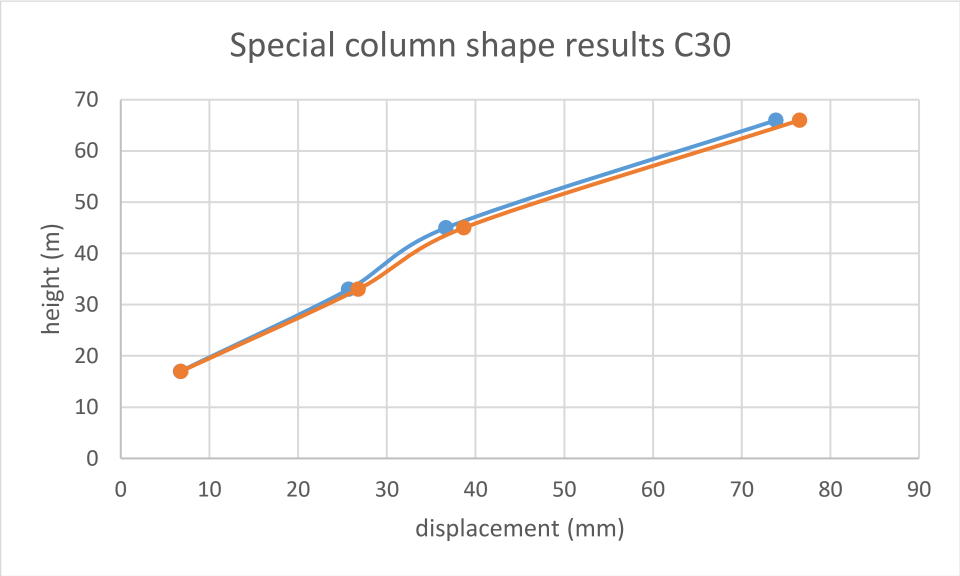

Figure 4.14: Special Column Shape and Wind Velocity 110 mph.

This figure compares rectangular column C30 results under a 96-mph wind load, plotting displacement (mm) versus height (m).

The blue curve represents my study, while the orange curve shows previous data, indicating closely matching trends with slight variations in displacement at different heights.

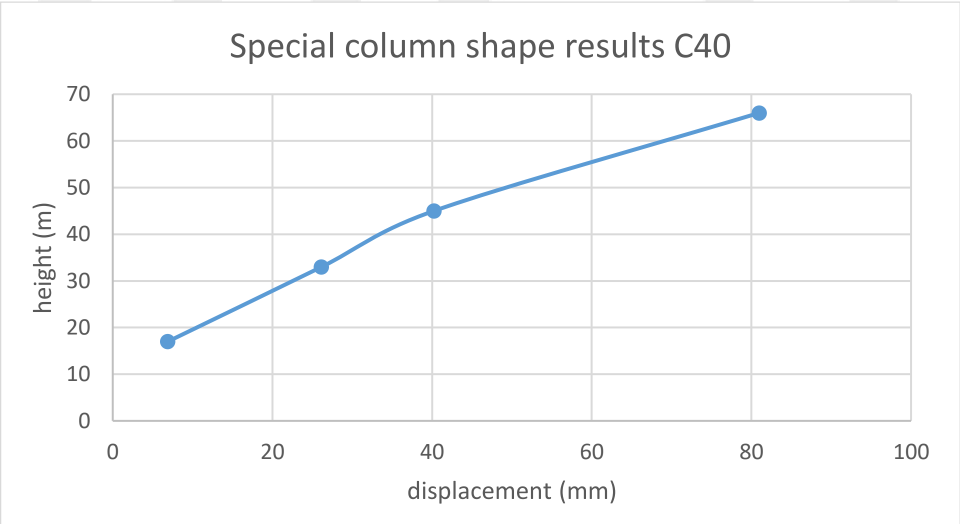

Figure 4.15: Special Column Shape and Wind Velocity 110 mph.
This figure compares special column shape C40 results under a 110-mph wind load, plotting displacement (mm) against height (m). The blue line shows my study, while the orange line represents previous studies, highlighting similar trends with slightly higher displacements in the earlier data.

A structure featuring L-shaped or T-shaped column sections is known as a "special-shaped column structure." Because of its drastically different shape from L-shaped and T-shaped columns, the shaped column has a far higher carrying capacity and ductility than the other three special-shaped columns mentioned before. Traditional reinforced concrete columns can be improved in performance by using specially designed columns that operate as a succedaneum. The special-shaped concrete column performs exceptionally well.

4.4 MODAL ANALYSIS L

Modal analysis is the examination of dynamic processes occurring inside a deforming area. Illustrating the movement of various structural elements under the influence of dynamic loading conditions, including those generated by electrostatic actuators, aids in determining the vibrational characteristics of a mechanical system. In other words, it reveals the fundamental mechanism of mechanical construction. When constructing a structure to handle dynamic loads, it is important to consider the center of modal forms. The linear mode analysis method evaluates and combines many mode forms to describe displacement patterns. It is sometimes referred to as the mode-superposition technique. Mode analysis is a synonym for the mode-analysis approach. Mode forms refer to the inherent configurations that a structure will naturally assume. The majority of respondents are concerned about the potential for a movement in either the left or right direction. For each structure with degrees of freedom, there should theoretically be a maximum of n possible modes of form. Novel patterns emerge when previous displacement patterns are consistently magnified and combined. Mode shapes are employed to analyze the behavior of an electrified system. A motion pattern characterized by the continuous and sinusoidal movement of the system's components. Modal analysis determines the linear behavior of structures when subjected to dynamic loads by examining their natural frequencies and mode shapes. Modal analysis involves decomposing the vibrational response of a structure into its constituent modes. The defining characteristics of a mode are its frequency and shape. Building models based on slopes exhibit a greater occurrence of various forms, with the reciprocal of this being the period.

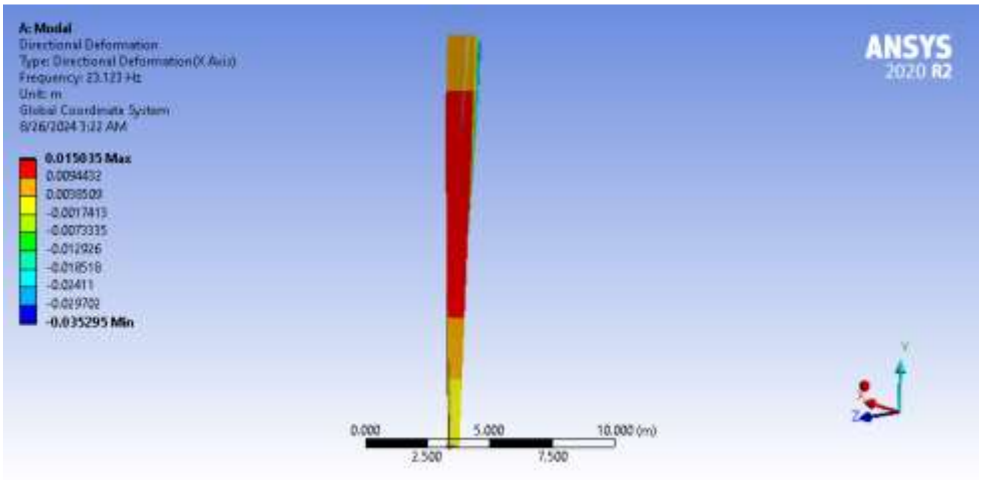

Figure 4.16: Modal Analysis L Shape Model 1.

This figure presents the first vibration mode of an L-shaped column from the ANSYS modal analysis. The natural frequency is 2.132 Hz, and deformation occurs along the X-axis. The color scale represents the magnitude of deformation: Red indicates the maximum displacement, Yellow/green represent moderate displacement, and Blue shows the minimum displacement (almost no movement).

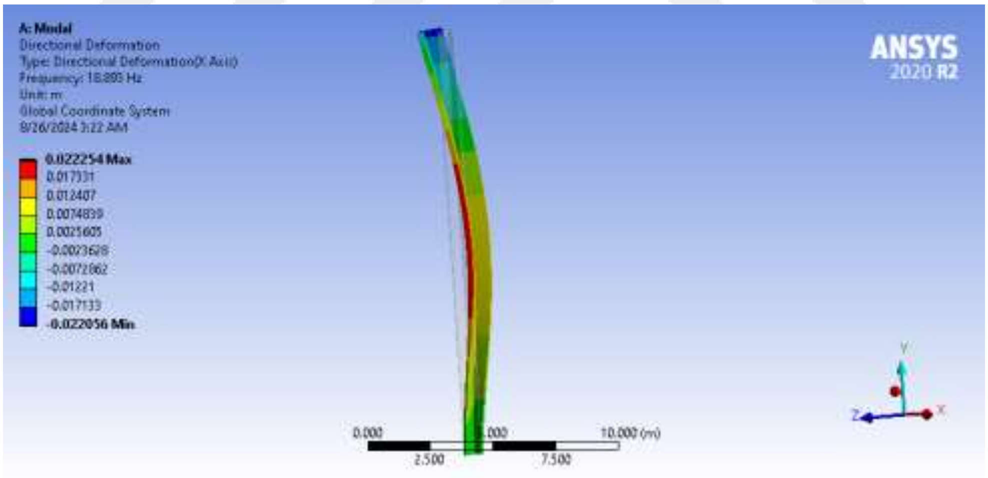

Figure 4.17: Modal Analysis L Shape Mode 2.

This figure shows the second vibration mode of the L-shaped column from the ANSYS modal analysis. The natural frequency is 18.893 Hz, and deformation occurs along the X-axis. The color scale represents the magnitude of displacement: Red indicates the maximum deformation, Yellow/green represent moderate deformation, and Blue indicates the minimum deformation (little to no movement).

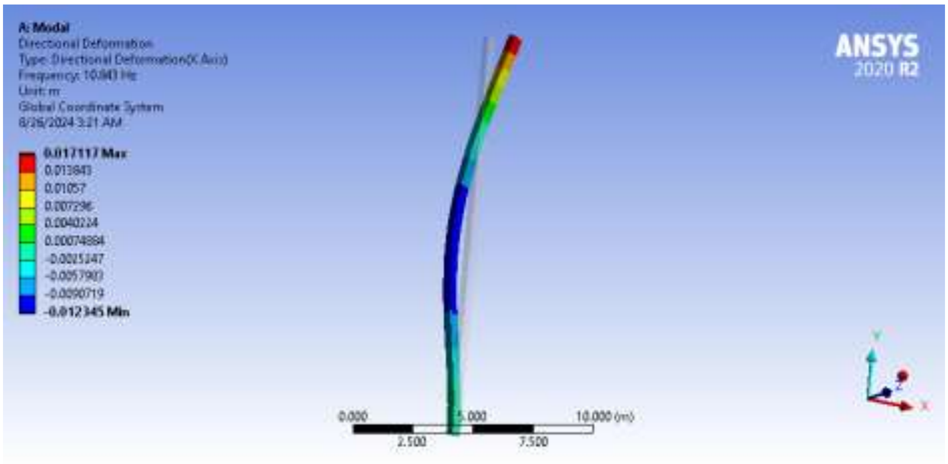

Figure 4.18: Modal Analysis L Shape Model 3.

This figure presents the third vibration mode of the L-shaped column from the ANSYS modal analysis. The natural frequency is 18.843 Hz, and the deformation occurs along the X-axis. The color legend shows the displacement magnitude: Red → maximum deformation regions, Yellow/green → moderate deformation, Blue → minimum deformation, indicating the areas with the least movement.

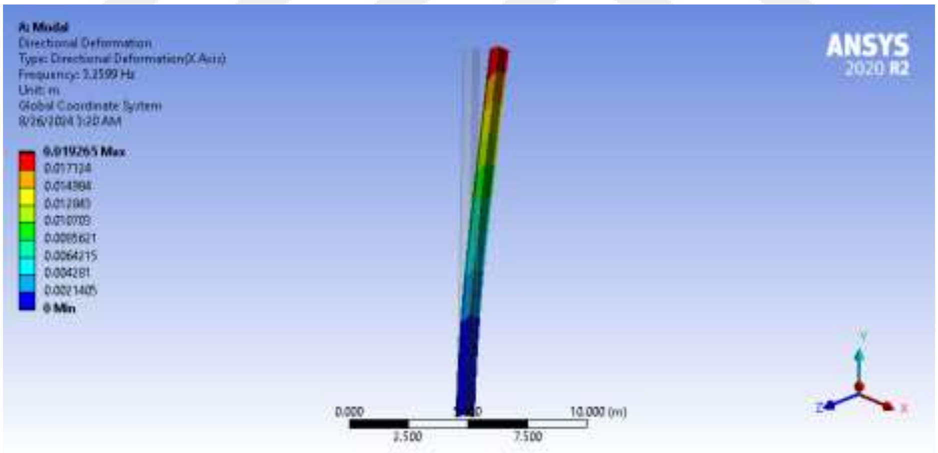

Figure 4.19: Modal Analysis L Shape Mode 4.

This figure shows the fourth vibration mode of the L-shaped column from the ANSYS modal analysis. The natural frequency is 3.6599 Hz, and the deformation occurs along the X-axis. The color scale represents displacement magnitude: Red → maximum deformation zones, Yellow/green → moderate displacement, Blue → minimum deformation, indicating areas with the least movement.

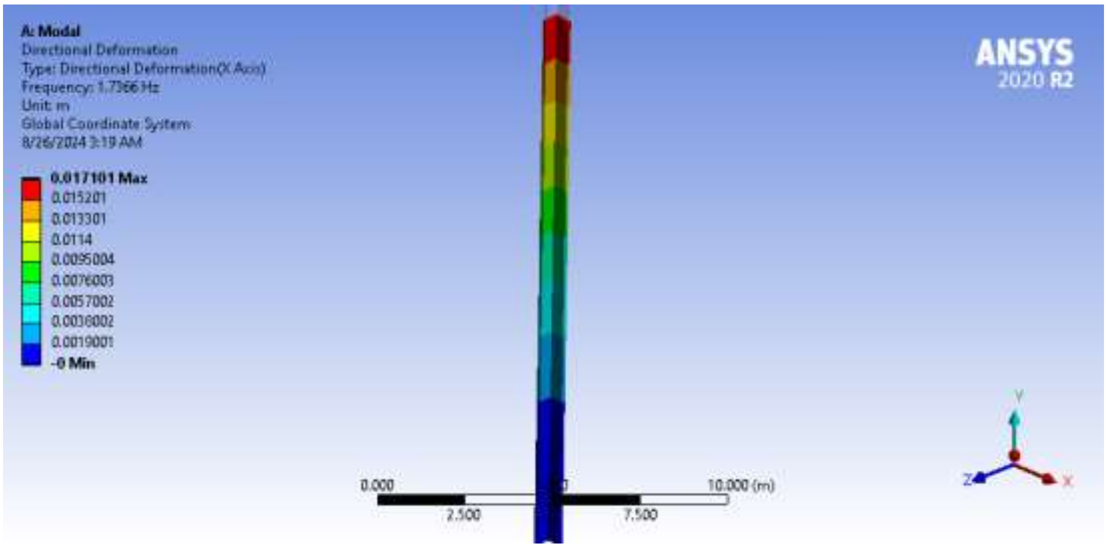

Figure 4.20: Modal Analysis L Shape Mode 5.

This figure presents the fifth vibration mode of the L-shaped column from the ANSYS modal analysis. The natural frequency is 1.7366 Hz, with deformation occurring along the X-axis. The color scale illustrates displacement magnitude: Red → maximum deformation zones (highest lateral movement), Yellow/green → moderate displacement, Blue → minimum deformation, indicating regions with negligible movement.

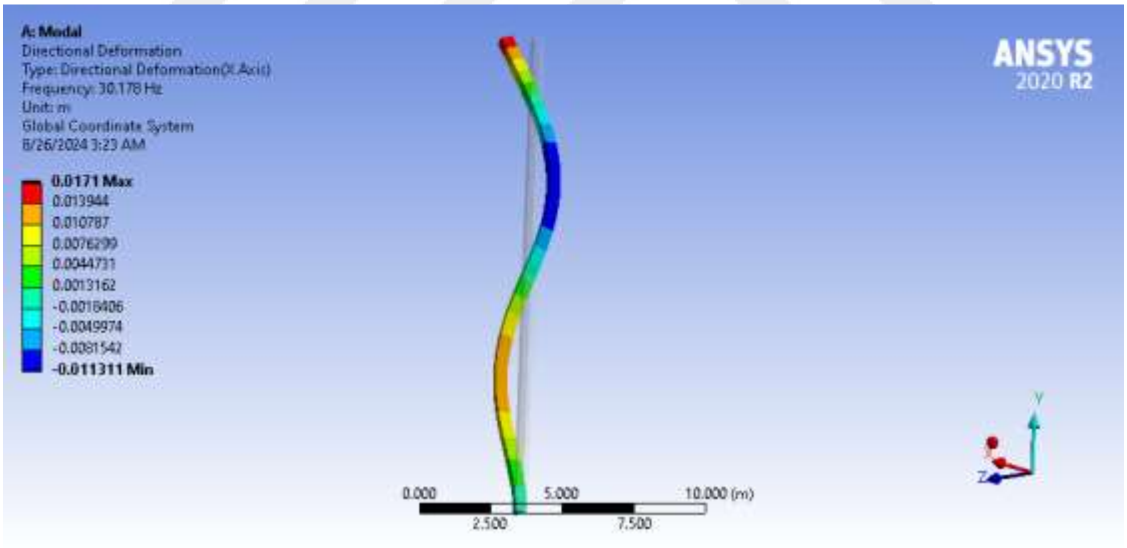

Figure 4.21: Modal Analysis L Shape Mode 6.

This figure shows the sixth vibration mode of the L-shaped column obtained from ANSYS modal analysis. The natural frequency is 30.178 Hz, with deformation occurring along the X-axis. The color legend indicates displacement magnitude: Red → maximum deformation regions (greatest lateral movement), Yellow/green → moderate displacement, Blue → minimum deformation, highlighting areas with very little motion.

A modal analysis examines the distinct characteristics of repeated connections over many frames. It helps to determine the mode states of a mechanical design or component by showing how different structural parts change under high stacking situations, such as lateral stress. The design concepts for dynamic stacking scenarios are considerably limited by regular mode forms. Mode-superposition methodology, commonly referred to as modal analysis, is a technique that directly evaluates and combines mode forms to define displacement designs. In the field of pattern recognition, the mode forms indicate the most often occurring starting locations. Parallel removal processes are necessary, as is widely recognized. If there are N possible outcomes, then there are also N possible modes. Each mode form corresponds to a unique and standardized method of uprooting; by expanding and combining them, one may develop a final relocation plan. The modal space offers a viewpoint on the fundamental distortion. When structures are stimulated at their specific frequencies, they undergo a transformation into mode shapes, which are distortions. In typical operational conditions, the process of creating a challenging combination involves incorporating all modes. Modal analysis simplifies a complex structure by breaking it down into several frameworks, each representing different possibilities on a single level.

4.5 MODAL ANALYSIS T

Mode shapes are used to describe the behavior of an electrified system. A motion pattern in which the system's components move in a consistent, sinusoidal manner. When structures are subjected to dynamic loads, modal analysis establishes their linear response by identifying the natural frequencies and mode shapes. Modal analysis is defined as the decomposition of a structure's response into its constituent vibrational modes. A mode is defined by its frequency and shape. For different mode forms, slope-based building models have a greater frequency, and the time period is the inverse of the condition.

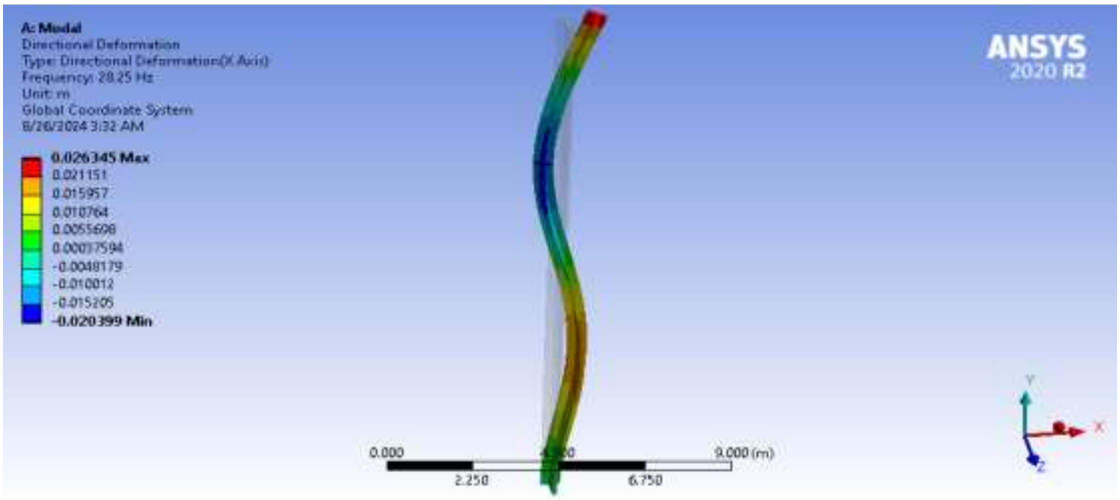

Figure 4.22: Modal Analysis T Shape Mode 1.

This figure presents the first vibration mode of the T-shaped column from ANSYS modal analysis. The natural frequency is 28.25 Hz, with deformation occurring along the X-axis.
The color scale represents displacement magnitude: Red → maximum deformation areas (largest lateral deflection), Yellow/green → moderate displacement, Blue → minimum deformation, where movement is negligible.

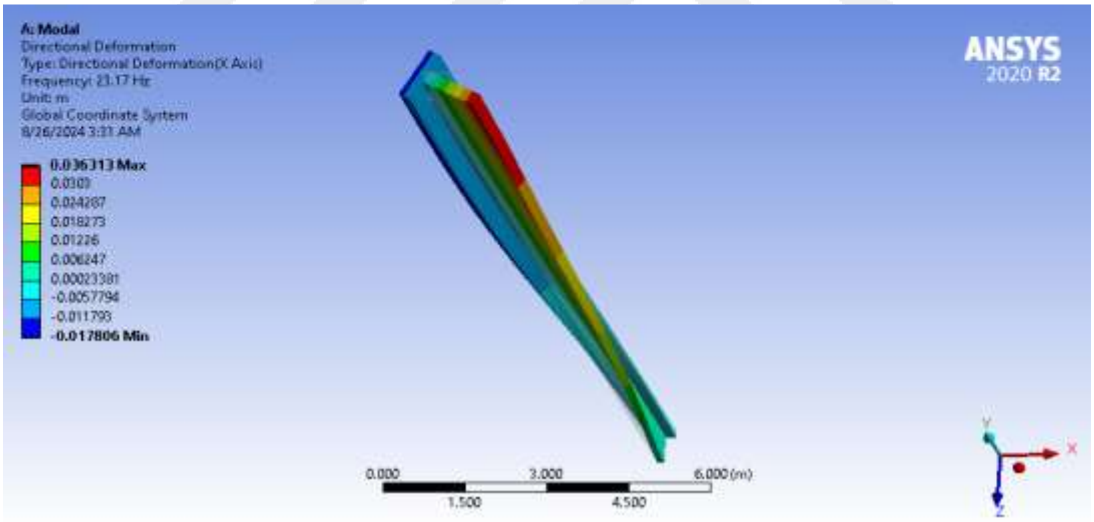

Figure 4.23: Modal Analysis T Shape Mode 2.

This figure shows the second vibration mode of the T-shaped column from ANSYS modal analysis. The natural frequency is 23.17 Hz, indicating a lower mode than the first.
The color legend represents deformation magnitude: Red → maximum displacement (highest bending regions), Yellow/green → moderate movement, Blue → minimum displacement, where deflection is least.

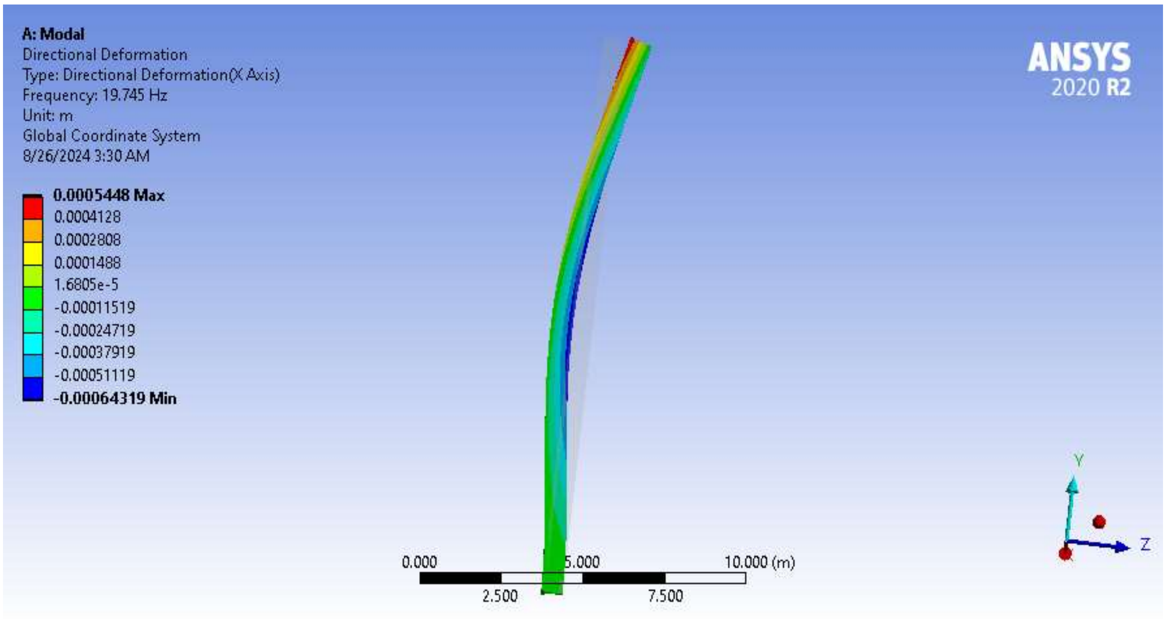

Figure 4.24: Modal Analysis T Shape Mode 3.

, This figure presents the third vibration mode of the T-shaped column from ANSYS modal analysis. The natural frequency is 19.145 Hz, indicating a higher-order deformation pattern. The color scale shows displacement magnitude: Red → maximum deflection, Yellow/green → moderate movement, Blue → minimum deflection, representing areas of least vibration.

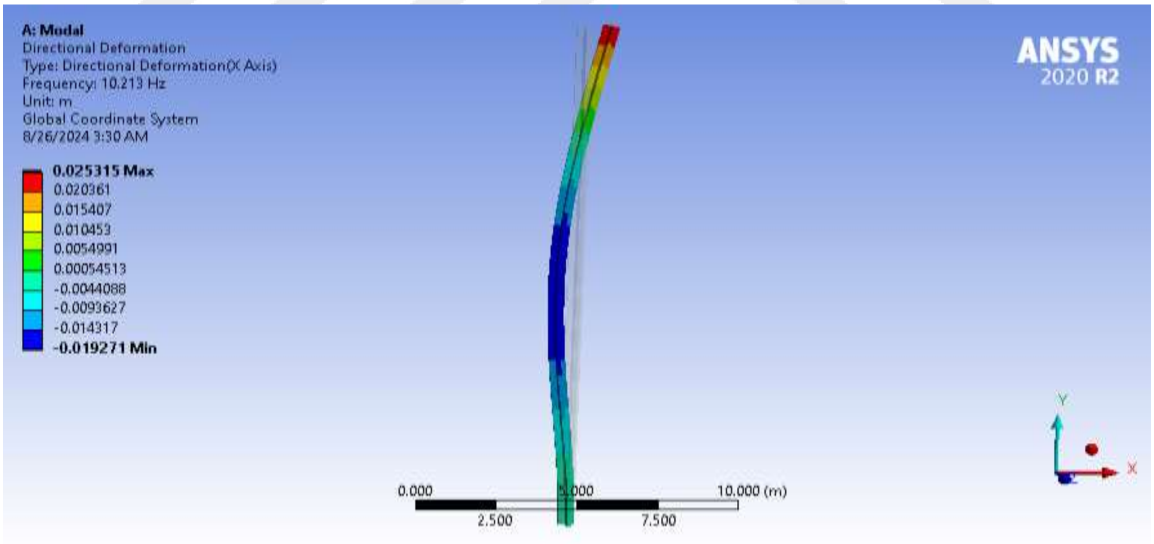

Figure 4.25: Modal Analysis T Shape Mode 4.

This figure shows the fourth vibration mode of the T-shaped column obtained from ANSYS modal analysis. The natural frequency is 10.213 Hz, indicating a lower-frequency deformation pattern. The color scale represents displacement magnitude: Red → maximum deflection, Yellow/green → moderate displacement, Blue → minimum movement, highlighting the most stable areas of the column.

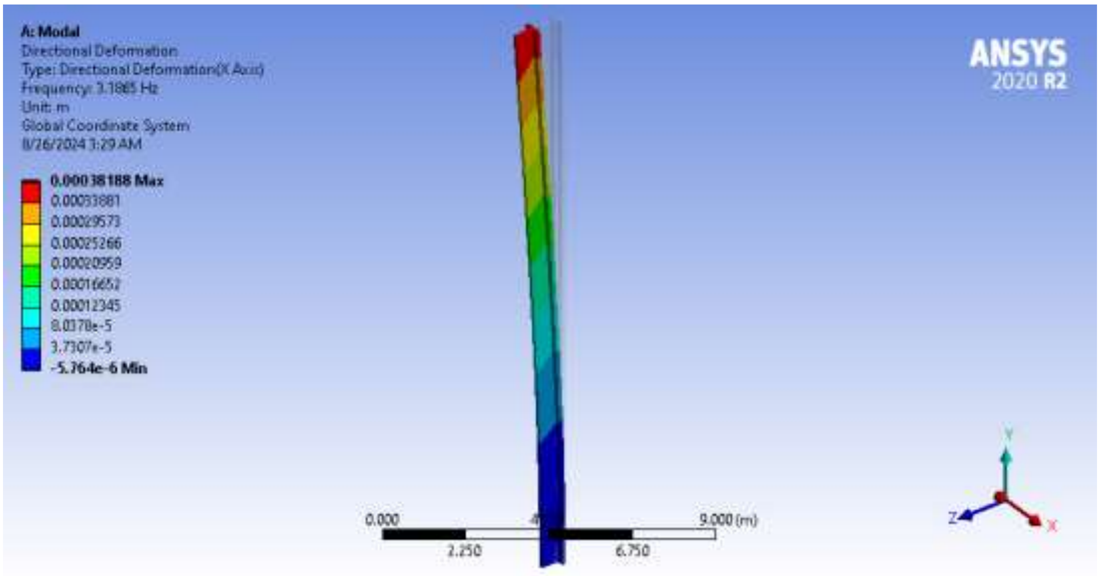

Figure 4.26: Modal Analysis T Shape Mode 5.

This figure presents the fifth vibration mode of the T-shaped column from ANSYS modal analysis. The natural frequency is 3.1865 Hz, reflecting a very low-frequency deformation. The color legend shows displacement intensity: Red → highest deflection zones, Yellow/green → moderate movement, Blue → minimum displacement, indicating the most stable parts of the structure.

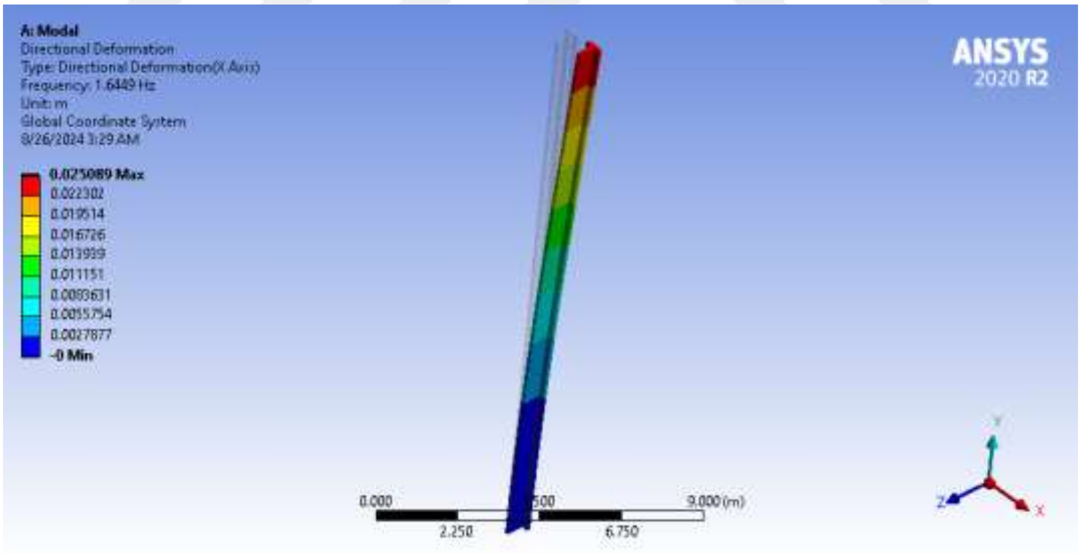

Figure 4.27: Modal Analysis T Shape Mode 6.

This figure shows the sixth vibration mode of the T-shaped column from the ANSYS modal analysis. The structure vibrates at a natural frequency of 1.6849 Hz, representing a very low-frequency mode. The color scale highlights displacement intensity: Red → maximum deformation (peak displacement zone), Yellow/green → moderate displacement, Blue → near-zero movement, indicating the most stable areas of the column.

The distinctive characteristics of recurring connections across multiple frames are investigated in a modal analysis. It assists in the determination of the mechanical design or mode states of the component by demonstrating the alteration of various structural elements under severe mounting conditions, including lateral stress. Design concepts for dynamic layering scenarios are substantially restricted by regular mode forms. Modal analysis, or mode-superposition methodology, is a direct, individual response approach that characterizes displacement designs by assessing and superimposing mode forms. The mode forms in pattern recognition are the most common starting locations. It is widely recognized that parallel elimination strategies are indispensable. If N outcomes are feasible, N mode forms are also feasible. The mode forms, each of which represents a distinct, standardized uprooting procedure, may be amplified and stacked to develop a final relocation strategy. One method involves examining the underlying distortion through the lens of modal space. Structures assume mode shapes, or distortions, when they are stimulated at their characteristic frequencies. The standard activity parameters encompass all options in the production of complex mixes. Furthermore, modal analysis simplifies a complex structure by dividing it into a series of distinct frameworks that represent distinct possibilities at a single level.

5. CONCLUSION AND RECOMMENDATIONS

The results of this study underscore the critical influence of column cross-sectional shape and dimensions on structural performance, particularly with respect to axial displacement, stiffness, and dynamic behaviour. The sectional characteristics, most notably the moment of inertia, play a decisive role in a column’s ability to resist loads and maintain serviceability under both static and dynamic conditions. The inverse relationship between the moment of inertia and deflection, especially when considering depth raised to the third power, highlights how geometric design directly impacts structural efficiency.

This investigation further emphasizes the increasing relevance of non-traditional column shapes, such as castellated and specially formed columns, in contemporary construction practices. These forms offer several structural and practical advantages, including increased bending stiffness, higher strength-to-weight ratios, enhanced deformation resistance, and reduced long-term maintenance costs. The use of form-based column designs allows for greater architectural flexibility and can contribute to more efficient material utilization without compromising load-bearing capacity.

A significant finding of this study is that rectangular columns tend to exhibit greater axial displacement compared to other tested geometries, indicating that alternative shapes may offer improved stability under axial and lateral loads. The inclusion of square openings in rectangular steel columns, modeled in SolidWorks, allowed for a more nuanced understanding of their load-deflection behavior. Both experimental and finite element analyses (FEA) showed a strong correlation, confirming the reliability of the simulation models in capturing real-world behavior and failure patterns.

Moreover, modal analysis provided valuable insights into the vibrational characteristics of various column shapes. The mode shapes representing different deformation patterns serve as a foundation for understanding the dynamic response of structural elements. In complex structures, multiple modes often interact, making it essential to consider superimposed modal responses for a comprehensive assessment. Modal space deformation was found to be a dominant factor in some scenarios, guiding how design engineers might prioritize mode-superposition techniques for displacement-based evaluations.

Ultimately, this research demonstrates that enhancing column design through shape optimization and advanced analysis techniques such as FEA and modal decomposition can lead to more robust, efficient, and resilient structures. The application of specially shaped columns, particularly those with castellated or non-standard geometries, shows great promise in improving structural performance across a range of loading conditions. Future studies should explore the long-term behaviour of these columns under cyclic or fatigue loading and consider integration with smart materials or sensor-embedded systems for real-time health monitoring.

REFERENCES

[1] M. Z. Aryan, P. Singh, and Zabihullah, “Selection of Optimum Structural System in the Design of Reinforced Concrete High-Rise Building under the Effect of Seismic Load,” *IOP Conf. Ser. Earth Environ. Sci.*, vol. 614, no. 1, 2020, doi: 10.1088/1755-1315/614/1/012072.

[2] M. M. Higazey, M. J. Alshannag, and A. S. Alqarni, “Numerical Investigation on the Performance of Exterior Beam–Column Joints Reinforced with Shape Memory Alloys,” *Buildings*, vol. 13, no. 7, 2023, doi: 10.3390/buildings13071801.

[3] P. Nagaprasad, D. R. Sahoo, and D. C. Rai, “Seismic strengthening of RC columns using external steel cage,” *Earthq. Eng. Struct. Dyn.*, vol. 38, no. 14, pp. 1563–1586, 2009, doi: 10.1002/eqe.917.

[4] A. Takino and S. Ikeuchi, “Analytical and experimental study on the seismic performance of roof structure of Japanese traditional temples,” *WCTE 2018 - World Conf. Timber Eng.*, 2018.

[5] G.-W. Kim, J.-K. Song, S.-J. Jung, Y.-H. Song, and T.-H. Yoon, “Lateral load distribution factor for modal pushover analysis,” *Proc. Counc. Tall Build. Urban Habitat*, 2004.

[6] K. Ramin and F. Mehrabpour, “Study of Short Column Behavior Originated from the Level Difference on Sloping Lots during Earthquake (Special Case: Reinforced Concrete Buildings),” *Open J. Civ. Eng.*, vol. 04, no. 01, pp. 23–34, 2014, doi: 10.4236/ojce.2014.41003.

[7] E. Işık, H. Ulutaş, E. Harirchian, F. Avcil, C. Aksoylu, and M. H. Arslan, “Performance-Based Assessment of RC Building with Short Columns Due to the Different Design Principles,” *Buildings*, vol. 13, no. 3, 2023, doi: 10.3390/buildings13030750.

[8] A. Thote, I. Dahat, and M. Tech, “COMPARATIVE STUDY OF FLOATING COLUMN & NON-FLOATING COLUMN WITHOUT SEISMIC BEHAVIOUR,” no. 07, pp. 1832–1836, 2023.

[9] R. C. Dekhn and K. K. Shadhan, “Structural behavior of tree-like steel columns subjected to combined axial and lateral loads,” *J. Mech. Behav. Mater.*, vol. 31, no. 1, pp. 314–322, 2022, doi: 10.1515/jmbm-2022-0030.

[10] Md. Rashedur Rahman, A. Anjum, and U. Mony, “Comparative Study Between Rectangular and Specially Shaped R . C . Column on Seismic Response for Multistoried Building Shaped R . C . Column on Seismic Response for Multistoried,” *J. KoNTekS 5*, no. March, pp. 0–9, 2020.

[11] D. S. K. H. Baviskar Vinita, “IRJET- Effect of Braced Special Shaped Column Cross Section on Response Modification Factor of Reinforced Concrete Building,” *Irjet*, vol. 8, no. 9, pp. 1620–1626, 2021.

[12] R. J. Aswathy, “Study on Effect of Concrete Compressive Strength and Column Shape on Punching Shear Stress in Flat Plate Systems,” *Int. J. Eng. Res. Technol.*, vol. 6, no. 06, pp. 2–5, 2018, [Online]. Available: www.ijert.org

[13] A. Abay and T. Wondimu, “Numerical Investigation of Bundled RC Column under Impact Load,” *Adv. Civ. Eng.*, vol. 2021, 2021, doi: 10.1155/2021/5587576.

[14] T. Islam, R. Yasar, and S. R. Chowdhury, “Numerical Analysis of Retrofitted RC Column under Lateral Load,” *Comput. Eng. Phys. Model.*, vol. 5, no. 3, pp. 82–95, 2022.

[15] S. Pan, R. Yue, H. Hui, and S. Fan, “Lateral cyclic behavior of bridge columns confined with pre-stressed shape memory alloy wires,” *J. Asian Archit. Build. Eng.*, vol. 21, no. 1, pp. 66–79, 2022, doi: 10.1080/13467581.2020.1818568.

[16] A. Rahaman, “Effect of Special Shaped Column on Lateral Load Resistance Capacity of Reinforced Concrete (RC) Building,” *Am. J. Civ. Eng.*, vol. 6, no. 5, p. 147, 2018, doi: 10.11648/j.ajce.20180605.12.

[17] D. Xu, Y. Yang, and Z. Chen, “Experimental study and damage model on the seismic behavior of reinforced concrete l-shaped columns under combined torsion,” *Appl. Sci.*, vol. 10, no. 19, pp. 1–18, 2020, doi: 10.3390/app10197008.

[18] G. Eslami and A. Rahai, “Experimental Investigation on the Behavior of Fiber Reinforced Lightweight Concrete Filled Double Steel Plate Shear Wall,” no. August, pp. 149–151, 2018, doi: 10.5075/epfl-ICSS12-2018-149-151.

[19] A. Arabzadeh, R. Aghayari, and A. R. Rahai, “Investigation of experimental and analytical shear strength of reinforced concrete deep beams,” *Int. J. Civ. Eng.*, vol. 9, no. 3, pp. 207–214, 2011.

[20] T. Terzioglu, K. Orakcal, and L. M. Massone, “Cyclic lateral load behavior of squat reinforced concrete walls,” *Eng. Struct.*, vol. 160, no. October 2016, pp. 147–160, 2018, doi: 10.1016/j.engstruct.2018.01.024.

[21] A. M. Mahmoud, “Finite element implementation of punching shear behaviors in shear-reinforced flat slabs,” *Ain Shams Eng. J.*, vol. 6, no. 3, pp. 735–754, 2015, doi: 10.1016/j.asej.2014.12.015.

[22] A. H. Shrigondekar, G. D. Parulekar, and V. R. Kasar, “Behaviour of RC Overhead Water Tank Under Different Staging Patterns,” *Int. J. Eng. Res.*, vol. V6, no. 04, pp. 538–541, 2017, doi: 10.17577/ijertv6is040442.

[23] B. Moo JIN, S. Jin JEON, S. Woon KIM, Y. Jin KIM, and C. Hun CHUNG, “Earthquake Response Analysis of Lng Storage Tank By Axisymmetric Finite Element Model and Comparison To the Results of the Simple Model,” *13th World Conf. Earthq. Eng.*, no. 13th World Conf. Earthq. Eng., p. 14, 2004.

[24] G. Gabbianelli, D. Perrone, E. Brunesi, and R. Monteiro, “Seismic acceleration and displacement demand profiles of non-structural elements in hospital buildings,” *Buildings*, vol. 10, no. 12, pp. 1–19, 2020, doi: 10.3390/buildings10120243.

[25] R. Sharpe, “Earthquake Engineering 2003 Pacific Conference on 7 Pacific Conference on Earthquake,” no. February, 2003.

[26] H. Jin, R. Song, and Y. Liu, "Sloshing motion in a real-scalewater storage tank under nonlinear ground motion," *Water (Switzerland)*, vol. 12, no. 8, 2020, doi: 10.3390/W12082098.

[27] M. Rafieeraad, "NONLINEAR SEISMIC RESPONSE OF GROUND SUPPORTED CYLINDRICAL REINFORCED CONCRETE by Maryam Rafieeraad Master of Applied Science , Sharif University of Technology , presented to Ryerson University requirements for the degree of in the program of," 2018.

[28] A. I. Celik, M. M. Kose, T. Akgul, and A. C. Alpay, "Directional-Deformation Analysis of Cylindrical Steel Water Tanks Subjected To El-Centro Earthquake Loading," *Nat Sci*, vol. 36, no. 4, pp. 1033–1046, 2018.

[29] C. B. Lee and J. H. Lee, "Nonlinear dynamic response of a concrete rectangular liquid storage tank on rigid soil subjected to three-directional ground motion," *Appl. Sci.*, vol. 11, no. 10, 2021, doi: 10.3390/app11104688.

[30] Kheyroddin, A, and Naderpour, H. (2011), "Investigation of the shear lag phenomenon in reinforced concrete buildings with tubular system", Journal of Modeling in Engineering, Ninth year, No. 26, Winter.

[31] S. Naimi, and M. Celikag, "Problems of Reinforced Concrete Building Construction in North Cyprus.", 12th International Conference on Inspection, Appraisal, Repairs & Maintenance of Structures, pp. 23-25, 2010.

[32] Kheyroddin. A, Aramesh, S, (2013) "Structural resistant systems in high buildings", Structural Book, 690, pp:1-800, Semnan University.

[33] Moghadasi, M. (2009), "Effect of Adding Internal Tube(s) on Behavior of Framed Tube Tall Buildings Subjected to Lateral Load", 7th Asian Pacific Structural Engineering and Construction Conference (APSEC) & 2nd European Asian Civil Engineering Forum(EACEF), Malaysia.

[34] S. Naimi, M. Celikag, and A. A. Hedayat, “Ductility enhancement of post-Northridge connections by multilongitudinal voids in the beam web.”, The Scientific World Journal, 2013.

[35] Paveloni, M. (2012), “Future Building Systems: A Look at Future's Architecture”, Translation by Dr. Mahmoud Golabchi, Tehran University Publishers..

[36] Sayyar Roudsari S, Sameer. A. Hamoush, Sayyed Soleimani,. M, Madandoust. R, (2018), “Evaluation of Large-Size Reinforced Concrete Columns Strengthened for Axial Load Using Fiber Reinforced Polymers” Engineering Structures Journal, DOI: 10.1016/j.engstruct.2018.09.071.

[37] A. Khaleel, and S. Naimi, “Automation of cost control process in construction project building information modeling (BIM).”, Periodicals of Engineering and Natural Sciences, 10(6), pp. 28-38, 2022.

[38] Sayyed Soleimani M, Sayyar Roudsari, S, 2015, “Analytical Study of Reinforced Concrete Beams Tested under Impact Loading “The Fifth International Workshop on Performance, Protection & Strengthening of Structures Under Extreme Loading (PROTECT 2015), - Page 620- 627, 1013.

[39] S. Amhaimedi, S. Naimi, and S. Alsallami, “Assessment of a Decision-Making Model for Monitoring the Success of a Project for Smart Buildings.”, Civil Engineering Journal, 9(1), 127-142, 2023. doi: 10.28991/CEJ-2023-09-01-010.

[40] Taranath, B.S., (1982)., “Structural Analysis and Design of Tall Buildings”, Mc Graw-Hill, New York..

[41] S. Naimi, H. Hrizi. "Risk Analysis of Slaving Floor in Construction Sites." International Journal of Electronics, Mechanical and Mechatronics Engineering, Vol. 9, no. 1, pp. 1637-1645, 2019.

[42] S. Naimi and M. A. Karimi, “Pavement Management System Investigation in Case of Afghanistan,” Cumhuriyet Science Journal, vol. 40, no. 1, pp. 221–232, Mar. 2019, doi: 10.17776/csj.471334.

[43] M. Reihanifar & S. Naimi (2018). Evaluation of road construction projects by value engineering approach as a tool for sustainability. Int J Ecosyst Ecol Sci (IJEES), 8, 339-346.

[44] L. Al Musawi, and S. Naimi, "The management of construction projects in Iraq and the most important reasons for the delay.", Acta Logistica, 10(1), 61-70, 2023.

[45] **V. Kavinkumar, R. Elangovan**, 2016, "An Analytical and Numerical Investigation on Punching Shear Behaviour of SCC Slab", **International Journal of Technology & Engineering**, Vol. 3, Issue 3.

[46] S. Saedi, ORUÇ Ş. The effects of nano bentonite and fatty arbocel on improving the behavior of warm mixture asphalt against moisture damage and rutting. Civil Engineering Journal-Tehran. 2020;6(5). http://dx.doi.org/10.28991/cej-2020-03091514.

[47] S. Saedi, Oruc S. The influence of SBS, viatop premium and FRP on the improvement of stone mastic asphalt performance. Fibers. 2020 Mar 27;8(4):20. https://doi.org/10.3390/fib8040020

[48] S. Saedi, Sadeghian Asl G, Yasrobi SH. The combined effect of SBS and proplast in improving the stone mastic asphalt performance. Quarterly Journal of Transportation Engineering. 2018 Dec 22;10(2):385-99. Doi:20.1001.1.20086598.1397.10.2.11.6.

[49] S. Saedi, Evaluation of the effect of para-aramid and micro-polyolefin fibers on permanent displacement in stone mastic asphalt. Journal of Sustainable Construction Materials and Technologies. 2024;9(2):106-13. https://doi.org/10.47481/jscmt.1501623

[50] S. Saedi, Laboratory investigation of the effect of de-icing solutions on moisture susceptibility of hot mix asphalt with biomass fibers. Innovative Infrastructure Solutions. 2024 Nov;9(11):442. https://doi.org/10.1007/s41062-024-01757-2

[51] B. Abdalhameed and S. Naimi, "Based BIM techniques to clash detection for construction projects," *Period. Eng. Nat. Sci.*, vol. 11, pp. 239–245, 2023.

[52] T. Vardar, M. F. Altan, and S. Naimi, “Economic and technological evaluation of transportation system, new trends,” *J. Sustain. Constr. Mater. Technol.*, vol. 1, no. 1, pp. 83–88, 2017, doi: 10.29187/jscmt.2018.11.

[53] R. Al-Musawi and S. Naimi, “Evaluation of construction project’s cost using BIM technology,” *Math. Model. Eng. Probl.*, vol. 10, pp. 469–476, 2023.

[54] S. Mahal and S. Naimi, “Impact of project management on success criteria,” *Int. J. Tech. Phys. Probl. Eng. (IJTPE)*, vol. 15, no. 1, pp. 318–326, Mar. 2023.

[55] A. H. N. Nimr and S. Naimi, “Improving performance of project through utilizing statistical control chart based on adaptive management and scientific engineering,” *Int. J. Intell. Syst. Appl. Eng.*, vol. 11, no. 4s, pp. 587–593, 2023.

[56] L. Mahmood and S. Naimi, “Investigating the potential of liquefaction issue of some Turkish dams during earthquakes,” *Period. Eng. Nat. Sci.*, vol. 10, no. 6, pp. 57–66, 2022.

[57] S. Naimi, H. A., & Alobadi, S. (2023). A Study of Construction Delays. International Journal on “Technical and Physical Problems of Engineering”(IJTPE), 15(54), 296-308.

[58] A. Emad, S. Naimi, M. R. Altaie, and M. R. A. Hameed, “Artificial intelligence based statistical process control for monitoring and quality control of water resources: A complete digital solution,” *Int. J. Intell. Syst. Appl. Eng.*, vol. 11, no. 5s, pp. 314–324, 2023.

[59] A. R. Mohammed and S. Naimi, “The effectiveness of thermal insulation of the exterior composite walls of buildings in Iraq based on different materials and climate regions using engineering applications,” *Int. J. Intell. Syst. Appl. Eng.*, vol. 11, no. 4s, pp. 594–601, 2023.

[60] S. Naimi and O. Peker, “Deprem etkileri altındaki farklı tiplerde çelik yapıların StaSTEEL ve SAP2000 kullanılarak karşılaştırılması,” *Iğdır Univ. J. Inst. Sci. Tech.*, vol. 12, no. 3, pp. 1577–1591, 2022.

[61] M. Olbak and S. Naimi, “Kentsel dönüşüm uygulanmış 5 katlı iki yapı örneğinin deneysel verileri kullanılarak doğrusal olmayan analiz yöntemleri ile güçlendirme sonuçlarının irdelenmesi,” *İstanbul Aydın Univ. Derg.*, no. 31, pp. 145–166, 2016.

[62] S. A. Mohammed, S. Naimi, and A. H. AbdulKareem, “The effect of geogrid reinforcement of embankment over soft foundation,” *Periodicals of Engineering and Natural Sciences (PEN)*, vol. 10, no. 6, pp. 5–5, Dec. 2022, doi: https://doi.org/10.21533/pen.v10i6.3345.

[63] Ahsan Hussain Khan and S. Naimi, “Effect of Construction Manager’s Political Skills on Relationship between Quality Management Practices and Inter-Organizational Project Success,” *Civil engineering journal*, vol. 10, no. 1, pp. 299–316, Jan. 2024, doi: https://doi.org/10.28991/cej-2024-010-01-019.

[64] Q. A. Saber *et al.*, “Structural Finite Element Analysis of Bridge Piers with Consideration of Hydrodynamic Forces and Earthquake Effects for a Sustainable Approach,” *Mathematical Modelling and Engineering Problems*, vol. 12, no. 3, Mar. 2025, doi: https://doi.org/10.18280/mmep.120334.

[65] S. Mohammed and S. Naimi, “Investigation of concrete properties using recycled waste concrete aggregate,” *Periodicals of Engineering and Natural Sciences (PEN)*, vol. 11, no. 1, pp. 15–15, Feb. 2023, doi: https://doi.org/10.21533/pen.v11i1.3368.